

# The relationship between brain network organization and variability in episodic memory outcomes and abilities

Kyle Kurkela

A dissertation

submitted to the faculty of

the department of Psychology and Neuroscience

in partial fulfillment

of the requirements for the degree of

Doctor of Philosophy

Boston College  
Morrissey College of Arts and Sciences  
Graduate School

August 2023



# **The relationship between brain network organization and variability in episodic memory outcomes and abilities**

Kyle Kurkela

Advisor: Maureen Ritchey, Ph.D.

Our brains afford us the remarkable ability to remember past events from our lives, to travel back in time in our minds' eye and relive our memories anew. What are the brain processes that support this ability? In this thesis I investigated this question across three experiments. In Chapter 1, I examined how the brain regions previously linked to episodic cognition (i.e., the hippocampus, parahippocampal cortex, retrosplenial cortex, posterior cingulate cortex, precuneus, angular gyrus, and medial prefrontal cortex) support recollection by building a model that incorporates both region-specific and network-level contributions. I found that these brain regions form ventral and dorsal subnetworks and that their contributions to recollection outcomes are largely explained by subnetwork-level rather than region-specific engagement. In Chapter 2, I used an openly available MRI dataset to test whether individual differences in functional connectivity were related to individual differences in memory ability, finding that network connectivity outside of the classic episodic networks supports individual differences in our ability to remember. In Chapter 3, I tested a neuroscience inspired hypothesis that individuals would have different capacities to bind their memories around social-emotional and visual-spatial content, ultimately finding inconclusive evidence for or against my hypothesis. Together, these results help to solidify our understanding of the brain as an interconnected network of brain regions and shed new light on how these networks support individual differences in memory.

# TABLE OF CONTENTS

<b>INTRODUCTION</b> .....	<b>1</b>
EPISODIC MEMORY AND THE BRAIN .....	2
INDIVIDUAL DIFFERENCES IN THE BRAIN .....	8
INDIVIDUAL DIFFERENCES IN MEMORY ABILITY .....	13
CURRENT DIRECTIONS.....	16
<b>1.0 CHAPTER 1</b> .....	<b>18</b>
1.1 OVERVIEW.....	18
1.2 METHODS .....	22
1.2.1 <i>Experiment</i> .....	22
1.2.2 <i>Analyses</i> .....	25
1.3 RESULTS.....	36
1.3.1 <i>Preliminary Analyses</i> .....	36
1.3.2 <i>Measurement Models</i> .....	36
1.3.3 <i>Structural Models</i> .....	40
1.4 SUMMARY .....	46
<b>2.0 CHAPTER 2</b> .....	<b>48</b>
2.1 OVERVIEW.....	48
2.2 METHODS .....	50
2.2.1 <i>Participants</i> .....	50
2.2.2 <i>MRI Data</i> .....	51
2.2.3 <i>Regions of Interest</i> .....	52
2.2.4 <i>Behavioral Data</i> .....	53
2.3 ANALYSIS.....	56
2.3.1 <i>MRI Quality Control</i> .....	56
2.3.2 <i>MRI Preprocessing</i> .....	56
2.3.3 <i>Functional Connectivity</i> .....	57
2.3.4 <i>Connectome Based Predictive Modeling</i> .....	59
2.3.5 <i>Statistical Modeling</i> .....	61
2.4 RESULTS.....	61
2.4.1 <i>Hypothesis Driven</i> .....	61
2.4.2 <i>Data Driven</i> .....	64

2.5 SUMMARY .....	71
<b>3.0 CHAPTER 3 .....</b>	<b>73</b>
3.1 OVERVIEW.....	73
3.2 METHODS .....	76
3.2.1 <i>Participants</i> .....	76
3.2.2 <i>Materials</i> .....	77
3.2.3 <i>Procedure</i> .....	78
3.2.3 <i>Analysis</i> .....	81
3.3 RESULTS.....	86
3.3.1 <i>Overall Accuracy</i> .....	86
3.3.2 <i>Evidence for Content Biases in Retrieval Dependency</i> .....	87
3.3.3 <i>Dependency and Overall Accuracy Are Strongly Related</i> .....	91
3.3.3 <i>Content Biases in Overall Accuracy</i> .....	96
3.4 SUMMARY .....	100
<b>4.0 DISCUSSION .....</b>	<b>103</b>
4.1 INTEGRATING REGIONAL AND NETWORK APPROACHES.....	104
4.2 FUNCTIONAL CONNECTIVITY AND MEMORY ABILITY .....	110
4.3 NEURAL INSPIRED ORGANIZATION OF MEMORY ABILITY .....	120
4.4 FUTURE DIRECTIONS & CONCLUDING THOUGHTS .....	125
<b>S.0 SUPPLEMENTAL MATERIAL.....</b>	<b>128</b>
S.1 CHAPTER 1 MODEL SUMMARIES .....	128
S.2 MEMORY FEATURE MODEL PARAMETERS .....	130
S.3 fMRIPREP BOILERPLATE.....	131
3.3.1 <i>Anatomical data preprocessing</i> .....	131
3.3.2 <i>Functional data preprocessing</i> .....	132
S.4 GLOBAL SIGNAL REGRESSION.....	135
S.5 CBPM CONNECTION DEFINING THRESHOLD .....	138
S.6 COMBINING DATA ACROSS TASKS.....	139
S.7 EXPERIMENTAL STIMULI.....	141
S.8 RESULTS IN WINSORIZED SUBSAMPLE.....	145
<b>REFERENCES.....</b>	<b>146</b>

## List of Tables

<b>TABLE 1: DESCRIPTIVE STATISTICS FOR VARIABLES OF INTEREST..</b> .....	35
<b>TABLE 2: COMMUNALITY VALUES. COMMUNALITY VALUE ESTIMATES FROM THE ONE FACTOR AND TWO FACTOR MEASUREMENT MODELS.</b> .....	38
<b>TABLE 3: MEASUREMENT MODEL STANDARDIZED PARAMETER ESTIMATES. SELECT STANDARDIZED PARAMETER ESTIMATES IN THE WITHIN-SUBJECT LEVEL MODEL.</b> .....	40
<b>TABLE 4: KEY PARAMETER ESTIMATES FROM REGION-SPECIFIC MODELS.</b> .....	41
<b>TABLE 5: MEMORY FEATURE MODELS: PARAMETER ESTIMATES.</b> .....	45
<b>TABLE 6: CAM CAN KEY DATA SUMMARY.</b> .....	55
<b>TABLE 7: COMPUTATIONAL LESION ANALYSIS RESULTS.</b> .....	68
<b>SUPPLEMENTAL TABLE 1. SUMMARIES OF ALL MODELS INCLUDED IN CHAPTER 1.</b> .....	129
<b>SUPPLEMENTAL TABLE 2: PARAMETER ESTIMATES FOR THE WITHIN-SUBJECTS PART OF OUR FEATURE SPECIFIC MEMORY MODEL.</b> .....	131
<b>SUPPLEMENTAL TABLE 3. REGRESSION RESULTS OF AVERAGE WITHIN DMN-C CONNECTIVITY ON MEMORY ABILITY REMOVING GSR FROM OUR ANALYSIS PIPELINE.</b> .....	136
<b>SUPPLEMENTAL TABLE 4: REGRESSION RESULTS OF AVERAGE DMNC--DMNA CONNECTIVITY ON MEMORY ABILITY REMOVING GSR FROM OUR ANALYSIS PIPELINE.</b> .....	136
<b>SUPPLEMENTAL TABLE 5: REGRESSION RESULTS OF AVERAGE DMNC CONNECTIVITY WITH THE REST OF THE BRAIN ON MEMORY ABILITY REMOVING GSR FROM OUR ANALYSIS PIPELINE.</b> .....	137
<b>SUPPLEMENTAL TABLE 6: REGRESSION RESULTS OF AVERAGE HIPPOCAMPAL CONNECTIVITY ON MEMORY ABILITY REMOVING GSR FROM OUR ANALYSIS PIPELINE.</b> .....	137
<b>SUPPLEMENTAL TABLE 7: HOW SIMILAR ARE CONNECTOMES CALCULATED USING DATA FROM DIFFERENT TASKS? SIMILARITY BETWEEN CONNECTOMES WAS CALCULATED USING A PEARSON'S CORRELATION.</b> .....	140
<b>SUPPLEMENTAL TABLE 8: FAMOUS PERSON, FAMOUS PLACE, AND COMMON OBJECT STIMULI USED IN CHAPTER 3.</b> .....	145

## List of Figures

<b>FIGURE 1.</b> <i>THE MAJOR NODES OF THE POSTERIOR MEDIAL NETWORK (PMN) AND DEFAULT MODE NETWORK (DMN)...</i>	6
<b>FIGURE 2:</b> <i>MEASUREMENT MODEL</i> .....	39
<b>FIGURE 3:</b> <i>PATH DIAGRAM</i> .....	42
<b>FIGURE 4:</b> <i>MEMORY FEATURE MODEL PATH DIAGRAM</i> .....	44
<b>FIGURE 5:</b> <i>REGIONS AND CONNECTIONS OF INTEREST</i> .....	59
<b>FIGURE 6:</b> <i>TARGETED HYPOTHESES</i> . .....	64
<b>FIGURE 7:</b> <i>EVALUATING FEATURE IMPORTANCE</i> . .....	70
<b>FIGURE 8:</b> <i>TRIADS TASK OVERVIEW</i> .....	81
<b>FIGURE 9:</b> <i>CALCULATION OF RETRIEVAL DEPENDENCY</i> .....	84
<b>FIGURE 10:</b> <i>OVERALL ACCURACY AS A FUNCTION OF SESSION AND TRIAD TYPE</i> .....	87
<b>FIGURE 11:</b> <i>RETRIEVAL DEPENDENCY AS A FUNCTION OF SESSION AND TRIAD TYPE</i> .....	89
<b>FIGURE 12:</b> <i>CONTENT BIASES IN RETRIEVAL DEPENDENCY</i> .....	91
<b>FIGURE 13:</b> <i>DEPENDENCY IS A QUADRATIC FUNCTION OF OVERALL ACCURACY</i> .....	93
<b>FIGURE 14:</b> <i>CONTENT BIASES IN OVERALL ACCURACY</i> .....	97
<b>FIGURE 15.</b> <i>FAMILIARITY OF FAMOUS EXPERIMENTAL STIMULI</i> .....	99
<b>SUPPLEMENTAL FIGURE 1:</b> <i>CBPM RESULTS ARE ROBUST TO SELECTION OF CONNECTION SELECTION THRESHOLD</i> ..	139
<b>SUPPLEMENTAL FIGURE 2:</b> <i>HOW DO PREDICTIVE MODELS BUILT USING CONNECTOMES FROM INDIVIDUAL TASKS COMPARE?</i> .....	140

## INTRODUCTION

About 3 years ago, I broke my arm riding my bike down Harvard Ave in Boston. I was in my second year of graduate school, and it was an unusually warm day for late February. It was late in the day, and I was in a rush to get back to my apartment before sunset. I was riding at speed, heading north on Harvard Ave, when I approached an intersection that had a traffic light that had just turned green. As I approached the intersection, I saw a car rapidly approaching from my right out of the corner of my eye. I instinctively grabbed at my brakes to avoid what I thought was going to be a collision. Unfortunately for me, I made the mistake of only using my front brakes to try and slow my momentum, causing me to tumble over the top of my handlebars, ultimately lying flat in the middle of the intersection. I can vividly recall much about that episode, from the searing pain in my left arm, the dark gray clouds overhead, the warm-for-February-but-still-quite-cold temperature. Episodic memory is defined as our ability to “mentally time travel”, reexperiencing past events anew (Tulving, 1983, 2002). Episodic memories, unlike sensorimotor, semantic, or short-term memory, are bound to a specific time and place and are accompanied by a sense of auto-noetic awareness – a distinctive awareness that you are reexperiencing something that has occurred before. It is this cognitive ability that is the focus of the present dissertation. The thing that particularly fascinates me about episodic memory is how the brain gives rise to this complex cognitive ability. Much like a mechanic, I have always been fascinated in getting “under the hood” of episodic memory, understanding the machinery that affords us this remarkable ability. In what

follows, I review the literature on the neural architecture of episodic memory, specifically focusing on how this neural machinery is organized and how it supports individual differences in our ability to remember past events.

## **EPISODIC MEMORY AND THE BRAIN**

The study of the brain basis of episodic memory has traditionally taken a region focused approach, examining how brain regions individually contribute to episodic memory. This is largely because early cognitive neuroscience work consisted of studying patients who experienced cognitive deficits after damage to circumscribed brain areas. In the field of episodic memory, the hippocampus became the focus of intense research following the discovery of a patient (referred to as Patient H.M.) who developed a profound case of anterograde amnesia following resection of his hippocampus (and surrounding medial temporal lobe tissue) due to intractable epilepsy (Corkin, 2002; Scoville & Milner, 1957). Evidence began to mount supporting the necessary role of the hippocampus in episodic memory, with many more documented cases of amnesia following hippocampal damage (Damasio et al., 1985; see Spiers et al., 2001 for review; Zola-Morgan et al., 1986) and studies of non-human primates (e.g., Zola-Morgan & Squire, 1985, 1986) and rodents (e.g., O'Keefe et al., 1975; Sutherland & McDonald, 1990) demonstrating memory deficits following surgical ablation of the hippocampus. More recent research has demonstrated not only the necessity of the hippocampus for memory, but also how the hippocampus is sufficient for driving memory retrieval. Specifically, recent research in rodents suggests that hippocampal neurons activated

during the formation of a fear memory that are tagged and subsequently artificially reactivated reinstates fear memories (Josselyn & Tonegawa, 2020; Ramirez et al., 2013).

Later research expanded our knowledge of the neural architecture supporting episodic memory beyond the hippocampus to structures surrounding the hippocampus within the medial temporal lobes. Specifically, these studies implicated the cortical areas surrounding the hippocampus, including regions such as the entorhinal cortex, the parahippocampal cortex (PHC), and the perirhinal cortex (PRC), in episodic memory. Studies in rodents and primates, for example, noted that memory deficits can be induced by lesioning the surrounding MTL cortices (e.g., Zola-Morgan et al., 1989) and lesions including the hippocampus and other MTL regions led to the most profound memory deficits (e.g., Squire & Zola-Morgan, 1991). It was on the basis of this work that theorists proposed that the entire medial temporal lobe – including the hippocampus and the surrounding cortex – served together as an integrated declarative memory system (Squire, 1992; Squire & Zola-Morgan, 1991). Early studies using functional magnetic resonance imaging (MRI) delegated mnemonic functions to the PHC and the PRC, with the PHC cooperating with the hippocampus to support memory that is accompanied with rich contextual details (i.e., based on a sense of recollection) and the PRC supporting memory that is acontextual (i.e., based on a sense of familiarity) (e.g., Davachi et al., 2003; Diana et al., 2010; Ranganath et al., 2004). Findings from these studies led theorists to propose an influential binding of items and contexts (BIC) model in which the PHC supports memory for contextual details, the PRC memory for specific items, and the hippocampus serving as the binding site for the two informational pathways (Diana et al., 2007; Ranganath, 2010). Importantly, these lines of research broadened the neural focus of

investigation for cognitive neuroscientists interested in episodic memory, suggesting that brain regions outside of the hippocampus serve complementary roles in the phenomenon.

Extending this line of inquiry even further, recent research suggests that episodic memory is reliant on a wide network of regions outside of just the medial temporal lobes. FMRI studies of episodic memory find that activation in a core network of regions—including the posterior parietal cortex, the medial prefrontal cortex, the retrosplenial cortex, and the precuneus—correlates with episodic memory success (H. Kim, 2011; Rugg & Vilberg, 2013; Spaniol et al., 2009). Further, these regions increase in their functional communication during successful memory retrieval (Fornito et al., 2012; Geib et al., 2017; King et al., 2015; Schedlbauer et al., 2014; Watrous et al., 2013). Perhaps most compellingly, there are documented cases of memory changes in patients with brain damage to the retrosplenial cortex, mammillary bodies, prefrontal cortex, and the posterior parietal cortex (Berryhill et al., 2007; Duarte et al., 2005; Gadian et al., 2000; Newsome et al., 2018; Simons et al., 2010; Valenstein et al., 1987). Interestingly, the PRC and the PHC show different patterns of whole brain functional connectivity and coactivation during tasks (Libby et al., 2012; Ritchey et al., 2014), leading to an influential proposal that they form the cores of anterior temporal (ATN) and posterior medial (PMN) hippocampal-cortical networks that support memory guided behavior (PMAT framework; Ranganath & Ritchey, 2012).

The set of cortical regions associated with episodic retrieval have also been shown to be co-active during rest. Early cognitive neuroscience research using fMRI found that a group of regions displayed greater activation during periods of rest compared to attention demanding tasks (Mazoyer et al., 2001) leading to the hypothesis that these

regions constituted the “default mode” of brain organization (Raichle et al., 2001). These default mode regions also tended to co-fluctuate during “resting-state” scans where participants were not given an explicit task (Greicius et al., 2003) and tended to co-activate in response to tasks that require internally directed attention (Spreng & Grady, 2010), including tasks that require participants to recall an event from their lives (i.e., autobiographical memory tasks), tasks that require participants to imagine a future event (i.e., prospection tasks), and tasks that require participants to read and consider the states of mind of other people (i.e., theory of mind tasks). Further work refined the default mode network, noting that many default mode regions co-fluctuate with the hippocampus during rest (Greicius et al., 2004; Vincent et al., 2006), leading to proposals that default mode network is also involved in episodic memory. The regions comprising the default mode network – the medial prefrontal cortex, posterior parietal cortex, the posterior midline, and the lateral temporal cortex – include the set of regions defined as part of the PMN in the PMAT framework (see **Figure 1a,b**).

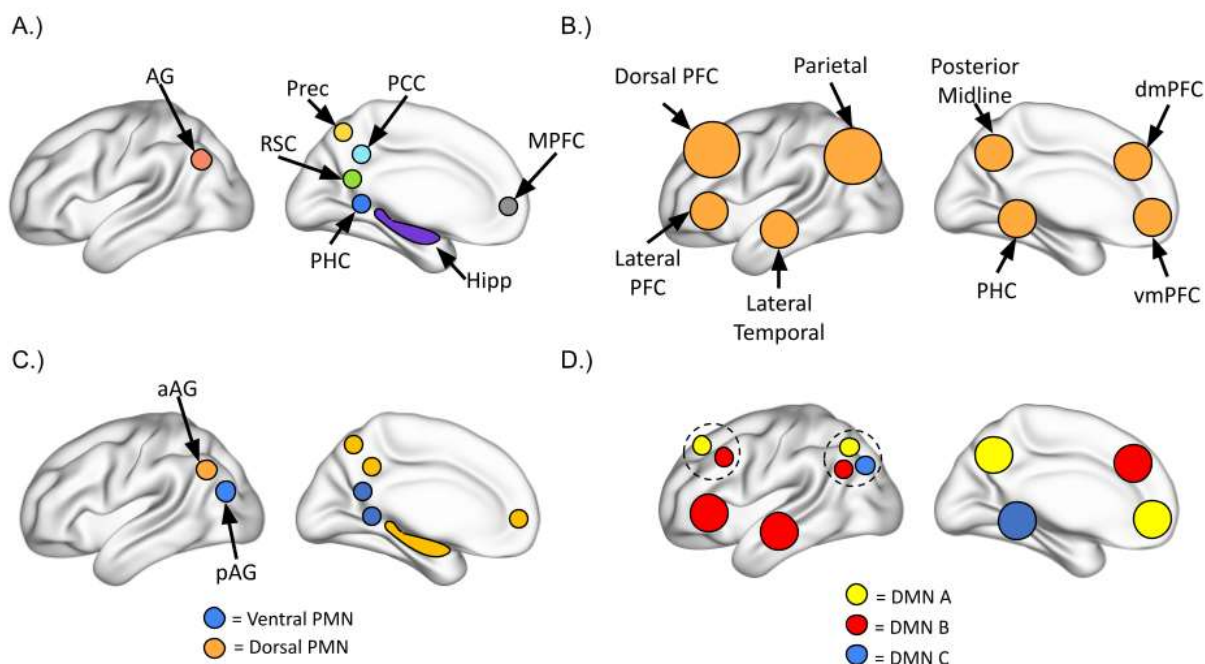


**Figure 1.** The Major Nodes of the posterior medial network (PMN) and default mode network (DMN). Many of the regions of the PMN (panel A) are also regions of the DMN (panel B), with the DMN having a few additional regions that are not a part of the PMN. Both the PMN and the DMN can be broken down into subnetworks (panel C,D). Subnetworks C and A of the DMN are closely aligned with the ventral and dorsal PMN subnetworks.

The latest research on brain wide neural networks supporting episodic memory suggests that these large-scale neural networks can be decomposed into highly related subnetworks. Evidence to this end has come from fMRI experiments examining functional connectivity during resting state scans (Andrews-Hanna et al., 2010; Barnett et al., 2021; Buckner & DiNicola, 2019; Yeo et al., 2011), patterns of whole brain functional connectivity during tasks (e.g., movie watching Cooper et al., 2021b), coactivation during tasks (Andrews-Hanna, Saxe, et al., 2014; DiNicola et al., 2020) and similar multivariate pattern information profiles during memory tasks (retrieval: Barnett et al., 2021; encoding: Ritchey et al., 2014). Cooper and colleagues (2021), for example, defined the nodes of the PM network using ROIs from a meta-analytic search for the term “episodic” in the *NeuroSynth* database. Cooper and colleagues (2021) then showed that

these regions clustered into ventral and dorsal subnetworks (see **Figure 1c**) based on their patterns of whole brain functional connectivity during a movie-watching task. They support this ventral/dorsal distinction by further showing that these subnetworks differentially respond during movie scene transitions. Evidence from clustering analyses on functional connectivity data similarly (Andrews-Hanna et al., 2010; Yeo et al., 2011) shows that the DMN can be decomposed into at least three different subnetworks – labeled by Yeo and colleagues (2011) as DMN “A”, “B”, and “C” (sketched in **Figure 1d**). Importantly, the subnetworks of the PMN and the DMN seem to perform related but dissociable roles in cognition, with the more ventral subnetworks (the ventral PMN and DMN-C) playing a stronger role in episodic cognition and the more dorsal subnetworks (dorsal PMN and DMN-A) playing a stronger role in social cognition (DiNicola et al., 2020). Interestingly, these subnetworks are highly overlapping, such that the ventral and dorsal PMN subnetworks are closely aligned with the DMN subnetworks C and A identified in other data (see **Figure 1c,d**). For the remainder of this dissertation, I will be considering the ventral and dorsal PMN and the DMN-C and DMN-A subnetworks as representing a parallel distinction with similar respective groupings of regions.

Taken together, the literature just reviewed suggests that episodic memory is a brain wide phenomenon supported by more than just structures within the medial temporal lobe. What remains lacking, however, is an integrated understanding of how these brain regions contribute to episodic memory within the context of these larger networks. In Chapter 1, I report the results of an fMRI study where I explicitly test whether the brain regions of the default mode network make region-unique contributions that are independent of network-wide contributions.

## INDIVIDUAL DIFFERENCES IN THE BRAIN

Human brains display a remarkable amount of normativity and idiosyncrasy. All human brains, for example, have the same basic shape and structure. They all have folds in the cortex in the form of sulci and gyri; they all have four basic lobes of the cortex and the same subcortical structures. Human brains also display remarkable normativity in how the brain functions. Activation in cortical regions fluctuates in such a way that cortical regions form large scale brain networks that are largely consistent across individuals (Yeo et al., 2011); patterns of brain activation while watching movies and recalling events can be so consistent from individual to individual that brain patterns from one individual can predict patterns of brain activation in another individual while both individuals are watching or recalling the same event (“intersubject synchrony” Chen et al., 2017). On top of this normative structure, however, lies an equally remarkable number of individual differences in the brain’s structure and function. The size of the folds of the cortex, for example, can vary substantially from individual to individual (e.g., Im et al., 2006) and the pattern of functional connectivity of large scale neural networks is unique enough to each individual to allow for the identification of an individual from a group (i.e., a brain fingerprint Finn et al., 2015). Do individual differences in brain structure and function relate to individual differences in cognition? If so, which brain properties are related to individual differences in memory ability in healthy young adults?

Individual differences in memory ability in healthy young adults have been hypothesized to be related to at least three different brain properties: gray matter volume of the hippocampus, the amplitude of BOLD responses during retrieval, and patterns of brain-wide functional connectivity. Some of the earliest studies linking individual

differences in memory to the brain studied the volume of the hippocampus. As reviewed earlier, the hippocampus has been the target of intensive study by cognitive neuroscientists following the discovery that hippocampal damage leads to profound cases of anterograde amnesia. Early studies using MRI to measure the volume of the hippocampus suggested that better rememberers have larger hippocampal volumes (Maguire et al., 2000; Mazzoni et al., 2019; Poppenk & Moscovitch, 2011). One influential example is a study on London taxi drivers. London Taxi drivers are required to memorize the dazzling complexity of London's streets and landmarks. Maguire and colleagues (2000) collected structural MRI scans of a sample of London taxi drivers and found that London taxi drivers had larger posterior hippocampal volumes compared with controls. These findings, however, have been contradicted by more recent, higher powered studies which suggest that the relationship between hippocampal volume and memory ability is small to nonexistent in the healthy young adult population (Clark et al., 2020; Van Petten, 2004). To date, it appears that although there are substantial individual differences in hippocampal volume it remains unclear whether these individual differences are related to memory ability in the healthy adult population.

Another line of research suggests that there are substantial individual differences in the topology of neural activation during episodic retrieval (Donovan & Miller, 2008; M. B. Miller et al., 2002, 2009, 2012). As reviewed earlier, successful episodic retrieval is on average characterized by increased activation in a number of brain areas, including in the hippocampus, medial temporal lobes, posterior midline, medial prefrontal cortex, and lateral parietal cortex – regions that have also been associated with the default mode network (Buckner & DiNicola, 2019; Ritchey & Cooper, 2020). Individuals also deviate

from this average pattern, often substantially so. In fact, individuals often deviate so much from this average pattern that this average pattern often becomes a poor representation of the brain activation pattern of individual subjects. Patterns of activation during an episodic retrieval task correlate more strongly within individuals over time than across individuals completing the same episodic retrieval task over time (M. B. Miller et al., 2002). Furthermore, patterns of activation while participants complete different retrieval tasks are more similar than the patterns of activation of different participants completing the same retrieval task (M. B. Miller et al., 2009). In other words, knowing that a brain scan came from the same person can be much more important than knowing that a brain scan came from a particular task – in this case, successful episodic retrieval. The substantial individual variability in retrieval-related brain activation topology appears to be explained, in part, by individual differences in anatomy, cognitive style, and specific strategy used during the memory test but, importantly for the present purposes, not to individual differences in overall memory performance (e.g., giving verbal names to non-verbal content, M. B. Miller et al., 2012). Taken together, this line of research highlights the need to account for individual differences when studying the neural correlates of episodic memory.

Measures of intrinsic functional connectivity, often obtained from resting-state scans that do not include an explicit cognitive task, have been widely used to study individual differences in cognition and are a strong candidate for explaining individual differences in memory ability. Studies of the resting-state have found that there is a normative pattern of functional connections in the brain, such that brain regions form stable networks (between 7-17, Yeo et al., 2011). Recent work suggests that the majority

of variability in the strength of these connections is attributable to stable individual differences away from this group-level pattern (as opposed to variation attributable to cognitive task or day-to-day variation (Gratton et al., 2018). Furthermore, the strength of intrinsic connections has been shown to be predictive of a number of different behavioral phenotypes including neuroticism and extraversion (Hsu et al., 2018), trait-level anxiety (Z. Wang et al., 2021), fluid intelligence (Finn et al., 2015), creativity (Beaty et al., 2018), sustained attention (Rosenberg et al., 2016), and working memory ability (Avery et al., 2020). Patterns within the intrinsic functional connectome are so identifiable that they can be used to identify an individual from a group, acting a sort of “brain fingerprint” (Finn et al., 2015). Thus, it seems reasonable to hypothesize that individual differences in intrinsic functional connectivity would be related to episodic memory ability.

Prior studies examining the relationship between functional connectivity and individual differences in memory have largely focused on the functional connectivity of the hippocampus due to its important role in memory function (Corkin, 2002; Riedel et al., 1999). These studies have generally found that increased hippocampal functional connectivity is associated with better memory ability, including its bilateral functional connectivity (L. Wang, Negreira, et al., 2010) and its functional connectivity with cortical areas such as the lateral occipital cortex (Tambini et al., 2010) and the posterior medial cortex (Touroutoglou et al., 2015; L. Wang, LaViolette, et al., 2010). This positive relationship between hippocampal connectivity and memory ability can be interpreted as reflecting greater responsiveness of the hippocampus to time-varying signals across the brain in individuals with better memory, or conversely, disruption in hippocampal

communication in individuals with worse memory. More recent experiments have looked at the relationship between memory and functional connectivity using larger samples (specifically of the hippocampus; Przeździecki et al., 2019), incorporating a broader set of brain regions (Sneve et al., 2017; van Buuren et al., 2019), or both (King et al., 2015; Lin et al., 2021). These studies suggest that there is a complex, distributed pattern of whole brain functional connectivity that is related to individual differences in episodic memory ability, but the exact nature of this relationship has varied from study to study. Some studies have shown that intrinsic functional connectivity calculated during a resting-state scan is related to episodic memory ability, but with contrasting results (Sneve et al., 2017; van Buuren et al., 2019). Some studies suggest that superior rememberers have default mode networks that are decoupled with perceptual regions of the brain (Sneve et al., 2017), whereas others suggest that superior rememberers are characterized by increased connectivity within the ventral default mode network and strong connectivity between the dorsal default mode network and the frontal-parietal control network (van Buuren et al., 2019). Still other studies suggest that functional connectivity calculated during a task is particularly important for predicting episodic memory ability (King et al., 2015; Lin et al., 2021). One study suggests that regions commonly associated with episodic memory, including many regions in the default mode network, increase in their connectivity with each other and the rest of the brain in better rememberers (King et al., 2015). Another study showed a similar pattern of results, but makes the additional note that functional connectivity limited to regions classically linked to episodic remembering were useful but not sufficient for predicting episodic memory ability (Lin et al., 2021).

Many of just reviewed studies, however, are underpowered, both in terms of the number of participants collected (Marek et al., 2022) and in terms of the amount of data collected per participant (Anderson et al., 2011; Gordon, Laumann, Gilmore, et al., 2017; Laumann et al., 2015). It has been recently demonstrated that brain-wide association studies require thousands of participants to achieve acceptable amounts of power (Marek et al., 2022), though this problem is mitigated by using a region of interest-based approach to reduce the number of comparisons or by focusing on multivariate patterns within the connectome. Functional connectivity studies may additionally benefit from more data being collected per participant, as it has been shown that at least 30 minutes of high quality MRI data is required to achieve good levels of reliability of the functional connectome (i.e.,  $r > 0.85$ ; Gordon and colleagues (2017)). This is important because the reliability of a measurement places a key constraint on the measurable effect size of the correlation between two constructs of interest (e.g., functional connectivity and behavior). Most existing studies relating functional connectivity to memory ability have typically used data from one MRI scan, often comprising 6-8 minutes of data. In Chapter 2 of my dissertation, I report the results of an analysis where I build and improve upon previous work by utilizing an openly available fMRI dataset that contains data from hundreds of individuals completing many different MRI scans.

### **INDIVIDUAL DIFFERENCES IN MEMORY ABILITY**

The cognitive neuroscience literature investigating individual differences in memory often assumes that memory ability is a unidimensional phenomenon – you are either a “good” rememberer or a “poor” rememberer. As a result, cognitive

neuroscientists often operationalize memory ability by observing how well participants perform on a single memory test. But is this all there is to say about individual differences in episodic memory ability? Do some people simply have better memory than others? Or can people differ in other, more nuanced ways? What does the psychometric literature say about how individual differences in memory ability are organized?

Psychologists have long been interested in individual differences in memory ability. Indeed, some of the pioneering researchers in the study of mnemonic processes noted the extent to which individuals differed in their memory ability (Ebbinghaus, 1885/1964). Many laboratory studies that sought to examine individual differences in memory ability have taken an exploratory approach, electing to administer extensive batteries of memory tests in order to measure people's long-term memory ability (Malmi et al., 1979; Nyberg, 1994; Underwood et al., 1978; Unsworth, 2010; Unsworth & Brewer, 2009, 2010). In one of the most extensive reviews on the literature studying individual differences in long-term memory ability to date, Unsworth (2019) performed a best-evidence synthesis of decades of psychometric research on memory ability. Unsworth (2019) examined 5 previously published datasets that, in the author's opinion, constituted the "best evidence" for examining the structure of individual differences in memory ability. Unsworth (2019) concluded that a model that organizes memory ability based on an overall memory ability subsumed by underlying memory test specific abilities was the best fit for the available data. In other words, Unsworth (2019) argues that individuals have an overall memory capacity whereby one person may have a better memory than another across different types of memory tests. Unsworth (2019) also argues that individuals also have specific capacities to perform on specific types of

memory tests. For example, Mary and Paul might have a similar overall memory capacity, but Mary might be better at a word-list free recall test than Paul, whereas Paul might be better at recognizing previously encountered faces than Mary. One oversight of the type of model suggested by Unsworth (2019) is that this model does not account for the underlying cognitive processes that underlie performance on different episodic memory tests. For example, presumably people do not have an “ability to freely recall words” but an underlying ability to implement a cognitive strategy that is particularly effective in that task. In support of this idea, Ngo and colleagues (2021) collected data that suggests that individuals systematically differ on their ability to perform two fundamental cognitive computations that underlie our long-term memory ability – the ability to “pattern separate” and our ability to “pattern complete”. A pattern separation ability refers to the ability to distinguish two highly similar representations in memory whereas a pattern completion ability is the ability to link disparate elements of an event together into a singular, coherent whole.

Psychological research on individual differences in memory has also examined how individuals differ in recalling their autobiographical memories. In a review of individual differences in autobiographical memory, Palombo and colleagues (2018) focused specifically on two extreme cases of autobiographical memory ability: highly superior autobiographical memory (HSAM) and severely deficient autobiographical memory (SDAM). Both syndromes fall at the extremes in terms of the level of detail of people’s autobiographical memories. Individuals with HSAM can remember remote days from their lives in an extraordinary amount of detail, whereas individuals with SDAM are unable to vividly recollect events from their lives. Importantly, individuals with HSAM

and SDAM perform similar to controls on laboratory tests of their memory and other cognitive abilities, suggesting that their syndrome is specific to autobiographical memory. Palombo and colleagues (2018) suggest research on individual differences in autobiographical memory outside of these extreme cases is limited, but offer three component processes on which individuals in the less extreme ends of population may differ: their visual imagery ability, their amount of self-awareness or self-consciousness, and their ability to process affective (i.e., emotional) information.

What is clear from the literature is that individuals differ on more than just a single memory continuum. What is interesting is that almost all of the research to date has not integrated an individual differences approach with what is known about the underlying neural architecture that underlies our episodic memory ability. And yet biological substrates should shape how individuals differ. Chapter 3 of my dissertation seeks to fill this gap in the literature by testing a neuroscience inspired hypothesis on how individuals differ in their memory ability, based on what is known about the organization of cortical networks involved in memory.

### **CURRENT DIRECTIONS**

The aims of the present dissertation are threefold. In Chapter 1, I aim to examine the relationship between regional and network-level contributions to episodic memory. The study of episodic memory has traditionally taken either a region-focused approach (e.g., how does damage to the hippocampus affect memory?) or a network-focused approach (i.e., functional communication increases between which brain regions in support of memory?), but much less is known about how these network accounts relate to

prior work on individual regional contributions. In Chapter 1 I reexamine a previously published dataset from my laboratory and use a structural equation model (SEM) to simultaneously capture region-specific and network-common contributions to successful episodic retrieval. In Chapter 2, I aim to investigate the relationship between individual differences in memory ability and intrinsic measures of functional brain connectivity. Because past research has typically not been well-powered to examine this question, here I examine an openly available dataset that contains data from a relatively large number of subjects and contains multiple fMRI scans. In Chapter 3, I aim to test a multidimensional hypothesis on the organization of individual differences in memory ability. Research on individual differences in memory ability has been performed by both cognitive neuroscientists and psychologists, but our understanding of the organization of individual differences in memory ability has not incorporated our understanding of how the brain is organized. In Chapter 3, I collect data on a novel behavioral paradigm designed to test a neuroscience inspired multidimensional hypothesis on how individuals differ in their memory ability.

# CHAPTER 1

## 1.1 OVERVIEW

As reviewed in the Introduction, there is a core set of brain regions that are reliably engaged in recollection and other forms of episodic construction, including the hippocampus, parahippocampal cortex, the retrosplenial cortex, the posterior cingulate cortex, the precuneus, the angular gyrus, and the medial prefrontal cortex. Exactly how this network supports episodic construction, however, remains unclear. Past research suggests that there are both regional- and network-level contributions of the PM network to episodic recollection. For instance, the hippocampus has long been known to be essential for episodic memory (Corkin, 2002; e.g., Riedel et al., 1999). Using neuroimaging to look beyond the hippocampus, however, it is apparent that the rest of the PM network is also reliably engaged during recollection (H. Kim, 2013; Rugg & Vilberg, 2013; Spaniol et al., 2009). These regions are robustly structurally and functionally connected with the hippocampus, supporting the idea that they constitute an integrated functional network, yet how this network-level involvement relates to their individual functions remains an open question. Here, we use multilevel structural equation modeling (SEM) to examine heterogeneity in the function of the PM network during an episodic retrieval task. Specifically, we investigated the subnetwork architecture of the PM network, as well as the contributions of individual PM regions to predicting memory outcomes.

A great deal of research has focused on the roles of individual brain regions in supporting episodic construction, delineating specific roles for the hippocampus, angular gyrus, and other regions of the PM network (Ritchey & Cooper, 2020). The hippocampus, for example, is posited to support the binding together of contextual details in memory (Davachi, 2006; Diana et al., 2007; Eichenbaum et al., 2007) and is thought to perform a pattern completion function in which partial representations evoked by memory cues are “completed” by reinstating related information stored in memory (Horner et al., 2015; Marr, 1971; Norman & O’Reilly, 2003). The angular gyrus, on the other hand, is thought to support the representation of multimodal episodic details brought to mind during recollection (Humphreys et al., 2021; Ramanan et al., 2018; Rugg & King, 2018). Some fMRI studies have directly tested for cognitive and temporal dissociations among the regions of the PM network, finding evidence for functional specialization in the context of both episodic memory (Richter et al., 2016; Vilberg & Rugg, 2012, 2014) and imagination (Thakral et al., 2020). For example, Richter et al. (2016) used fMRI to identify brain activity that tracked the success, precision, and subjective vividness of episodic recollection. The authors modeled these measures jointly and found that the hippocampus uniquely tracked whether retrieval was successful, the angular gyrus uniquely tracked the precision of remembered information, and the precuneus uniquely tracked subjective memory vividness. These findings suggest that individual regions of the PM network make distinct contributions to the recollection process.

Prior research has made it clear that activity in default mode network regions is related to memory and to one another, but it remains unclear whether their contributions

to memory are regionally specific or shared across the network. In other words, do any regions of the network make contributions to episodic recollection that go above and beyond those of the other regions of the network? Or can episodic recollection be better thought of as arising from joint coactivation of the network and it is this network wide coactivation that is contributing to episodic recollection? Structural equation modeling (SEM) is a well suited tool for delineating regional and network-level contributions to behavior (Bolt et al., 2018), allowing for the capturing of common, distributed, network-level contributions by estimating latent variables that capture the covariance amongst regions of a network. Structural models can then estimate the statistical dependency between these network latent variables and some behavioral variable while also estimating the regional-specific effect of each of the regions, statistically controlling for their membership within larger networks. For instance, Bolt and colleagues (2018) used SEM to parse the unique contributions of the right dorsolateral prefrontal cortex to cognitive control from those of the larger frontoparietal control network, showing that the unit of behavioral significance for many common cognitive control tasks was not the right dorsolateral prefrontal cortex, but the shared contributions of the frontoparietal control network. This approach differs from common applications of SEM to study functional interactions supporting cognition (see McIntosh & Protzner, 2012 for a review), which in the context of episodic memory, have largely focused on building models of the effective connectivity among brain regions (Addis et al., 2010; Iidaka et al., 2006; McCormick et al., 2010, 2015; Rajah & McIntosh, 2005; Rosenbaum et al., 2010). For instance, past work taking this approach has shown that episodic retrieval involves increased communication among left frontal and parietal regions (Iidaka et al., 2006) as

well as between the hippocampus and regions in the frontal lobes (McCormick et al., 2010, 2015) and sensory cortex (McCormick et al., 2015). Here, rather than focusing on interactions among brain regions, I report a published study (Kurkela et al., 2022b) that applied SEM to estimate the specific regional and common network contributions to episodic remembering within a single statistical model.

Taken together, the literature suggests that the regions of the PM network perform dissociable yet interrelated functions and, as a result, make separable contributions to the recollection process. It remains unclear, however, exactly how to combine the findings from experiments taking region-focused approaches and network-focused approaches—highlighting the need for an approach that can simultaneously consider network-wide and region-specific contributions to episodic retrieval. The present study uses SEM to model heterogeneity of function of the PM network. We sought to model two key aspects of functional heterogeneity within the network: that larger networks fracture into related subnetworks and that regions of the network make extra network contributions to cognition. To this end, I first compared a single network model to a two related subnetworks model, motivated by previous evidence for dissociable ventral and dorsal PM subnetworks that exhibit distinct patterns of functional connectivity during movie-watching (Cooper et al., 2021b). Next, I modeled region-specific contributions to behavior, controlling for network-level effects (c.f., Bolt et al., 2018), to determine whether any regions acted outside of their networks in support of episodic recollection.

## 1.2 METHODS

### 1.2.1 Experiment

#### 1.2.1.1 Participants

Twenty-eight participants from Cooper & Ritchey (2019) were included in the final set of analyses after excluding participants who did not complete the study or who had inadequate memory performance (see Cooper & Ritchey, 2019). Participants were selected such that they were between the ages of 18 and 35 ( $M = 21.82$ ,  $SD = 3.57$ , 16 females, 12 males) and had no history of neurological or psychiatric illness. Participants' self-reported ethnicity was as follows: Not Hispanic or Latino ( $n = 22$ ) and Hispanic or Latino ( $n = 6$ ). Race was self-reported as White ( $n = 18$ ), Asian ( $n = 3$ ), More Than One Race ( $n = 3$ ), Black or African American ( $n = 2$ ), Other ( $n = 1$ ), with one participant electing not to report their race ( $n = 1$ ). Participants reported an average years of education of  $M = 15.2$  years ( $SD = 1.67$ ). Informed consent was obtained from all participants prior to the experiment and participants were reimbursed for their time. All procedures were approved by the Boston College Institutional Review Board.

With respect to statistical power, our analyses focused on trial-to-trial variability in brain activity and memory outcomes. Our dataset had a total of 3888 trials nested within 28 subjects (22 subjects contributing 144 trials; 6 subjects contributing 120 trials – see Cooper & Ritchey 2019). Wolf and colleagues (2013) ran a series of Monte Carlo simulations to determine the minimum sample size required to achieve SEMs that had at least 80% power to detect nonzero parameters with an  $\alpha = 0.05$ . To determine if our models were sufficiently powered, we compared the number of observations that we had

at the within subject, across trial level (i.e., 3888 observations) to the most conservative recommendations made for achieving adequate power in the Wolf simulations, which argue for 460 observations. However, we note that, unlike our study, the Wolf simulations did not use a multilevel model and they did not use categorical variables. There does not currently exist any published recommendations for the required N to achieve sufficient power using the type of multilevel SEM that we use in this manuscript. In the absence of alternative recommendations, we argue that our models are likely to be sufficiently powered given that our number of observations at the within subjects, across trials level far exceeds the most conservative recommendations made by Wolf and colleagues (2013). Although we have sufficient power to model trial-to-trial variability in this dataset, we remain underpowered to model between-subjects variability, and thus we refrain from interpreting any existing subject-to-subject variability in our analyses.

### **1.2.1.2 Materials**

Memoranda consisted of 144 unique events that were constructed using a combination of 144 episode-unique object stimuli from Brady and colleagues (2013), 6 panoramic scenes from the SUN 360 database (Xiao et al., 2012), and 12 sounds from the International Affective Digitized Sounds (IADS) database (Bradley & Lang, 2007). The grayscale object images were altered such that they took on 1 of 120 unique colors taken from the equally spaced positions in CIELAB color space. In a similar manner, the 360-degree panoramic background images were transformed into 120 equally spaced 100° field of view images taken at regular intervals around the panorama. Events consisted of the simultaneous presentation of the colored object on top of a randomly chosen view from the panorama coupled with the presentation of one of the affective sounds.

Participants were encouraged to integrate the three features together into a single meaningful event. For example, a red radio could be placed on top of a beach scene with a view of the ocean while the sound of a woman screaming played in the background. See Cooper & Ritchey (2019) for further information.

### **1.2.1.3 Procedure**

Participants completed six interleaved encoding and retrieval phases while undergoing MRI scanning (see Cooper & Ritchey, 2019). To summarize, during scanned encoding phases participants were told that they would encounter 24 events consisting of a foreground object, a background scene, and an emotionally evocative sound. Participants were asked to remember each of the events in as much detail as possible, with explicit instructions to try and remember the color of the foreground object, the position of the object within the background scene, and the emotional valence of the sound. During scanned retrieval phases, participants were tested on their ability to reconstruct episode features from memory. At the beginning of each retrieval trial, participants were shown grayscale versions of the object stimuli from the previous encoding phase. During this remember period, participants were asked to bring to mind the cued episode in as much detail as possible. Immediately after the remember period, participants were asked to report the emotional valence of the episode's sound using a confidence scale. The confidence scale asked participants to identify their response to the emotional valence question as either with high confidence or with low confidence. After reporting the sound's valence, participants were asked to report the quality of their memory for the remaining two features in a counterbalanced order. Specifically, participants were presented with the object image in a random color on top of a random

view from the correct background scene. Participants were instructed to reconstruct the color of the target image using an interactive 360-degree color wheel and to position the object within the background scene using a similar interactive 360-degree panoramic scale.

#### **1.2.1.4 FMRI data acquisition**

MRI scanning was performed at the Harvard Center for Brain Science using a 3T Siemens Prisma MRI scanner with a 32-channel head coil. Structural MRI images were collected using a T-1 weighted multiecho MPRAGE protocol with a field of view = 256 mm, 1 mm isotropic voxels, 176 sagittal slices with an interleaved acquisition, TR = 2530 ms, TE = 1.69/3.55/5.41/7.27 ms, flip angle = 7 degrees, phase encoding from anterior-posterior, parallel imaging = GRAPPA, and an acceleration factor of 2. Functional images were acquired using a whole brain multiband echo-planar imaging sequence with a field of view of 208 mm, 2 mm isotropic voxels, 69 slices at T > C -25.0 with interleaved acquisition, TR = 1500 ms, TE = 28 ms, flip angle = 75 degrees, anterior-posterior phase encoding, parallel imaging with GRAPPA, and an acceleration factor of 2. A total of 6 scan runs were collected, each of which consisted of 466 TRs.

### **1.2.2 Analyses**

#### **1.2.2.1 Behavioral Data**

Behavioral data from the dataset consisted of trialwise error values measured in degrees for the object color and scene position features and of binary data (i.e., 1: correct; 0: incorrect) for the sound valence feature (i.e., collapsed across confidence). For

consistency across behavioral measures, we transformed the object color and scene position measures into binary measures representing whether a response was correct (1) or incorrect (0), like what we have done previously (see Cooper & Ritchey, 2019). This was done by taking any trial with an error smaller than the accuracy threshold (see below) and giving it a score of 1 and taking any trial with an error greater than the accuracy threshold and giving it a score of 0. Descriptive statistics of our behavioral variables are detailed in **Table 1**.

The accuracy threshold was determined by fitting two probability density functions to group aggregate data within a mixture modeling framework and is described in detail in Cooper and Ritchey (2019). In brief, Cooper and Ritchey (2019) estimated (for the color and scene features separately) the probability that each error resulted from the von Mises as opposed to the uniform distribution. Errors that had less than a 50% chance of fitting the von Mises distribution were labeled as incorrect. This analysis resulted in a threshold of +/- 57 degrees for the object color feature and +/- 30 degrees for the scene position feature and served as our threshold for labeling a response as “correct” or “incorrect”.

#### **1.2.2.2 MRI Preprocessing**

All preprocessing of the MRI data was performed using FMRIPrep v1.0.3 (Esteban et al., 2019). Data were preprocessed using the same steps as in Cooper & Ritchey (2019). First, each T1w volume was corrected for intensity non uniformity and skull stripped. Spatial normalization to the ICBM 152 Nonlinear Asymmetrical template version 2009c was performed through nonlinear registration, using brain-extracted versions of both the T1w volume and template. All analyses reported here use structural

and functional data in MNI space. Brain tissue segmentation of cerebrospinal fluid (CSF), white-matter (WM), and gray-matter (GM) was performed on the brain-extracted T1w image. Functional data was slice time corrected, motion corrected, and corrected for field distortion. This was followed by co-registration to the corresponding T1w using boundary-based registration with 9 degrees of freedom. Physiological noise regressors were extracted using CompCor. A mask to exclude signals with cortical origin was obtained by eroding the brain mask, ensuring it only contained subcortical structures. Six aCompCor components were calculated within the intersection of the subcortical mask and the union of CSF and WM masks calculated in T1w space, after their projection to the native space of each functional run. Framewise displacement was also calculated for each functional run. No smoothing of the data was performed. For further details of the pipeline please refer to the online documentation:

<https://fmriprep.readthedocs.io/en/1.0.3/index.html>. Entire scan runs were excluded from further analysis if more than 20% of frames had a framewise displacement exceeding 0.3mm. Spike regressors were additionally created and added to our trialwise models (detailed below) by flagging all frames that had a framewise displacement greater than 0.6mm. In total, 6 subjects had a single scan run excluded from further analysis due to excessive motion.

### **1.2.2.3 Trialwise Response Estimates**

To estimate trialwise response estimates, we used a multi-model approach proposed by Mumford and colleagues (2012) and implemented in SPM12 (<https://www.fil.ion.ucl.ac.uk/spm/>) using in house MATLAB (<https://www.mathworks.com/products/matlab.html>) scripts. In this approach, a separate

general linear model (GLM) is built to estimate the amplitude of the BOLD response for each trial by modeling the response for each trial using its own dedicated regressor and modeling all other trials as a separate regressor (including the following nuisance regressors: translation in the x, y, and z dimensions; rotation in pitch, roll, and yaw; the first 5 principal component from aCompCorr, framewise displacement, and spike regressors censoring high motion frames). In total, 3888 GLMs were constructed – one for each trial in our dataset. Encoding and retrieval phases for our experiment were interleaved, such that each scan run had 24 encoding trials followed by 24 retrieval trials. The GLMs for the current study were restricted to TRs encompassing the retrieval trials from Cooper and Ritchey (2019), i.e., excluding the encoding trials. Each retrieval trial was modeled by convolving SPM12’s hemodynamic response function with a stick function placed at the onset of the remember period of each retrieval trial. The statistic used as our estimate of the BOLD response was the t-statistic for the regressor corresponding to each individual trial. The t-statistic provides a more sensitive measure than beta values when searching for information within the brain (Misaki et al., 2010) and downweights noisy voxels, allowing them to have a smaller influence on results. Trialwise response estimates were extracted from our regions of interest (ROIs) averaged within each ROI and submitted to further analysis.

#### **1.2.2.4 ROIs**

The ROIs for the present analysis are the same ones used in a previous study from our lab investigating interactions among PM regions (Cooper et al., 2021a). The ROIs were created using a combination of cortical ROIs from the ‘Default A’ and ‘Default C’ subnetworks from the Schaefer Atlas (Schaefer et al., 2018) and a hippocampal ROI from

a probabilistic parcellation (Ritchey et al., 2015). These anatomical ROIs were combined with a meta-analytic map generated using *Neurosynth* (Yarkoni et al., 2011) using the search term “episodic”. Functional peaks from this map within regions of the PM network were selected and ROIs were drawn around these peaks such that they were of equal size and each contained 100 contiguous voxels. These ROIs were additionally constrained to the left hemisphere because cortical memory retrieval effects are often found to be strongest in the left hemisphere of the brain, which was also evident in the meta-analytic map used to create the ROIs. The final set of ROIs included the posterior hippocampus (pHipp), the parahippocampal cortex (PHC), the retrosplenial cortex (RSC), the precuneus (Prec), posterior cingulate cortex (PCC), posterior angular gyrus (pAG), anterior angular gyrus (aAG), and the medial prefrontal cortex (MPFC). We previously examined the functional connectivity of these ROIs in an independent dataset (Cooper et al., 2021a). In a community detection analysis, we found evidence for subnetwork organization of the PM network, including a ventral PM subnetwork including RSC, PHC, and pAG and a dorsal PM subnetwork including the MPFC, pHipp, Prec, PCC, and aAG. Although there exist multiple possible subnetwork organizations of the PM network, we were motivated by these previous findings to examine a ventral-dorsal subnetwork architecture. We additionally note that this subnetwork grouping appears to align with correlations among the ROIs observed in the current dataset (see **Table 1**).

#### **1.2.2.5 Multilevel Structural Equation Modeling**

The present study took a multilevel structural equation modeling (SEM) approach to investigate functional heterogeneity in the PM network. Multilevel SEM allows for the estimation of latent constructs and for modeling of structural paths amongst those latent

constructs in datasets that have a nested structure. This approach is optimal for the current dataset that contains observations of ROI activity across trials that are nested within subjects. In our data, trials are the level-1 units and subjects are the level-2 units. Because of the nested structure, the data have two sources of variation: one due to the difference between trials within subjects and the other due to the difference between subjects. For the neural data, the former represents where the BOLD response estimate (i.e., the t value) is relative to that subject's own average across all trials and the latter represents where each subject's average t value compared to other subjects' average t values. Our primary interest was in modeling within-subject, trial-to-trial variability. The between-subject variability in the neural data could represent meaningful differences in individual characteristics, but we did not have *a-priori* hypotheses about these individual differences in the present sample. Therefore, in the multilevel model for the neural data (see below), the between-subject model is specified only so that this source of variability is accounted for and therefore the statistical validity of the within-subject model is not compromised. For the behavioral data, the two sources of variation represent differences in overall memory quality on a trial-to-trial basis and differences in overall accuracy across trials on a subject-to-subject basis.

All modeling was performed using *Mplus* software version 8.2 (Muthén & Muthén, 1997-2017). Models were determined to have acceptable levels of model fit if they displayed the following fit indices: root mean squared error of approximation (RMSEA) < .06, comparative fit index (CFI) > .95, and a standardized root mean squared residual (SRMR) < .08 (Hu & Bentler, 1999). For SRMR, a separate index was calculated for the within cluster (i.e., within subject) and between cluster (i.e., between

subject) levels. I also report two information criterion per model to assist with model selection: Akaike information criterion (AIC) and the Bayesian information criterion (BIC). These criteria indicate the relative quality of model fit between candidate models. The model with the smaller AIC/BIC value indicates a better fitting model. The models were estimated using the MLR (maximum likelihood with robust standard errors) and the WLSMV (weighted least squares means and variances adjusted) estimators in *Mplus*. The cutoff values cited above are ones that are commonly applied in the SEM literature. We note that these values were originally determined based on simulations of SEMs on continuous variables estimated using a maximum likelihood estimator, whereas our behavioral data contains binary variables and all of our models that contain the behavioral variables use the WLSMV estimator. A recently published report by Xia and Yang (2019) suggests that models fit on categorical data using an estimator similar to *MPlus*' WLSMV estimator may be overly optimistic when using traditional fit index cutoffs. In the absence of alternative model fit thresholds, we interpret our results with respect to traditional model fit index thresholds. We do, however, use caution and carefully examine all statistics available to make a judgment with respect to model fit. For a summary of all of the models fit in the current manuscript, see **Supplemental Table 1**.

#### 1.2.2.5.1 Preliminary Analyses

Prior to performing our multilevel SEM analysis, we verified the necessity of a multilevel analysis by calculating intraclass correlations (ICCs) for each of our variables of interest and by fitting a “null” model designed to test if there is any structure in the between-subjects covariance matrix (see Jak et al., 2013). The ICC is a statistic that

reflects the proportion of variance of a variable that can be attributed to individual differences amongst our subjects. Datasets that contain variables that have ICCs close to 0 will not see an additional benefit from multilevel modeling. In the null model, a saturated (i.e., a model that estimates parameters for all possible variances and covariances amongst variables) was specified for the within-subject covariance structure, and a *null* model in which all the variances and covariances are constrained to be zero was specified for the between-subject covariance structure. If this model fails to satisfactorily fit the data, it suggests that the between-subject variances need to be allowed in the model and therefore calls for a two-level model. If the ICCs are greater than 0.1 or the null model fits the data poorly, we will conclude that multilevel modeling is required for our dataset.

#### 1.2.2.5.2 Measurement Models

After verifying the necessity of multilevel modeling, we examined the measurement structure underlying our eight ROIs. We tested two measurement models: a single-factor model for the integrated PM network hypothesis and a two-factor model for the two subnetworks hypothesis. In the single-factor model, the eight PM network regions loaded onto a single latent factor at the within-subject level. We did not impose any restriction at the between-subject level because we did not have a-priori hypotheses about the nature of the between-subject variability in neural data. In the two-factor model, RSC, PHC, and pAG loaded on one factor representing the ventral posterior medial network (vPMN), and MPFC, pHipp, Prec, PCC, and aAG loaded on the other factor representing the dorsal posterior medial network (dPMN) (see **Figure 2**). Again,

we did not impose any restriction at the between-subject level. For the measurement models for neural data, the MLR estimator was used.

We next fit a two-level categorical factor model to the behavioral data. This model contained a single latent factor that loaded onto each of our memory measures (i.e., scene position memory, object color memory, and sound valence memory). We placed restrictions on this model such that it had cross-level metric invariance – the factor loadings for level 1 (i.e., within-subjects, across trials) of the model were set equal to the corresponding factor loadings for level 2 (i.e., between-subjects, across subjects) of the model. These restrictions were placed on the model for two reasons. First, the cross-level metric invariance model facilitates the interpretation of the latent construct at both levels as being the within-subjects and between-subjects components of the same underlying construct. In this context, the level 1 latent variable represents overall memory for each episode whereas the level 2 latent variable represents participant’s overall memory ability. Second, the cross-level metric invariance model limits the number of free parameters in the model, avoiding possible estimation problems common to overparameterized models (see Jak, 2019). Because the behavioral variables were binary, the WLSVM estimator in MPLUS was used to estimate this model. This behavioral model with cross-level metric invariance was then stitched together with the neural model to form our final measurement model.

#### 1.2.2.5.3 Structural Models

After establishing good-fitting measurement models, the neural and behavioral models were stitched together to form a single model (see **Figure 2**). We subsequently fit a series of models to the data to quantify the contribution of the PM network (or PM

subnetworks) to memory quality and whether any of the regions made a region-specific contribution to memory quality over and above their network (or subnetwork) contribution. For these models, the WLSMV estimator was used. The baseline structural model contained a structural path from the PM Network (or PM subnetworks) latent variable(s) to the memory quality latent variable at the within-subjects level. After fitting the baseline model, a series of models were fit to test for region-specific contributions (i.e., one at a time). Each of these models included an additional structural path from the region to memory quality. This direct path reflects the predictive effect of the region after accounting for its participation in the network (or subnetwork). In a secondary set of analyses, we examined paths between the neural variables and memory outcomes for each individual event feature, allowing memory features to covary but removing the latent variable for overall memory quality.

	mean	sd	min	max	ICC	Correlations										
						RSC	PHC	pAG	aAG	pHipp	Prec	PCC	MPFC	SCENE	COLOR	
RSC	0.049	0.170	-0.567	0.808	0.138											
PHC	-0.028	0.181	-0.763	1.048	0.155	0.324										
pAG	-0.007	0.315	-1.292	1.232	0.138	0.296	0.330									
aAG	0.188	0.352	-1.346	1.648	0.184	0.296	0.119	0.295								
pHipp	0.077	0.156	-0.614	1.182	0.022	0.191	0.184	0.135	0.276							
Prec	0.116	0.215	-0.923	0.971	0.123	0.326	0.265	0.247	0.356	0.285						
PCC	0.144	0.218	-0.614	1.044	0.142	0.282	0.173	0.189	0.418	0.283	0.410					
MPFC	0.135	0.279	-1.176	1.308	0.036	0.162	0.101	0.066	0.342	0.285	0.282	0.402				
SCENE	0.675	0.468	0.000	1.000	0.205	0.194	0.130	0.086	0.050	0.051	0.094	0.055	-0.026			
COLOR	0.724	0.447	0.000	1.000	0.135	0.070	0.046	0.024	0.046	0.032	0.081	0.061	-0.033	0.251		
SOUND	0.758	0.429	0.000	1.000	0.118	0.091	0.070	0.034	0.039	0.066	0.099	0.078	0.021	0.229	0.170	

**Table 1: Descriptive Statistics for Variables of Interest.** Neural measures (RSC-MPFC) are the mean t-value across all voxels within that ROI from the single-trial estimation step. Behavioral measures (SCENE, COLOR, SOUND) are binary, coded such that 1 = correct and 0 = incorrect. Correlations between neural measures are Pearson's Correlation Coefficients. Correlations between the behavioral and neural variables are Point-Biserial Correlations Coefficients. All descriptive statistics, excluding the ICCs, were calculated ignoring the nested structure. Correlation values are highlighted such that greens indicate positive values and reds indicate negative values. pHipp = posterior hippocampus, Prec = precuneus, PCC = posterior cingulate cortex, MPFC = medial prefrontal cortex, PHC = parahippocampal cortex, RSC = retrosplenial cortex, aAG = anterior angular gyrus, pAG = posterior angular gyrus, SCENE = Scene Position Correct, COLOR = Object Color Correct, SOUND = Sound Valence Correct, sd = standard deviation, ICC = interclass correlation coefficient.

## 1.3 RESULTS

### 1.3.1 Preliminary Analyses

The ICCs were larger than 0.1 for the neural measures, except for pHipp whose ICC was .022 and MPFC whose ICC was .036. The null model for the neural data did not fit the data well (*Model 1*:  $\chi^2 = 2951.578$ ,  $df = 36$ ,  $p < .001$ , RMSEA = 0.144, CFI = 0.000, SRMR<sub>within</sub> = 0.047, SRMR<sub>between</sub> = 0.352, AIC = -10496.752, BIC = -10221.064). Thus, we concluded that multilevel modeling was appropriate for our neural data. For the behavioral measures, the ICCs ranged from .118 to .205, indicating that about 10 to 20% of the variance in the memory measures are due to between-subjects differences. The null model resulted in adequate fit to the data (*Model 2*:  $\chi^2 = 20.882$ ,  $df = 6$ ,  $p < .01$ , RMSEA = 0.025, CFI = 0.958, SRMR<sub>within</sub> = 0.000, SRMR<sub>between</sub> = 0.634). However, the fit statistics for the behavioral null model were obtained with the WLSMV estimator (because the behavioral memory measures were binary) and applying the same criteria for the WLSMV fit statistics have been shown to be less sensitive to discover model-data misfit (Xia & Yang, 2019). Thus, considering the large ICC values and the limitation in the performance of the WLSMV fit statistics, we concluded that adopting a multilevel model was also appropriate for the behavioral data.

### 1.3.2 Measurement Models

The one factor model for the neural data resulted in the following fit statistics (*Model 3*:  $\chi^2 = 290.442$ ,  $df = 20$ ,  $p < .001$ , RMSEA = 0.059, CFI = 0.905, SRMR<sub>within</sub> = 0.063, SRMR<sub>between</sub> = 0.005, AIC = -12584.469, BIC = -12208.530). The two-factor model fit the data well and better

than the one factor model (*Model 4*:  $\chi^2 = 90.096$ ,  $df = 19$ ,  $p < .001$ ,  $RMSEA = 0.031$ ,  $CFI = 0.975$ ,  $SRMR_{within} = 0.035$ ,  $SRMR_{between} = 0.003$ ,  $AIC = -13145.343$ ,  $BIC = -12763.138$ ). To further compare model fits, we examined the estimated correlation between the two latent factors in the two-factor model and compared the estimated communality values of the two models. We reasoned that additional evidence in favor of the two-factor model would be seen if the correlation between the latent factors was estimated to be low-moderate *and* if the estimated communality values were all equivalent or higher for the two-factor model relative to the one factor model. We note that the correlation between the vPMN and dPMN latent variables was high, but not perfect ( $r = 0.630$  or  $\sim 39.7\%$  of variance shared) and the communality values in the two-factor model were all equivalent or higher compared with the one factor model (see **Table 2**). Taken together, these results suggest that a two-factor model was a better model for the neural data.

	One Factor			Two Factor		
param	est	se	pval	est	se	pval
pHipp	0.188	0.024	< 0.001	0.193	0.025	< 0.001
Prec	0.397	0.039	< 0.001	0.395	0.039	< 0.001
PCC	0.437	0.029	< 0.001	0.479	0.024	< 0.001
MPFC	0.251	0.030	< 0.001	0.286	0.032	< 0.001
PHC	0.177	0.027	< 0.001	0.344	0.030	< 0.001
RSC	0.231	0.036	< 0.001	0.391	0.035	< 0.001
aAG	0.472	0.030	< 0.001	0.485	0.032	< 0.001
pAG	0.215	0.038	< 0.001	0.363	0.036	< 0.001

**Table 2: Communalities Values.** Communalities value estimates from the One Factor and Two Factor measurement models. All of the estimated communalities values are equivalent or higher in the Two Factor model compared with the One Factor model. param = parameter, est = estimate, se = standard error, pval = p value. pHipp = posterior hippocampus, Prec = precuneus, PCC = posterior cingulate cortex, MPFC = medial prefrontal cortex, PHC = parahippocampal cortex, RSC = retrosplenial cortex, aAG = anterior angular gyrus, pAG = posterior angular gyrus.

For the behavioral data, the two-level categorical single factor model with equality constraints on the factor loadings across levels fit the data well (*Model 5*:  $\chi^2 = 0.163$ ,  $df = 2$ ,  $p < .9218$ , RMSEA = 0.000, CFI = 1.00, SRMR<sub>within</sub> = 0.001, SRMR<sub>between</sub> = 0.022). This model has cross-level metric invariance, meaning that the latent variables at each level can be interpreted as the within-subject and between-subject components, respectively, of the same construct “overall memory quality.” Cross-level metric invariance additionally allowed us to calculate the proportion of variance in the overall memory quality factor that is attributable to individual differences and trial-to-trial differences. The memory quality factor had an ICC of .329, meaning that 32.9% of the variability in memory quality comes from individual differences and 67.1% of the variability comes from trial-to-trial differences. This is advantageous for our purposes since our primary interest was explaining trial-to-trial variability in memory quality.

After finding good fitting neural and behavioral measurement models, we proceeded to fit a joint measurement model by stitching the two-factor neural model and the cross-level metric invariance behavioral model together (see **Figure 2**; *Model 6*). At the between subjects level, the regions were allowed to covary with one another and allowed to covary with the between-subject memory quality factor. This joint measurement model fit the data adequately (*Model 6*:  $\chi^2 = 534.782$ ,  $df = 59$ ,  $p < .001$ , RMSEA = 0.046, CFI = 0.974, SRMR<sub>within</sub> = 0.034, SRMR<sub>between</sub> = 0.043). The key parameter estimates for the within-subjects part of this model are reported in **Table 3**. This is the model that we then incorporated into our SEM linking the neural and behavioral variables.

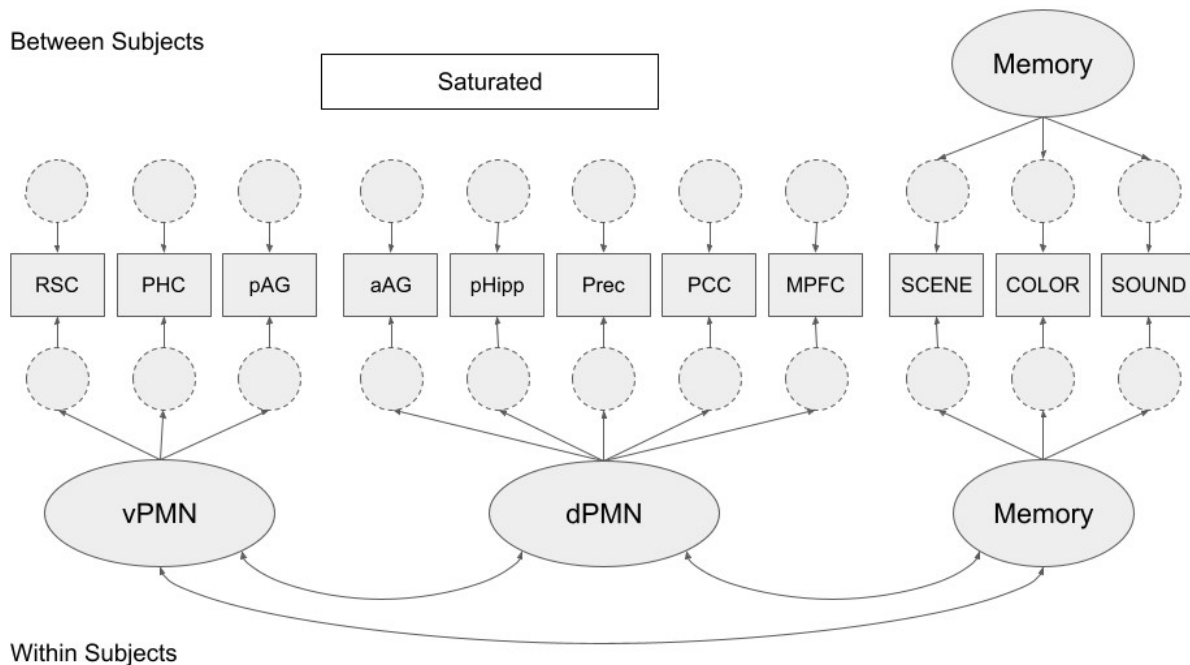


**Figure 2: Measurement Model.** A graphical representation of our combined measurement model including both neural and behavioral variables (Model 6), following the graphing conventions of E. Kim and colleagues (2016). Our measurement model contained two latent variables for the neural data at the within-subjects level, a single latent variable for the behavioral data at the within-subjects level, and a single latent variable representing the behavioral data at the between-subjects level. The factor loadings for the Memory latent variable were set equal across the levels. At the between subject level, the eight neural variables were allowed to covary with one another and with the Memory factor. See **Table 3** for standardized parameters of the within-subjects part of the model. vPMN = ventral posterior medial network, dPMN = dorsal posterior medial network, Memory = overall memory quality, pHipp = posterior hippocampus, Prec = precuneus, PCC = posterior cingulate cortex, MPFC = medial prefrontal cortex, PHC = parahippocampal cortex, RSC = retrosplenial cortex, aAG = anterior angular gyrus, pAG = posterior angular gyrus, Scene = scene position feature correct, Color = object color feature correct, Sound = sound valence feature correct.

paramHeader	param	est	se	pval
vPMN.BY	RSC	0.627	0.006	< 0.001
	PHC	0.567	0.008	< 0.001
	pAG	0.608	0.007	< 0.001
dPMN.BY	MPFC	0.516	0.006	< 0.001
	pHipp	0.437	0.008	< 0.001
	Prec	0.647	0.007	< 0.001
	PCC	0.685	0.004	< 0.001

	aAG	0.711	0.005	< 0.001
Memory.BY	SCENE	0.707	0.057	< 0.001
	COLOR	0.465	0.044	< 0.001
	SOUND	0.460	0.030	< 0.001
dPMN.WITH	vPMN	0.634	0.008	< 0.001
Memory.WITH	vPMN	0.200	0.025	< 0.001
	dPMN	0.102	0.026	< 0.001

**Table 3:** *Measurement Model Standardized Parameter Estimates.* Select standardized parameter estimates in the within-subject level model (Model 6). This table was created using the R package *MplusAutomation* (Hallquist & Wiley, 2018). Parameter headers (paramHeader) follow standard Mplus syntax, where the BY keyword indicates a loading parameter (lambda  $\lambda$ ) and the WITH keyword indicates a covariance parameter (theta  $\theta$ ). param = parameter, est = estimate, se = standard error, pval = p value. See **Figure 2** caption for abbreviations.

### 1.3.3 Structural Models

#### 1.3.3.1 Overall Memory Quality Models

We next estimated a series of structural models to tease apart network and region-specific contributions to overall memory. In the first model (*Model 7*), each of the two subnetworks was allowed to have a structural path to overall memory quality. In this baseline model, the vPMN uniquely (i.e., when statistically controlling for the dPMN) predicted the overall quality with which events were remembered while the dPMN did not (see **Figure 3**). When modeled separately, however, both the vPMN ( $\beta = 0.190$ ,  $S.E. = 0.021$ ,  $p < 0.001$ ) and the dPMN ( $\beta = 0.170$ ,  $S.E. = 0.022$ ,  $p < 0.001$ ) predicted Memory Quality (i.e., in models that included only one of the two paths). Models estimating region-specific contributions to overall memory quality are depicted in **Figure 3** and structural path parameter estimates for these models are reported in **Table 4**. Of the PM network regions, only the MPFC displayed a statistically significant region-specific ability to predict Memory Quality when controlling for its participation in its PM subnetwork (see **Table 4**;  $\alpha = 0.05$ , FWE corrected for multiple comparisons). Inspection of

the parameter estimates from this alternate model (*Model 07<sub>MPFC</sub>*) suggests that the MPFC had a negative relationship with Memory Quality when controlling for its participation in the dPMN. The absence of other region-specific effects suggests that the contributions of the other PM regions were well described by the subnetwork level effects.

Title	paramHeader	param	est	se	pval
Model 07 <sub>pHipp</sub>	MEMQ.ON	PHIPP	0.059	0.030	0.048
Model 07 <sub>Prec</sub>	MEMQ.ON	PREC	0.110	0.045	0.016
Model 07 <sub>PCC</sub>	MEMQ.ON	PCC	0.066	0.081	0.420
Model 07 <sub>MPFC</sub>	MEMQ.ON	MPFC	-0.158	0.037	< 0.001
Model 07 <sub>PHC</sub>	MEMQ.ON	PHC	0.097	0.090	0.282
Model 07 <sub>RSC</sub>	MEMQ.ON	RSC	0.026	0.045	0.575
Model 07 <sub>aAG</sub>	MEMQ.ON	AAG	0.047	0.057	0.415
Model 07 <sub>pAG</sub>	MEMQ.ON	PAG	-0.063	0.051	0.218

**Table 4:** *Key Parameter Estimates from Region-Specific Models.* The table reports the key parameter estimates for the family of models delineating region-specific contributions. This table was created using the R package *MplusAutomation* (Hallquist & Wiley, 2018). Parameter headers (paramHeader) follow standard Mplus syntax, where the ON keyword indicates a path parameter ( $\beta$ ). param = parameter, est = estimate, se = standard error, pval = p value. See **Figure 2** caption for abbreviations. Listed p values are uncorrected for multiple comparisons.

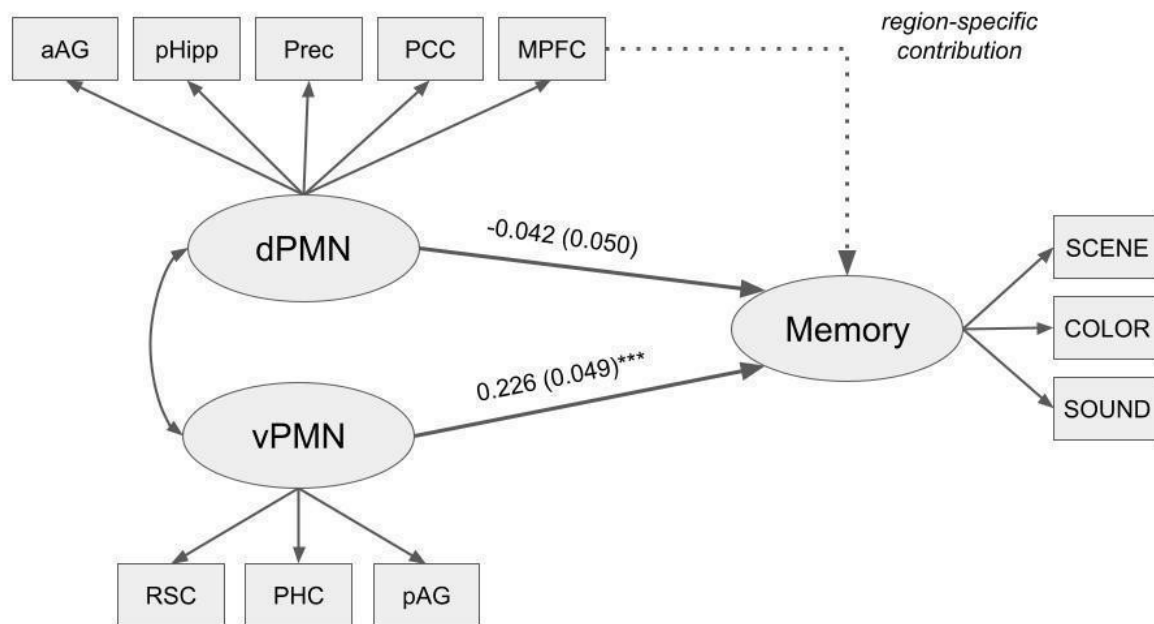


**Figure 3: Path Diagram.** Path diagram representing the within-subject level of our two-level baseline model (i.e., Model 7) with standardized parameter estimates (standard error in parentheses). The dotted line depicts the additional region-specific contribution path added in the region-specific family of models detailed in **Table 4**. See **Figure 2** caption for abbreviations. \* =  $p < .05$ , \*\* =  $p < .01$ , \*\*\* =  $p < .001$ .

### 1.3.3.2 Memory Feature Models

Our primary aim was to examine the region-specific and network-level contributions of PM regions to overall memory quality during retrieval. Our experimental design, however, also afforded us the opportunity to examine their contributions to the retrieval of different memory features (i.e., scene perspective, object color, sound valence). To examine this, we updated our joint measurement model so that the behavioral measures simply covaried with one another instead of loading onto a common factor. This updated measurement model fit the data well (*Model 8*:  $\chi^2 = 683.198$ ,  $df = 37$ ,  $p < .001$ ,  $RMSEA = 0.067$ ,  $CFI = 0.965$ ,  $SRMR_{within} = 0.030$ ,  $SRMR_{between} = 0.000$ ). Using this measurement model, we then fit a series of structural models to examine the network-level and region-specific contributions to each of the features of our events (see **Figure 3**). Key parameter estimates from this family of models can be found in **Table 5**.

The baseline model (*Model 9*; see **Figure 4**) suggests that there were statistically significant network-level contributions of the vPMN and the dPMN to scene feature memory, such that the vPMN contributed positively to scene memory whereas the dPMN contributed negatively. No other network-level effects were statistically significant, although it is worth noting that in contrast to its negative relationship with scene memory, the dPMN trended toward positive relationships with sound memory. Interestingly, the parameter estimates for the covariances amongst the residuals of the behavioral variables suggest that there remains a joint “holistic” remembering property that is not explained by PM network activity (see **Supplemental Table 2** for a full table of model parameters). The results from a family of models containing region-specific paths from each region to each memory feature (see **Figure 4, Table 5**) suggest that the MPFC made a region-specific negative contribution to object color memory. No other regions made a region-specific contribution after controlling for family-wise error using a Bonferroni correction.

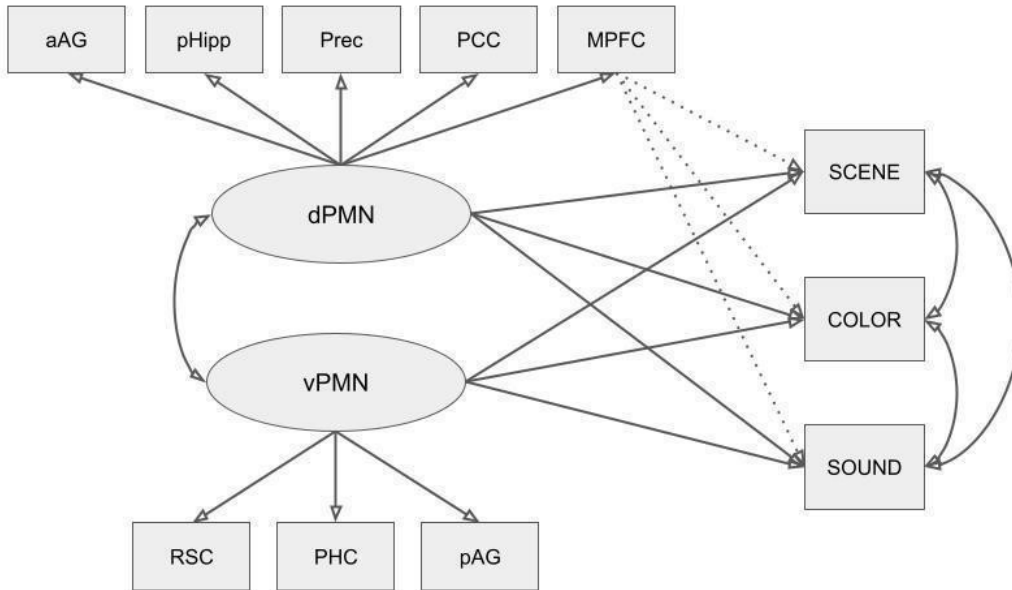


**Figure 4: Memory Feature Model Path Diagram.** Path diagram representing our feature specific memory model (Model 9) capturing network-level and region-specific contributions to feature memory. The baseline model contained paths from each subnetwork latent variable to each memory feature (i.e., 6 in total, solid lines). The region-specific models contained all of the paths from the baseline model with the addition of paths from a single region to each memory feature (i.e., 3 additional paths, dotted lines), iterated across the entire set of regions. See **Table 5** for parameter estimates.

Model	paramHeader	param	est	se	pval
Model 9	COLOR.ON	VPMN	-0.004	0.047	0.933
	COLOR.ON	DPMN	0.041	0.050	0.417
	SOUND.ON	VPMN	0.006	0.043	0.882
	SOUND.ON	DPMN	0.114	0.059	0.052
	SCENE.ON	VPMN	0.277	0.043	0.000
	SCENE.ON	DPMN	-0.147	0.040	0.000
Model 9 <sub>pHIPP</sub>	COLOR.ON	PHIPP	0.015	0.024	0.544
	SOUND.ON	PHIPP	0.038	0.032	0.234
	SCENE.ON	PHIPP	0.045	0.033	0.163
Model 9 <sub>PREC</sub>	COLOR.ON	PREC	0.073	0.049	0.135

	SOUND.ON	PREC	-0.001	0.040	0.971
	SCENE.ON	PREC	0.061	0.087	0.485
Model 9 <sub>PCC</sub>	COLOR.ON	PCC	0.026	0.050	0.600
	SOUND.ON	PCC	0.014	0.078	0.863
	SCENE.ON	PCC	0.083	0.126	0.511
Model 9 <sub>MPFC</sub>	COLOR.ON	MPFC	-0.096	0.027	0.000
	SOUND.ON	MPFC	-0.040	0.036	0.272
	SCENE.ON	MPFC	-0.089	0.038	0.020
Model 9 <sub>PHC</sub>	COLOR.ON	PHC	0.012	0.105	0.907
	SOUND.ON	PHC	-0.004	0.094	0.966
	SCENE.ON	PHC	0.052	0.046	0.261
Model 9 <sub>RSC</sub>	COLOR.ON	RSC	-0.027	0.055	0.616
	SOUND.ON	RSC	0.008	0.043	0.847
	SCENE.ON	RSC	0.062	0.046	0.177
Model 9 <sub>PAG</sub>	COLOR.ON	PAG	0.025	0.060	0.674
	SOUND.ON	PAG	-0.004	0.037	0.923
	SCENE.ON	PAG	-0.079	0.033	0.016
Model 9 <sub>AAG</sub>	COLOR.ON	AAG	0.013	0.066	0.845
	SOUND.ON	AAG	-0.056	0.053	0.285
	SCENE.ON	AAG	0.047	0.089	0.596

**Table 5: Memory Feature Models: Parameter Estimates.** Key parameter estimates from a family of memory feature specific models. Statistically significant path estimates that survive a Bonferroni correction are highlighted in yellow. This table was created using the R package *MplusAutomation* (Hallquist & Wiley, 2018). Parameter headers (paramHeader) follow standard Mplus syntax, where the ON keyword indicates a path parameter from the variable listed in the “param” column to variable listed in the “paramHeader” column. param = parameter, est = standardized estimate, se = standard error, pval = p value. See **Figure 2** caption for abbreviations. See **Figure 4** for path diagram. Listed p values are uncorrected for multiple comparisons.

## 1.4 SUMMARY

In Chapter 1, I examined heterogeneity in the function of the default mode network using a multilevel SEM framework. Supporting prior work, my measurement models indicated that a two-factor model with latent factors representing ventral and dorsal subnetworks was the better model for trialwise responses estimates than a single-factor model grouping all default mode regions together. My structural models indicated that the contributions of individual regions of the default mode network to memory quality are largely subsumed by subnetwork-level contributions, apart from the MPFC which made a unique, region-specific contribution to memory quality. Interestingly, the region-specific contribution of the MPFC was found to be negative, such that less MPFC activation (when controlling for subnetwork membership) was associated with more accurate recollections. Feature-specific analyses revealed that the dissociation between vPMN and dPMN was driven largely by their distinct contributions to memory for scene information, compared with object color or sound valence information. Together, these results reveal new insights into how memory outcomes can be explained by a combination of network-level and region-specific factors. I discuss these findings further and their implications for the neural organization of memory in the **Discussion**.

The current set of analyses was able to capture variability at multiple levels (i.e., across trials and across subjects) across two domains (i.e., brain and behavior). This was a major strength of the current study and is something that has rarely been done in the cognitive neuroscience of memory. Unfortunately, due to a relatively small sample size at the across subjects level ( $n = 28$ ), we were hesitant to draw strong conclusions about how default mode subnetwork function across subjects relates to individual differences in episodic memory ability. The next two chapters of this dissertation seek to address this level of analysis by using a higher-

powered cognitive neuroscience dataset (Chapter 2) and by running a behavioral study (Chapter 3).

## CHAPTER 2

### 2.1 OVERVIEW

Have you ever spoken with a family member about an event that happened long ago and admired the level of detail with which they could recall the event? While important differences exist at the extreme ends of the spectrum of memory ability, such as in patients with hippocampal damage (e.g., Patient H.M. Corkin, 2002) or in individuals with superior autobiographical memory (LePort et al., 2012; Parker et al., 2006), experiences like these reinforce that there is substantial variation within the neurotypical population in the ability to recall the details of past events. Interestingly, little is known about the brain processes that explain such individual differences within the healthy young adult population. As reviewed in the **Introduction**, one brain process that has been shown to be related to individual differences in cognition is the functional communication and connectivity of remote brain regions. The goal of Chapter 2 is to investigate the relationship between brain connectivity and memory ability found within the healthy adult population.

Episodic memory has been linked to the default mode network (DMN), a set of brain regions that tend to be co-activated during rest and during tasks involving episodic construction (Buckner & DiNicola, 2019; Ritchey & Cooper, 2020). In particular, memory tasks have been shown to recruit a ventral subnetwork of the DMN that is strongly interconnected with the medial temporal lobes (Andrews-Hanna et al., 2010; Barnett et al., 2021; Buckner & DiNicola, 2019). This DMN subnetwork, which has been labeled DMN-C in recent parcellations of the DMN (Schaefer et al., 2018; Yeo et al., 2011), consists of the retrosplenial cortex,

parahippocampal cortex, and the posterior angular gyrus. The DMN-C is commonly co-activated with an adjacent, more dorsal DMN subnetwork, labeled DMN-A, which consists of medial frontal and parietal regions. Recent work has shown that these two subnetworks are dissociable in terms of their functional connectivity during event perception (Cooper et al., 2021b) as well as their contributions to memory retrieval (Kurkela et al., 2022a). In the latter study, when both ventral and dorsal DMN regions were included in a model, only the ventral regions significantly predicted retrieval success (Kurkela et al., 2022a). Based on these findings, I hypothesize that the functioning of the DMN-C subnetwork may be central in determining individual differences in episodic memory ability. Specifically, I believe that the functional connectivity of this subnetwork may be crucial for determining an individual's memory ability.

The goal of Chapter 2 is to build upon previous efforts to elucidate the relationship between episodic memory ability and the intrinsic functional brain connectivity by coupling a series of hypothesis-driven analyses with a data-driven predictive modeling analysis. First, I examined whether connections within the DMN-C subnetwork (within-network), between the DMN-C and DMN-A subnetworks (between-network), and between DMN-C and other brain regions (extra-network) were predictive of individual differences in memory ability. I also examined whether hippocampal connections were predictive of memory ability given extensive evidence linking the hippocampus to memory. Second, I examined the entire functional connectome using connectome based predictive modeling (CBPM; Shen et al., 2017) -- a data-driven approach that determined if there were any patterns of whole-brain connectivity that were predictive of memory ability.

## 2.2 METHODS

To answer our research questions, we analyzed data from the Cambridge Center for Aging and Neuroscience (CamCAN) repository (available at <http://www.mrc-cbu.cam.ac.uk/datasets/camcan/>; Taylor et al., (2017), Shafto et al., (2014)). The CamCAN repository is a large-scale, cross-sectional, openly available cognitive neuroscience dataset collected by the University of Cambridge. Below we summarize the key characteristics of the CamCAN dataset, focusing specifically on the subsets of the dataset that were utilized in the present report. Analysis plans were preregistered on the Open Science Framework: [https://osf.io/9xcu3/?view\\_only=1ac6856b773249cfa0767dd3d005a9ae](https://osf.io/9xcu3/?view_only=1ac6856b773249cfa0767dd3d005a9ae).

### 2.2.1 Participants

Participants included 243 participants between the ages of 18 and 50 sampled from the original set of 653 CamCAN participants who had data available at the time of our access. Participants in the original set were equally sampled from each decile of age from 18-87 years of age with approximately equal numbers of men and women in each decile. They were required to be cognitively healthy, to not have a serious psychiatric condition, to have met hearing and English language requirements for experiment participation, and to be eligible for MRI scanning (Shafto et al., 2014). Of the 653 subjects, 7 were missing at least one of the five MRI scans (see “2.2.2 MRI Data”), 1 was missing data from Logical portion of the Wechsler Memory Scale, 341 were missing data from the Emotional Memory data, 19 were missing Cattell Fluid Intelligence scores, and 1 subject was missing ACE-R data (see **2.2.4 Behavioral Data**). To deal with

missing data, we took a listwise deletion approach such that if a participant was missing any of the variables of interest, they were removed from further analysis.

Participants were excluded from the current set of analyses if they met the following exclusion criteria. First, participants were excluded from the analysis if they had 2 or more functional runs that had a mean framewise displacement greater than 0.3mm, to mitigate the effects of motion on functional connectivity estimates. Second, participants were excluded from the analysis if they were older than 50 years of age to mitigate the influence of advanced aging on our results. After applying these additional exclusion criteria, we were left with 243 subjects to analyze. These 243 subjects were on average 36.28 years old and 123 self-reported as female and 122 as male.

### **2.2.2 MRI Data**

The subset of the CamCAN dataset analyzed in the present report contained a single high resolution T1-weighted anatomical scan, three functional scans, and a single field map to correct for magnetic field inhomogeneities. The three functional scans included a movie-watching scan, a resting-state scan, and a sensorimotor scan (detailed below). The anatomical and field map images were used during the preprocessing of the functional scans. The three functional scans were used to estimate each subject's intrinsic functional connectome (see **2.3.3 Functional Connectivity**). The anatomical scan was acquired using a Magnetization Prepared Rapid Gradient Echo (MPRAGE) sequence with the following parameters: Repetition Time (TR) = 2250 ms; Echo Time (TE) = 2.99 ms; Inversion Time (TI) = 900 ms; flip angle = 9 degrees; field of view (FOV) = 256mm x 240mm x 192mm; voxel size = 1mm isotropic; GRAPPA acceleration factor = 2; acquisition time of 4 min and 32 sec. The movie watching scan involved participants

watching an edited version of Alfred Hitchcock's movie "Bang, You're Dead". A total of 193 volumes were acquired using a multi-echo, T2\*-weighted EPI sequence (TR =2470 milliseconds, five echoes [TE =9.4 milliseconds, 21.2 milliseconds, 33 milliseconds, 45 milliseconds, 57 milliseconds], flip angle =78 degrees, 32 axial slices of thickness of 3.7 mm with an interslice gap of 20%, FOV =192mm × 192 mm, voxel-size =3 mm × 3mm × 4.44 mm) with an acquisition time of 8 minutes and 13 seconds. The resting-state scan involved participants resting in the scanner with their eyes closed. During the sensorimotor scan, participants were presented with visual checkerboards and auditory tones, either in isolation or simultaneously. They were instructed to respond with a button press when they were presented with any stimuli (either visual, auditory, or both visual and auditory). The resting state and sensorimotor scans had the same scanning parameters: a total of 261 volumes were acquired, each containing 32 axial slices acquired in descending order, slice thickness of 3.7 mm with an interslice gap of 20%; TR = 1970 ms; TE = 30 ms; flip angle = 78 degrees; FOV =192 mm × 192 mm; voxel-size = 3 mm × 3 mm × 4.44 mm) and an acquisition time of 8 min and 40 sec. The fieldmap consisted of an SPGR gradient-echo sequence with the same parameters as the resting state and sensorimotor tasks, but with two TEs (5.19 ms and 7.65 ms).

### **2.2.3 Regions of Interest**

Regions of interest (ROIs) were taken from the Schaefer cortical parcellation (Schaefer et al., 2018). Specifically, we used the 400-area resolution, 17-network parcellation. We focused our analyses *a-priori* on three sets of parcels from this atlas: DMN-C regions (number of parcels: left hemisphere = 7, right hemisphere = 6), DMN-A regions (number of parcels: left hemisphere = 18, right hemisphere = 16), and all other regions (number of parcels: left hemisphere = 176,

right hemisphere = 178). DMN-C regions consisted of the bilateral parahippocampal gyrus, bilateral retrosplenial cortex, and the bilateral posterior angular gyrus (see **Figure 5a**, blue regions). DMN-A regions included the bilateral posterior cingulate cortex, the bilateral precuneus, the bilateral medial prefrontal cortex, the bilateral anterior angular gyrus, and a bilateral section of the dorsal prefrontal cortex (see **Figure 5a**, yellow regions). We focused on regions in the DMN-C and DMN-A networks due to their roles in episodic memory and simulation (Buckner & DiNicola, 2019; Ritchey & Cooper, 2020). To supplement this cortical atlas, we included hippocampal ROIs created using the anatomical delineations from Ritchey and colleagues (2015). Specifically, we used hippocampal ROIs comprising the hippocampal head, the hippocampal body, and the hippocampal tail from the right and left hemispheres. These six hippocampal ROIs were added to the 400 cortical ROIs to form the functional connectome (i.e., 406x406 ROI-to-ROI connectivity matrix).

#### **2.2.4 Behavioral Data**

Summary statistics for the behavioral and neural variables of interest are presented in **Table 6**. Behavioral data included performance on the following cognitive assessments: the logical memory subtest from the Wechsler Memory Scale Third UK edition (Wechsler, 1999), the Addenbrook Cognitive Examination-Revised (variable name: ACER), and the Cattell Test of Fluid Intelligence (variable name: Cattell). The logical memory subtest from Wechsler Memory Scale involved having participants read two short passages and subsequently verbally recall as many story details as possible at two different time points: first immediately after reading the short passages and then again after a ~20 min delay. Verbal recalls were scored for the number of story details correctly recalled at each point in time. The number of story details recalled at

both points in time were averaged together to form a memory ability index (variable name: “memory”). The Addenbrook Cognitive Examination-Revised is a standardized cognitive battery originally designed for dementia screening. The battery is designed to test participants’ ability in 5 different cognitive domains, including attention, memory, fluency, language, and visual-spatial. The total score on this battery was used as an index of general cognitive functioning. The Cattell Test of Fluid Intelligence is a timed pen and paper task where participants are required to solve a series of non-verbal puzzles. Here we use the total score on this task as a general index of fluid intelligence.

Variable	mean	min	max	sd	n	Correlations								
						memory	Age	Sex	Cattell	ACER	fd	within	between	extra
memory	15.28	2.50	23	3.50	243									
Age	36.28	18.50	49.83	8.42	243	-0.13								
Sex <sup>a</sup>	0.50	0	1		243	0.14	-0.07							
Cattell	36.35	22	44	4.23	235 <sup>b</sup>	0.35	-0.25	-0.19						
ACER	96.54	74	100	3.63	243	0.40	0.12	0.03	0.39					
fd	0.14	0.05	0.25	0.04	243	-0.10	0.23	0.02	-0.22	-0.14				
within	0.31	0.17	0.50	0.06	243	0.02	-0.21	0.02	0.09	0.04	-0.23			
between	0.15	0.03	0.26	0.05	243	0.04	-0.01	0.09	-0.06	0.03	-0.10	0.53		
extra	-0.02	-0.06	0.02	0.01	243	-0.09	0.14	0.02	-0.06	-0.07	0.14	-0.55	-0.63	
hipp	0.00	-0.03	0.04	0.01	243	-0.10	-0.02	-0.18	0.01	-0.03	-0.07	0.02	-0.19	0.28

<sup>a</sup>Sex was coded such that Female = 1, Male = 0

<sup>b</sup>8 Subjects Missing Cattell Scores

**Table 6:** *Cam Can Key Data Summary.* Statistical summary of data analyzed for Chapter 2. memory = number of story details recalled in the logical portion of the Wechsler Memory task (immediate + delayed)/2, Cattell = total score on the Cattell Test of Fluid Intelligence, ACE-R = total score on the Addenbrook Cognitive Evaluation Revised (ACE-R), fd = mean framewise displacement, within = average functional connectivity estimate for within vPMN connections, between = average functional connectivity estimate for vPMN-dPMN connections, extra = average functional connectivity estimate for vPMN-rest of the brain connections, n = number of complete observations. Correlations were calculated using all available complete pairs of data. All values are rounded to two decimal places where appropriate.

## 2.3 ANALYSIS

### 2.3.1 MRI Quality Control

The quality of the functional MRI data was assessed using the *MRIQC* software package (Esteban et al., 2017). Quality reports generated from this software package were visually inspected for scanner artifacts and motion-related corruption. All scans that had a mean framewise displacement greater than 0.3mm were excluded from further analysis. If subjects had 2 or more scans with a mean framewise displacement greater than 0.3mm, then the subject was excluded from further analysis (see **2.2.1 Participants**). This conservative approach was adopted in order to limit the effects of head motion on functional connectivity measures (see Cooper et al., 2021b for a similar exclusion criterion; Power et al., 2012, 2014).

### 2.3.2 MRI Preprocessing

MRI data were preprocessed using *fMRIPrep* 20.2.0 (Esteban et al., 2018, 2019). Processing steps for the T1w images included correction for intensity non-uniformity, skull stripping, brain tissue segmentation, and volume-based spatial normalization to the ICBM 152 Nonlinear Asymmetrical template version 2009c. Processing steps for the 3 BOLD runs included slice-timing correction, realignment, using the fieldmap to optimize co-registration of the functional images to the anatomical reference image, normalization of the BOLD images to the ICBM 152 Nonlinear Asymmetrical template version 2009c, and the calculation of confounding time-series including basic 6 head-motion parameters (x,y,z translation; pitch, roll, yaw rotation), temporal derivatives and the quadratic terms of the head-motion parameters, noise components

from a principal components analysis based denoising routine (*CompCorr*), framewise displacement, and DVARS. For a much more detailed description of the processing pipeline please refer to **S.3 FMRIprep Boilerplate** which contains the recommended *fMRIprep* boilerplate.

### 2.3.3 Functional Connectivity

Functional connectivity analyses were performed using the *CONN* toolbox (Whitfield-Gabrieli & Nieto-Castanon, 2012) in MATLAB (Inc., 2022). Confounds removed from each voxel's time series included six head motion parameters and their temporal derivatives, up to the first six *aCompCor* components from a combined WM and CSF mask, framewise displacement, and the global signal<sup>1</sup> as calculated by *fMRIprep*. Additional spike regressors were included for any time points that exceeded a FD of 0.6 mm and/or a standardized DVARS of 2. After regression of motion confounds, BOLD data was band-pass filtered with a high-pass filter of 0.008 Hz and a low-pass filter of 0.1 Hz. No additional modeling was performed for the movie-watching and the resting state data. For the sensorimotor task, task-related activations were regressed out of the time series prior to calculation of functional connectivity. Specifically, task related activation was modeled in the sensorimotor task by convolving stick functions placed at stimulus onsets with SPM12's hemodynamic response function using the *CONN* toolbox. ROI-

---

<sup>1</sup> Global signal regression (GSR) was not included in the pre-registered analysis plan. However, since pre-registration, we have been persuaded by recent publications suggesting that GSR optimizes predicting individual differences in behavior from functional connectivity estimates. We report the results without global signal regression in the **S.4 Global Signal Regression**. Note that the results are largely consistent across methods; however, without global signal regression hippocampal connectivity is inversely related to memory ability and the ability of the functional connectome to predict memory ability is substantially weaker.

to-ROI functional connectivity was calculated using the Pearson's correlation coefficient after denoising and task modeling. The ROI-to-ROI intrinsic functional connectivity estimates were created by averaging functional connectomes calculated from all available functional scans, resulting in a measure of “generalized” functional connectivity intrinsic to each individual (Elliott et al., 2019). The resulting ROI-to-ROI intrinsic functional connectomes were then summarized into three terms to test our research hypotheses. *Within* DMN-C connectivity was operationalized as the average of all functional connections among DMN-C nodes in the Schafer (2018) atlas, *between* subnetwork connectivity as the average connectivity between all DMN-C and DMN-A nodes, and *extra* network connectivity as the average of all connections between the DMN-C nodes and all other nodes not contained in DMN-C or DMN-A. See **Figure 5b** for an illustration.

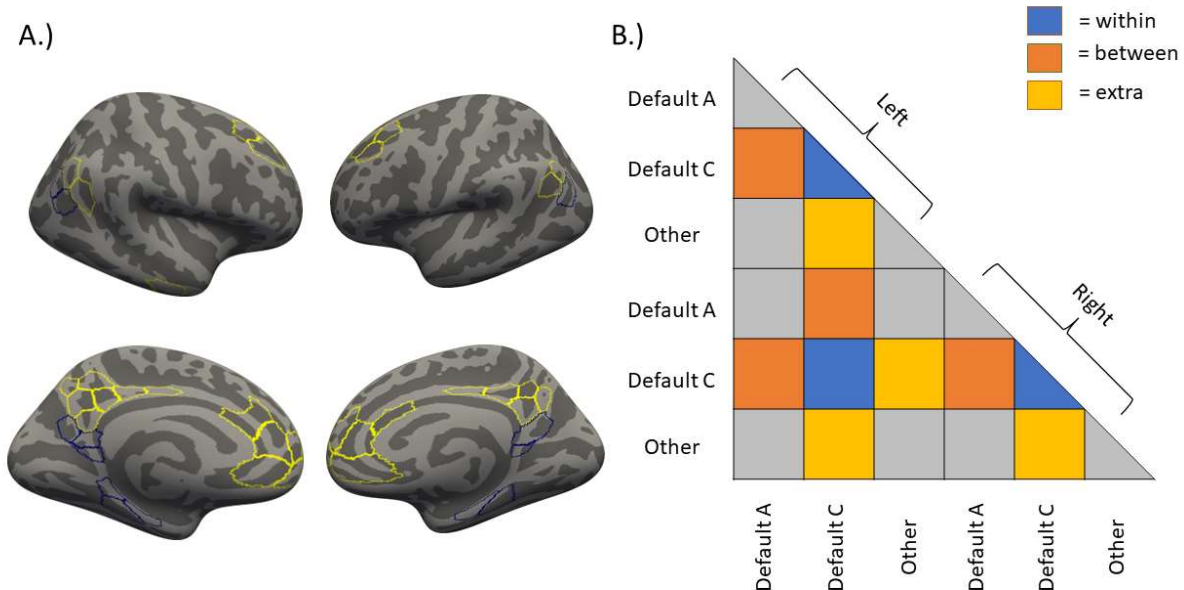


**Figure 5: Regions and Connections of Interest.** A.) Regions of interest were based on the 400 parcel 17-network parcellation from the Schaefer atlas (Schaefer et al., 2018). Here we highlight the DMN-C (blue) and DMN-A (yellow) networks from this atlas. This visualization was created in freeview (citation) using the fsaverage inflated surface template provided in the Schaefer et al. (2018) atlas. B.) The lower triangle of the functional connectome. Connections of interest are highlighted, including “within” connections (blue), “between” connections (orange), and “extra” network connections (yellow) of the DMN-C. Connections of no interest are shown in gray.

### 2.3.4 Connectome Based Predictive Modeling

To complement the hypothesis driven approach described above, the current report used connectome based predictive modeling (CBPM; Shen et al., 2017) to determine if there is any pattern of connections in the functional connectome related to memory ability. CBPM involves calculating a functional connectome for each individual and determining which connections are statistically related to a behavioral variable of interest. All connections that are related to behavior above some arbitrarily defined threshold (e.g., at  $p < .01$ ) are then summarized by separating out connections with a significant positive correlation with behavior from those that have a significant negative correlation with behavior. The connections in the connectome with

significant positive and negative correlations with behavior are then summed into separate positive and negative terms for use in a linear regression predicting behavior. The analysis method then estimates a linear regression using these summed positive and negative connection terms to predict the behavior of a left-out participant in a leave-one-out cross validation procedure. Successful prediction of a behavioral variable using the functional connectome is then determined by correlating the predicted behavioral scores for each participant with the observed behavioral scores with statistical significance determined using a null permutation procedure that reruns the entire analysis a given number of times, each time randomly pairing connectomes with behavioral scores and recording the correlation between predicted and observed behavior. For the current report, all CBPM analyses were performed using a connection selection threshold of  $p < .01$  and the null distribution of correlations between observed and predicted behaviors using 100 null simulations. Statistical significance of the CBPM analysis was determined by estimating the proportion of null simulations that resulted in better predictive performance than the actual analysis. All CBPM analyses were performed using modified analysis code published by Shen and colleagues (2017). To control for nuisance variables, the CBPM analysis code published by Shen and colleagues was modified to use the MATLAB function `partialcorr` when selecting connections used for prediction. See the accompanying GitHub repository for more detail ([https://github.com/memobc/CamCAN\\_IndDifs](https://github.com/memobc/CamCAN_IndDifs)). To determine which connections in the connectome the models were relying on to make their predictions, I also performed computational lesion analyses. In a computational lesion analysis, a predictive model is iteratively fit while excluding a set of features. If model performance is hindered by the removal of a set of features, then it is inferred that the model is relying on these features to make successful out-of-sample predictions.

### 2.3.5 Statistical Modeling

All statistical models, tables, and figures were created using *R* (R Core Team, 2022). All Bayesian regressions were performed in *R* using the *BayesFactor* package (Morey & Rouder, 2021) with interpretations of Bayes Factors made using the *effectsize* package's (Ben-Shachar et al., 2020) *interpret\_bf* function using the interpretation rules originally outlined by Jeffreys (1961). Bayes Factors represent the ratio of evidence in support of one model to evidence in support of a competing model. Bayes Factors equal to 1 represent no evidence for one model over another, Bayes Factors greater than 1 represent relatively more evidence in favor of the null model, and Bayes Factors less than 1 represent relatively more evidence in favor of an alternative model. Bayes Factors between 1 and 3 represent weak or “anecdotal” evidence in favor the null hypothesis, Bayes Factors between 3 and 10 “moderate” evidence in favor of the null hypothesis, and Bayes Factors between 10 and 30 “strong” evidence in favor of the null hypothesis. Similar interpretations can be made for evidence in favor of the alternative hypothesis by taking the inverse of these cutoff values (e.g., “anecdotal” evidence in favor of the alternative indicated by Bayes Factors between 1 and 1/3). Summary tables for the linear regressions were created using a combination of the R packages *gtsummary* (Sjoberg et al., 2021) and *flextable* (Gohel & Skintzos, 2023). All figures were created using the R package *ggplot2* (Wickham, 2016).

## 2.4 RESULTS

### 2.4.1 Hypothesis Driven

*Average intrinsic functional connectivity within the Default C subnetwork does not predict memory ability.* To answer our first research question, I conducted a set of regression

analyses to examine the relationship between memory ability and average within-DMN-C network connectivity. Average intrinsic functional connectivity among DMN-C regions was not related to memory ability ( $\beta = 1.08$ ,  $SE = 3.86$ ,  $t(241) = 0.28$ ,  $p = 0.78$ ; see **Figure 6a**). This pattern did not change after controlling for age, sex, and average framewise displacement ( $\beta = -1.65$ ,  $SE = 3.96$ ,  $t(238) = -0.42$ ,  $p = 0.68$ ) or after also controlling for fluid intelligence and cognitive capacity ( $\beta = -0.99$ ,  $SE = 3.59$ ,  $t(228) = -0.28$ ,  $p = 0.78$ ). Because frequentist linear regression models cannot provide evidence in favor of the null hypothesis, I supplemented these linear regression models with a Bayesian regression model. Specifically, I ran a Bayesian regression model that was analogous to the first model without nuisance regressors (i.e.,  $\text{memory} \sim 1 + \text{within}$ ). This Bayesian regression model suggested that there is moderate evidence in favor of the absence of an effect of DMN-C–DMN-C connectivity on memory ability ( $BF = 6.86$ ).

*Average intrinsic functional connectivity between the Default C and Default A subnetworks does not predict memory ability.* To answer our second research question, we conducted a similar set of regression analyses. Average between-subnetwork connectivity did not predict memory ability on its own ( $\beta = 3.25$ ,  $SE = 4.95$ ,  $t(241) = 0.66$ ,  $p = 0.51$ ; see **Figure 6b**), nor did it predict memory ability when controlling for age, sex, and gross measure of in-scanner movement ( $\beta = 1.63$ ,  $SE = 4.92$ ,  $t(238) = 0.33$ ,  $p = 0.74$ ), nor did it predict memory ability when additionally controlling for fluid intelligence and cognitive capacity ( $\beta = 4.26$ ,  $SE = 4.45$ ,  $t(228) = 0.96$ ,  $p = 0.34$ ). As in the previous set of analyses, we conducted a Bayesian regression analysis to determine the strength of evidence in favor of the null hypothesis. Specifically, we ran a Bayesian regression model (i.e.,  $\text{memory} \sim 1 + \text{between}$ ). This Bayesian regression model

suggested that there is moderate evidence in favor of an absence of an effect of between subnetwork (DMN-C — DMN-A) connectivity on memory ability ( $BF = 5.81$ ).

*Average intrinsic functional connectivity between the Default C subnetwork and all other brain regions does not predict memory ability.* To answer our third research question, we again tested a similar set of regression analyses. The average strength of functional connections from DMN-C regions to regions in networks other than the DMN-A and DMN-C did not predict memory ability on its own ( $\beta = -23.6$ ,  $SE = 16.98$ ,  $t(241) = -1.39$ ,  $p = 0.17$ ; see **Figure 6c**), when controlling for age, sex, and frame displacement ( $\beta = -17.92$ ,  $SE = 17.04$ ,  $t(238) = -1.05$ ,  $p = 0.29$ ), nor when additionally controlling for fluid intelligence and cognitive capacity ( $\beta = -18.92$ ,  $SE = 15.37$ ,  $t(228) = -1.23$ ,  $p = 0.22$ ). To determine the strength of evidence in favor of this null result, we ran a Bayesian regression model (i.e.,  $\text{memory} \sim 1 + \text{extra}$ ). This Bayesian regression model suggested that there was anecdotal evidence against the null hypothesis that extra network connections do not predict memory ability ( $BF = 1/2.86$ ).

*Average intrinsic functional connectivity of the hippocampus does not predict memory ability.* Although not part of my preregistered set of analyses, I decided to look at the relationship between memory ability and intrinsic functional connectivity of the hippocampus given prior research linking this region to individual differences in memory (Touroutoglou et al., 2015; L. Wang, LaViolette, et al., 2010; L. Wang, Negreira, et al., 2010). I set about testing this in a similar manner to our preregistered set of analyses. I found that the average strength of all hippocampal connections was not a significant predictor of memory ability on its own ( $\beta = -27.21$ ,  $SE = 18.09$ ,  $t(241) = -1.5$ ,  $p = 0.13$ ; see **Figure 6d**). This result held when we statistically controlled for age, sex, and framewise displacement ( $\beta = -23.21$ ,  $SE = 18.2$ ,  $t(238) = -1.28$ ,  $p = 0.2$ ), and when we further controlled for fluid intelligence and cognitive capacity ( $\beta = -21.02$ ,  $SE$

= 16.18,  $t(228) = -1.3, p = 0.2$ ). To determine the strength of evidence in favor of this null result, I ran a Bayesian regression model (i.e.,  $\text{memory} \sim 1 + \text{hipp}$ ). This Bayesian regression model suggested that there was anecdotal evidence against the null hypothesis that hippocampal connections do not predict memory ability ( $BF = 1/2.45$ ).

### Targeted Hypotheses

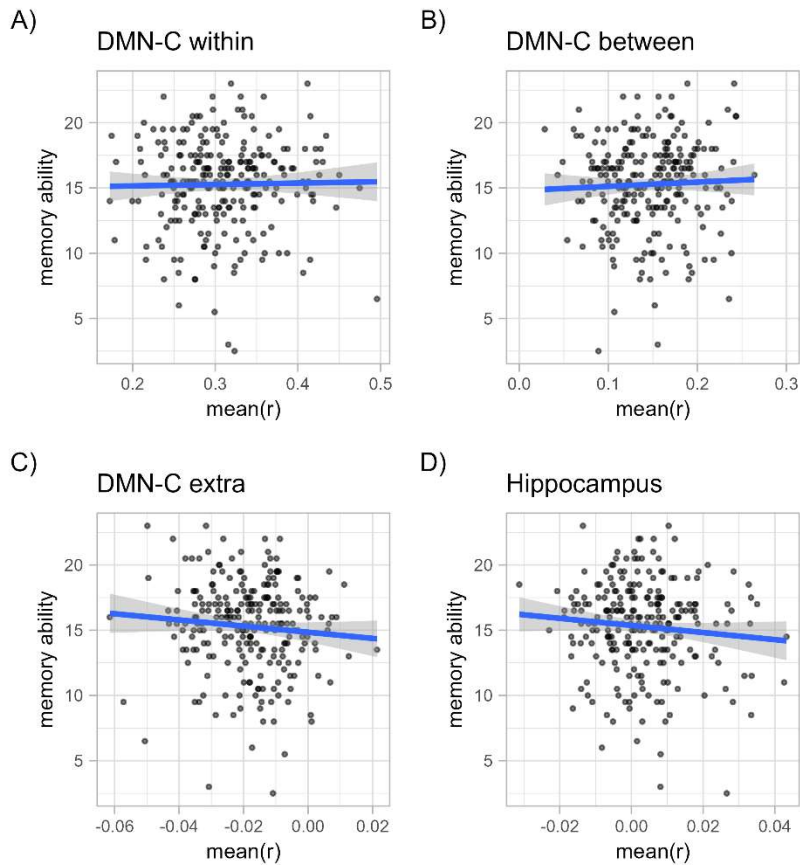


**Figure 6: Targeted Hypotheses.** Scatter plots and best fit linear regression line of memory ability on average intrinsic connection strength A) among DMN-C regions, B) between DMN-C and DMN-A regions, C) DMN-C and all other regions, and D) the Hippocampus and all regions. I found little evidence to suggest that the strength of these connections was predictive of individual differences in memory ability.

### 2.4.2 Data Driven

The intrinsic functional connectome can predict memory ability. This finding appears to be driven by connectivity of the SomMotB network. In a planned exploratory analysis, I ran a

connectome based predictive modeling (CBPM) analysis to see if I could predict memory ability using the entire intrinsic functional connectome. The first analysis—where I used the entire 406 x 406 intrinsic functional connectome to predict memory ability—resulted in a significant correlation between observed and predicted memory ability scores ( $r_{\{\text{observed}, \text{predicted}\}} = 0.164$ ,  $p = 0.027$ ). To ensure that this result was independent of age, sex, and in-scanner motion, I reran the CBPM analysis controlling for these variables when selecting connections to be used for predicting left out subjects (using the MATLAB function `partialcorr`, see Shen et al. 2017). I saw that predictive performance of the intrinsic connectome held when controlling for age, self-reported biological sex, and average framewise displacement ( $r_{\{\text{observed}, \text{predicted}\}} = 0.1498$ ,  $p < 0.01$ ).

To ensure the robustness of this predictive model, I reran the CBPM analysis under a couple of different conditions. First, I tested whether this result held when selecting different connection selection thresholds (see **2.3.4 Connectome Based Predictive Modeling**). In line with previous reports that the CBPM method is robust to selection of threshold (Finn et al., 2015; Jangraw et al., 2018; Shen et al., 2017), rerunning the CBPM analysis controlling for age, sex, and framewise displacement using connection selection thresholds of  $p = [0.001, 0.005, 0.01, 0.5, 0.1]$  had similar outcomes (see **S.5 CBPM Connection Defining Threshold, Supplemental Figure 1**). Next, I examined how combining functional connectomes from different tasks influenced the model. I reran the CBPM analysis on functional connectomes calculated using the movie watching, resting-state, and sensorimotor task scans separately. Models built using functional connectomes from each task individually underperformed compared to the model built using the combined intrinsic functional connectome. Among the three tasks, the model built using functional connectomes from the movie-watching scan was the only one able to predict

memory ability better than chance. Interestingly, models built using resting-state data performed particularly poorly, with almost no relationship between observed and predicted memory ability scores in out of sample data (see **S.6 Combining Data Across Tasks, Supplemental Table 7**).

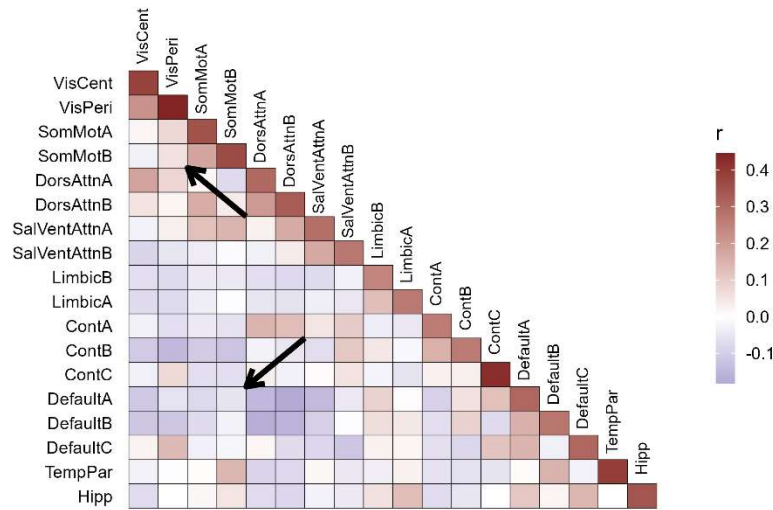
I was further interested in determining which features were driving performance. To figure out which network connections were driving model performance, I ran a computational lesion analysis. In the computational lesion analysis, I reran my CBPM analysis excluding each network from the analysis in turn. Network importance in this computational lesion analysis was determined via a significant drop in model performance with the exclusion of a network and its connections. The results of my computational lesion analyses are reported in **Table 7**. The SomMotB was the only network whose exclusion led to a significant drop in model performance. To further figure out which network connections were driving model performance, I created the matrices depicted in **Figure 7**. First, I looked at the average strength of intrinsic connections (**Figure 7a**) to get a baseline understanding of how different networks communicate with one another in my dataset. I next examined how network connections correlated with memory ability after controlling for age, sex, and average in-scanner motion (**Figure 7b**). Because the CBPM analysis approach selects connections that are statistically significantly correlated with behavior when building the predictive model (see **2.3.4 Connectome Based Predictive Modeling**), I next decided to create the matrices displayed in **Figure 7c,d**. Specifically, I separated connections that were negatively correlated with memory from those that were positively correlated with memory, and I counted the number of connections that were statistically significant at my connection selection threshold of  $p < 0.01$ . I then calculated the difference between the number of statistically significant negatively and positively weighted features (**Figure 7c**). One issue with using a simple count to interpret which connections are driving model performance is that a

count measure may overrepresent the contribution of networks that simply have a larger number of regions and thus a larger number of connections. To combat this possibility, I calculated the proportion of connections between regions that were significantly positively related to memory ability and subtracted away the proportion of connections that were significantly negatively related to memory ability (**Figure 7d**). **Figure 7b-d** reveals that my CBPM model is relying on connections throughout the connectome to successfully predict memory ability in out-of-sample subjects. Connectivity between SomMotB and Default A and connectivity between SomMotB and VisPeri, however, appear to be the primary drivers of model performance given the results of my computational lesion analysis. Closer examination of the grand mean connectivity matrix (see **Figure 7a**) suggests that connectivity between these networks tends to be negative and positive respectively. Thus, it appears that my CBPM model is relying on decoupling between SomMotB and Default A regions and increased coupling of SomMotB and VisPeri regions when making successful model predictions.

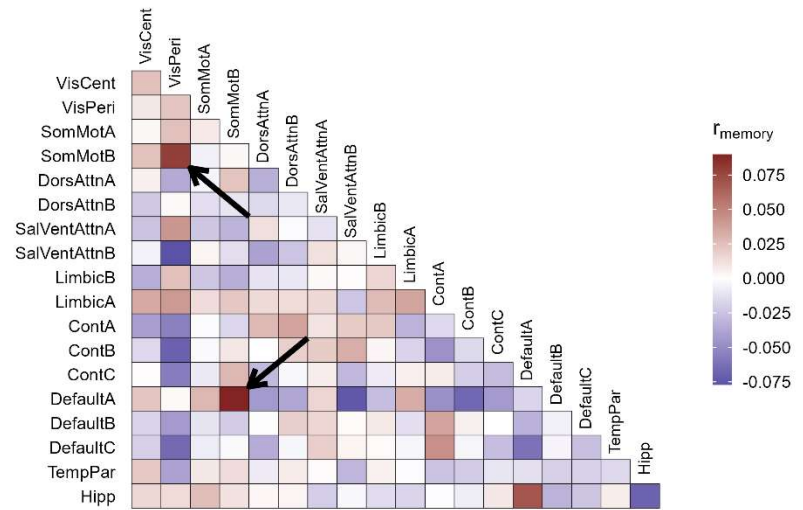
analysis	results	p
VisCent_exclude	0.156	0.000
VisPeri_exclude	0.152	0.010
SomMotA_exclude	0.169	0.000
SomMotB_exclude	-0.012	0.386
DorsAttnA_exclude	0.175	0.000
DorsAttnB_exclude	0.143	0.000
SalVentAttnA_exclude	0.168	0.000
SalVentAttnB_exclude	0.165	0.000
LimbicB_exclude	0.130	0.010
LimbicA_exclude	0.143	0.000
ContA_exclude	0.139	0.010
ContB_exclude	0.155	0.000
ContC_exclude	0.148	0.000
DefaultA_exclude	0.169	0.000
DefaultB_exclude	0.094	0.040
DefaultC_exclude	0.166	0.000
TempPar_exclude	0.133	0.010
Hipp_exclude	0.154	0.000

**Table 7: Computational Lesion Analysis Results.** Excluding SomMotB regions from the analysis resulted in a significant drop in model performance. analysis = network excluded, results = Pearson's correlation between observed and predicted memory ability scores, p = proportion of null simulations that were more extreme than the observed.

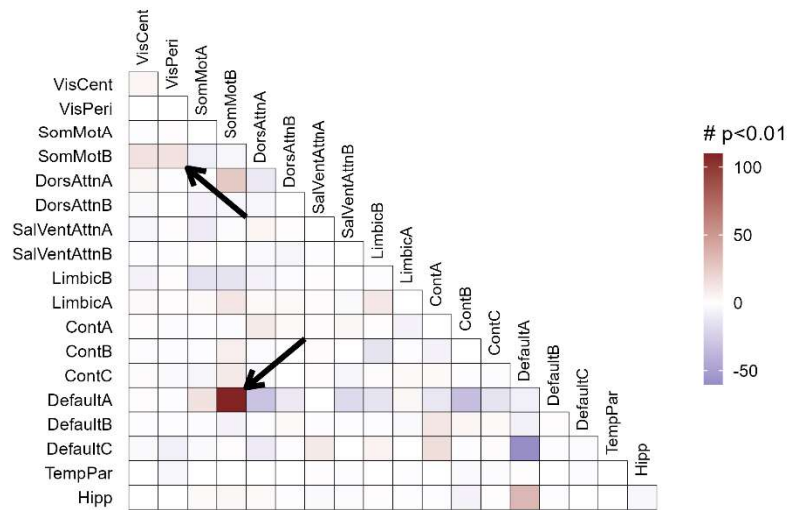
A)



B)



C)



D)

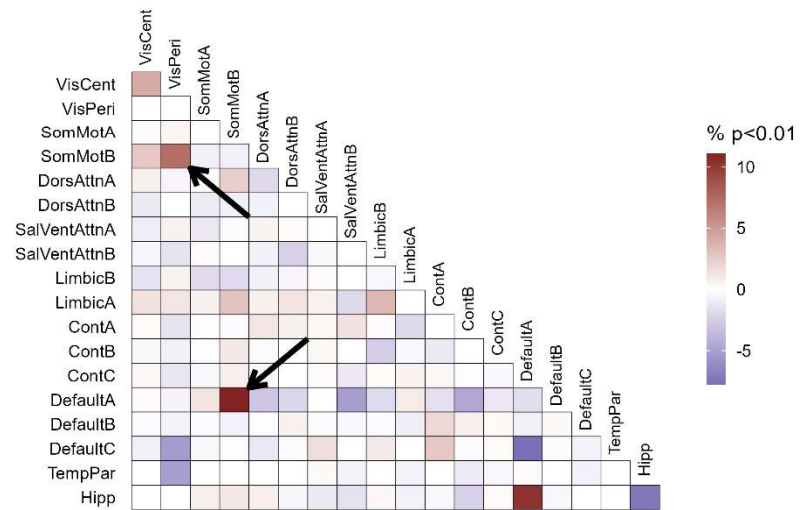


**Figure 7: Evaluating Feature Importance.** A.) Average strength of network connections, measured as the Pearson's correlation ( $r$ ) between region time courses. B) The partial correlation of connection strength with memory ability after controlling for age, sex, and average in-scanner motion. C) The number of connections that are significantly positively correlated with memory ability at  $p < 0.01$  minus the number of connections that significantly negatively correlated with memory ability at  $p < 0.01$ . D) The proportion of connections that are significantly positively correlated with memory ability at  $p < 0.01$  minus the proportion of connections that significantly negatively correlated with memory ability at  $p < 0.01$ . Arrows highlight connections between SomMotB and Default A and SomMotB and VisPeri regions.

## 2.5 SUMMARY

In Chapter 2, I examined how the functional connectome related to one's episodic memory ability. I placed a theoretically driven focus on connections of the Default C subnetwork – a subnetwork of the larger default mode network that has been strongly implicated in high fidelity, successful episodic remembering (Kurkela et al., 2022b; Chapter 1). Using a large openly available dataset, I determined that the strength of intrinsic functional connections among Default C regions, connections between Default C and Default A regions, connections between Default C regions and all other brain regions, and connections involving the hippocampus were not reliably related to one's episodic memory ability. In a data-driven predictive modeling approach, I found that there was information concerning memory ability found within the functional connectome. My connectome based predictive models relied on connections found throughout the connectome to make accurate predictions in out-of-sample subjects. A computational lesion analysis suggested that functional connections of the Somatomotor Network B were necessary for model success. Follow up analyses suggested the Somatomotor Network B regions decoupled with Default A regions and increased their communication with peripheral visual regions in individuals with better memory. This conclusion, however, contrasts with several previously published findings. As described in the **Introduction**, studies relating functional connectivity to memory have often implicated default mode regions or the hippocampus, though these findings have been somewhat mixed (King et al., 2015; Lin et al., 2021; e.g., Sneve et al., 2017; van Buuren et al., 2019).

One possible explanation for the current results is that there is a relationship between the functional connectome and memory ability, but the memory test data available in the CamCan dataset is inadequate to capture an individual's episodic memory ability. Using only a single

measure of memory ability is typically seen as suboptimal when attempting to capture an individual's overall memory ability. Unsworth (2019), for example, suggests that the factor structure underlying episodic memory is best characterized by a hierarchical structure, such that individuals have particular aptitudes for completing different types of memory tasks in addition to an overall memory capacity. If this is the case, then using any single task would be a biased estimation of an individual's overall memory ability. Chapter 3 of this dissertation aims to tackle this exact problem of how to properly model individual differences in episodic memory ability.

## CHAPTER 3

### 3.1 OVERVIEW

The ability to remember the past is one of our most important and ubiquitous cognitive capacities. We can remember vast amounts of information from our lives and this ability is advantageous for us in making decisions and predicting the future. It is also apparent, however, that individuals vary greatly in the quality with which they can remember the past (Palombo et al., 2018; Unsworth, 2019). Some of us can remember passwords, recognize people we met at parties, or recall the family Christmas party in 1999 with relative ease and in great detail. Others struggle to remember the same information, often forgetting passwords, needing to be reintroduced to individuals that we have already met, and only vaguely remembering that Uncle Walter dressed up as Santa Claus at the family Christmas party in 1999. Importantly, these individual differences in memory ability can be seen within the neurologically healthy population. Chapter 3 seeks to better understand the nature of individual differences in memory ability by testing a specific neuroscience-inspired hypothesis on the organization of individual differences in memory ability.

Episodic memory is supported by a set of interacting cortical and subcortical brain regions, including the hippocampus, the angular gyrus, the retrosplenial cortex, posterior parietal cortex, the precuneus, the parahippocampal cortex, and the medial prefrontal cortex. Collectively these regions have been referred to as the “recollection network” due to their activation during episodic recollection tasks (Rugg & Vilberg, 2013), as one of two large-scale hippocampal-cortical networks that support memory guided cognition (Posterior Medial Network: Ranganath

& Ritchey, 2012; Ritchey & Cooper, 2020), or as subnetworks within the larger default mode network (Andrews-Hanna et al., 2010). Recent work focusing on this set of brain regions suggests that instead of comprising a single homogenous network, the regions fracture into two highly related subnetworks (Barnett et al., 2021; Buckner & DiNicola, 2019; Cooper et al., 2021b; Kurkela et al., 2022a) that may support different cognitive processes (DiNicola et al., 2020). Specifically, some studies have argued that the more dorsal network supports theory of mind and mentalizing tasks (Spunt et al., 2011) and the more ventral network more specifically supports episodic recollection (Andrews-Hanna, Saxe, et al., 2014; Andrews-Hanna, Smallwood, et al., 2014; DiNicola et al., 2020). Others have argued that the more ventral subnetwork supports memory for more detailed space/place information, while the other more dorsal subnetwork supports memory for more abstract socioemotional information (Gurguryan & Sheldon, 2019; Peer et al., 2015; Silson et al., 2019). We hypothesize that this distinction among neural systems may have implications for individual differences in memory abilities. If either of these accounts is true and the functioning of these subnetworks also naturally differs between individuals, then I would expect to see individuals differ in the primary function of each of these subnetworks. In other words, we expect to see dissociable individual differences in the ability to recall socioemotional information from memory and in the ability to recall detailed spatial/temporal information from memory.

There is a relative dearth of studies that have investigated individual differences in long-term episodic memory abilities among healthy young adults. The few that have suggest that individuals differ on either an overall memory capacity (Unsworth, 2019) or along several cognitive components of the episodic recollection process (Ngo et al., 2021; Palombo et al., 2018). Recent research on the neurobiological architecture underlying episodic recollection

suggests that there are at least two highly related subnetworks that support different aspects of the recollection process. Specifically, these subnetworks may differentially support the processing of specific visual-spatial episodic information and more social-emotional information. It seems logical to hypothesize that individuals would differ in the effectiveness of their underlying brain networks and as a result may differ on the processing of visual-spatial and social emotional processing respectively. To the best of my knowledge, no study to date has systematically investigated individuals' ability to recall spatial/temporal information from memory and more social information from memory in a highly controlled laboratory setting.

Because the subnetworks of the default mode network are statistically dissociable but highly correlated (Kurkela et al., 2022a), I believe that the primary dimension along which people differ is an overall episodic memory dimension. This would be reflective of the efficiency with which both subnetworks function within an individual. The key to my hypothesis, however, is the existence of a second dimension along which people differ. This dimension is a visual-spatial–social-emotional dimension, which is caused by naturally occurring differences in the *relative* efficiency of individuals' ventral and dorsal default mode subnetworks respectively. If this state of affairs is correct, then I would expect to see a consistent content bias in individuals' memory such that some individuals are better at recalling events that are centered around places while others are better at recalling events that are centered around people. To test my hypothesis, I ran the following behavioral experiment in which I characterize the efficiency of individual episodic memory for different types of information (i.e., social-emotional/visual-spatial) using a well-established multielement episodic memory paradigm.

## 3.2 METHODS

### 3.2.1 Participants

A total of 60 participants were collected. Participants were recruited using the online platform Prolific (<https://www.prolific.co/>). Participants were recruited such that they resided in the United States, self-reported fluency in the English language, were between the ages of 18 and 40 years of age ( $M = 31.6$ ,  $SD = 5.7$ ,  $min = 20$ ,  $max = 40$ ), and had a minimum approval rate of 95% when completing studies on Prolific. Our sample of 60 participants were majority female ( $n = 35$  or 58.33%), and majority White (White = 70%, Black = 8.33%, Asian = 8.33%, Mixed = 8.33%, and Other = 5%). Informed consent was obtained from all participants prior to participating and participants were compensated for their time. All procedures were approved by the Boston College Institutional Review Board. The study methods were preregistered in advance of data collection; see:

[https://osf.io/nmjde/?view\\_only=8e5fa7b8949d45559884e1d0c8c8f887](https://osf.io/nmjde/?view_only=8e5fa7b8949d45559884e1d0c8c8f887).

60 participants were collected based on the results of a preregistered independent segments stopping procedure (J. Miller & Ulrich, 2021). The independent segments stopping procedure is a procedure designed to make efficient use of experimental resources when evaluating a scientific hypothesis. In this procedure, a maximum sample size is selected, and  $k$  equally sized and independent segments of this sample are collected one at a time. In each independent segment of data, a key statistical test of the scientific hypothesis is evaluated to determine if data collection continues to the next segment. Data collection continues if evidence for or against the null hypothesis is ambiguous. If the key statistical test determines that there is already strong evidence against the null hypothesis or very weak evidence against the null

hypothesis, data collection is stopped. Importantly, the parameters of this procedure are selected to control the overall alpha value of the entire procedure. For this experiment, we *a-priori* decided to collect a total possible sample of 240 subjects over 4 independent segments. To control the overall alpha value at 0.05, we stopped data collection if our key statistical test had a p-value less than 0.035 or a p-value greater than 0.282 in any segment. Here, this occurred in the first segment and thus data collection was stopped with a sample size of 60. The key statistical test of my hypothesis is described further in “Analysis” and the results of this test are reported in “Results”.

### 3.2.2 Materials

Memoranda were composed of sets of written English words. Each word came from one of three categories: famous persons, famous places, or common objects. A bank of the first and last names of 112 famous individuals was created via online searches. A bank of 84 famous place names were collected from the places images originally collected by Cooper and colleagues (Cooper et al., 2017) supplemented by a series of online searches. A bank of object names were collected from the Bank of Standardized Stimuli (BOSS) (Brodeur et al., 2010, 2014) by filtering the database for images of non-living objects and selecting the 124 images that had the high modal name agreement. I expected images in this database with the designation non-living and high modal name agreement to be most likely to be common, easily identifiable objects. All stimuli to be used in the current proposal can be found in **Supplemental Table 8**. Memoranda were composed of a set of three written words presented in a triad (see **Figure 8a**). One half of the triads were composed of a famous person and two common objects, and the other half were composed of a famous place and two common objects. A total of 28 memoranda were

presented to each participant during each session (14 famous person–object–object triads; 14 famous place–object–object triads). All words were unique to each triad. Participants also completed three questionnaires concerning their perceived episodic memory, visual imagery, and mentalizing abilities: the survey of autobiographical memory (Palombo et al., 2013), the Vividness of Visual Imagery Questionnaire (Marks, 1973), and the Interpersonal Reactivity Index (M. H. Davis, 1983).

### **3.2.3 Procedure**

Participants completed two experimental sessions. Each session included a multi element episodic memory task (Horner & Burgess, 2014) designed to measure their episodic memory ability for events containing different types of information. Before the task began, participants completed surveys probing participant’s familiarity with the famous persons and famous places selected for the experiment. Each of the two surveys randomly selected 28 famous people or 28 famous places, with separate stimuli chosen for each session. For each of the 28 famous persons/places, participants were given a Likert scale (1- unfamiliar – 6 - Very Familiar) to indicate how familiar they were with each stimulus. The familiarity ratings gathered in this survey were used to prescreen stimuli to be used during the multi element episodic memory task for each participant. Stimuli were selected for the experiment such that the top 14 most familiar persons and the top 14 most familiar places were used to construct the famous place and famous person triads described previously (see **3.2.2 Materials**). This was done to ensure that all stimuli used in the memory task were familiar to participants. A total of 28 triads were constructed by randomly selecting 56 object names from my database of names, randomly pairing them, and

then randomly assigning each object pair to one of the 14 famous names and 14 famous places selected as familiar to each participant.

After completing the famous person/places surveys, participants completed an encoding task. During the encoding task, participants were presented with each of the 28 triad memoranda (i.e., 14 famous person triads and 14 famous place triads) and they vividly imagined a scenario linking the elements of the triad together. Participants were given a total of 12 seconds to imagine a scenario for each triad. Following this 12 second period, participants were asked to indicate on a scale from 0-100 how successful they were in imagining a scenario linking the 3 triad elements together. To get insight into what exactly participants were imagining during encoding, I randomly selected 2 of the 14 person triads and 2 of the 14 place triads to serve as catch trials. On these catch trials, participants imagined a scenario linking the 3 triad elements together, rated how successful they were in imagining a scenario, and then report using a written free text response exactly what they were imagining during the 12 second imagination interval (see **Figure 8b**). Memory for the triads from the 4 catch trials were not tested in subsequent retrieval rounds.

After completing the encoding task, participants completed a backwards digit span task to get a measurement independent of the episodic memory task of their cognitive capacity and task engagement. In this task, participants were presented with a string of numbers one at a time. Each number was presented for 500ms with a 500ms intertrial interval. After the numbers were presented, participants were presented with a free text response box and were asked to report the number that they just saw in reverse order. For example, if participants were presented with the digits “1-1-8-9” then they were tasked with reporting back “9-8-1-1”. Backwards digit span trials

progressed in difficulty, from 3 digits to 7 digits. Participants completed two trials at each difficulty level, for a total of 10 trials.

After completing the backwards digit span task, participants were tested on their memory for the previously presented triads. The retrieval task consisted of a series of cued free recall trials (see **Figure 8c**). Each trial was self-paced. Trials presented one of the three elements of the triads from the encoding task as a memory cue, asking participants to report the other two corresponding elements. Each element in the triads served as a memory cue. This results in 72 total retrieval trials (24 triads that did not serve as catch trials during encoding x 3 triad elements). All retrieval trials were completely in a randomized presentation order.

After completing the experimental tasks, participants completed questionnaires on their self-perceived episodic memory (Survey of Autobiographical Memory, Palombo et al., 2013), visual imagery ability (Vividness of Visual Imagery Questionnaire, Marks, 1973), and mentalizing ability (Interpersonal Reactivity Index, M. H. Davis, 1983). After completion of these questionnaires, participants were presented with a screen that invited them to participate in the next session of the experiment. The second session of the experiment was identical to Session 1 of the experiment in their procedure, except for the completion of the demographics and individual differences questionnaires. A new set of famous person, famous place, and common object stimuli were used on each subsequent session. Participants completed two sessions of the experiment to estimate each participant's intrinsic level of dependency in the famous person triad and famous place triad conditions (see **3.2.3 Analysis**).

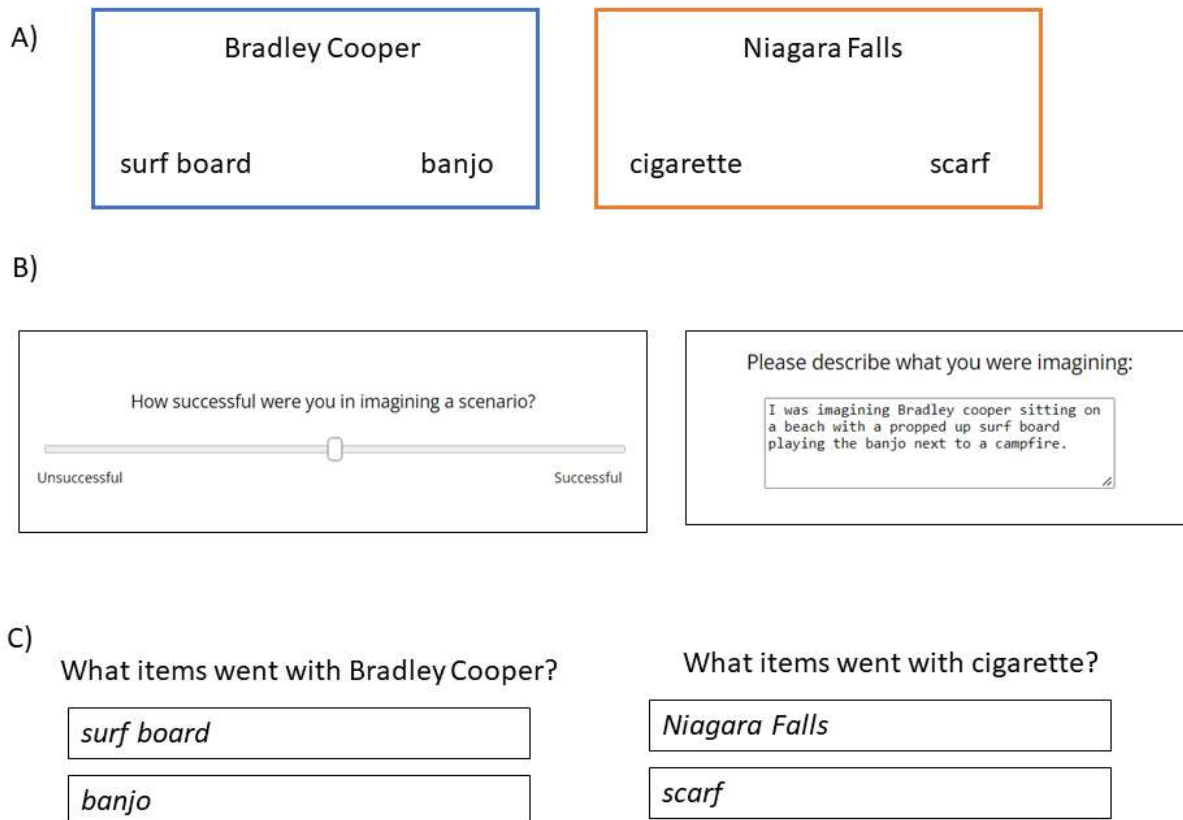


**Figure 8: Triads Task Overview.** A.) Example famous person (blue) and famous place (orange) memoranda. All memoranda were presented for 12 seconds during the encoding task, during which time participants imagined a scenario linking the 3 items together. B.) Example encoding trial. After spending 12 seconds imagining, participants rated on a scale of 0-100 how successful they were in imagining a scenario. For a subset of 4 catch trials (i.e., 2 famous person trials and 2 famous place trials), participants described in writing what they were imagining during encoding. C.) During an immediate retrieval task, participants were cued with one of the items from the triads and attempted to report the two corresponding items from the triad. Each of the three items from the triads served as a memory cue for a total of 72 retrieval trials.

### 3.2.3 Analysis

All statistical analyses were run in the R statistical environment (R Core Team, 2022). All mixed effects models were fit using the R package *lme4* (Bates et al., 2015), paired t-tests using the package *stats* (R Core Team, 2022), partial correlations using the *ppcorr* package (S. Kim, 2015), statistical reporting of paired t-tests and mixed models using the R package *report*

(Makowski et al., 2023), and all figures using *ggplot2* (Wickham, 2016). All code needed to recreate the analyses from this experiment are publicly available in a GitHub repository which can be found here: <https://github.com/memobc/indivTriadJS>.

Cued recall responses during retrieval were automatically graded using the *agrepl* function available in the *base* package in the R statistical environment (R Core Team, 2022). This function takes a string as input and tries to match it to a vector of strings using a fuzzy matching algorithm. The algorithm works by attempting to match the strings by limiting the number of substitutions, additions, or deletions necessary to make two strings match. For example, the pattern string “lasy” will match the string “lazy” when the algorithm is set to allow for 1 substitution, addition, or deletion (substituting “z” for “s”). The algorithm also allows the user to set the number of substitutions, additions, or deletions to be a proportion of the length of the pattern string. Written responses were considered correct IFF the correct response matched either of the subject’s written responses allowing for up to 30% of the correct answer’s length in substitutions, deletions, or additions with one exception. To match cued recall responses where the correct answer was a famous place, the algorithm was modified to allow for 65% of the correct answer’s length in substitutions, deletions, or additions. I reasoned that 30% was a reasonable amount of fuzziness to allow close typos and misspellings of the correct answer to be counted as correct. I made the exception for my famous place stimuli because my famous place stimuli included both the canonical name of the famous location alongside its geographical location (e.g., “Fenway Park, Boston”; see **Supplemental Table 8**). In a pilot sample of 14 subjects, I noticed that most participants reported only the canonical name of the famous place during cued recall (e.g., “Fenway Park”). I reasoned that 65% allowed for enough fuzziness to capture these types of responses as being correct, at the risk of some false positives. The

feasibility of this automatic grading algorithm with the 30%/65% fuzziness parameters was tested in a pilot dataset of 14 subjects. The pilot dataset was first graded by a single human grader and the grades from this human grader were compared to those from the just described *agrepI* algorithm. Grades produced by the algorithm agreed with those from the human grader 98.8% of the time.

A key feature of episodic memory is the fact that representations of events are thought to be “coherent wholes”. This implies that when retrieving an event, retrieval of one element of the event should be dependent on the retrieval of the other elements of that same event. This idea is referred to as *retrieval dependency* (Horner & Burgess, 2014; Ngo et al., 2021) and can be measured in my multielement episodic memory task by examining contingency in participants' recalls (see **Figure 9a**). For the following explanation, each element of a triad will be arbitrarily represented by a letter (e.g., A-C), with a capital letter representing which element is serving as the memory cue and lower-case letters representing which element is being retrieved (example: Ab would be when element A is being used as a memory cue to retrieve element b; see **Figure 9a**). *Retrieval dependency* is calculated by examining 6 contingency tables – three contingency tables when each element of a triad is used as a memory cue to retrieve the other two elements (AbAc, BaBc, CaCb) and three contingency tables where a common element is cued by the other two elements of a triad (BaCa, AbCb, AcBc). For each contingency table, the proportion of associations that were jointly remembered or jointly forgotten is calculated (in other words, the proportion of associations that fall into the top left and bottom right cells of each contingency table; see **Figure 9**). This proportion is averaged across the 6 contingency tables. This average proportion is then subtracted from the expected number of joint recalls under a model that assumes both associations in each contingency table are recalled independently (the independent

model). The expected number of joint recalls is calculated as a function of the probability of recalling each association in a contingency table across all events (see **Figure 9b**). Retrieval dependency was operationalized as the proportion of joint recalls observed in the data minus the expected proportion of joint recalls assuming independent retrieval. This value can theoretically range [-1, 1] with 0 indicating a complete absence of retrieval dependency (in other words, the independent model fits well), 1 indicating perfect retrieval dependency, and -1 indicating the opposite of retrieval dependency (i.e., retrieving an element of an event makes it *less likely* that you will retrieve the other element of an event).

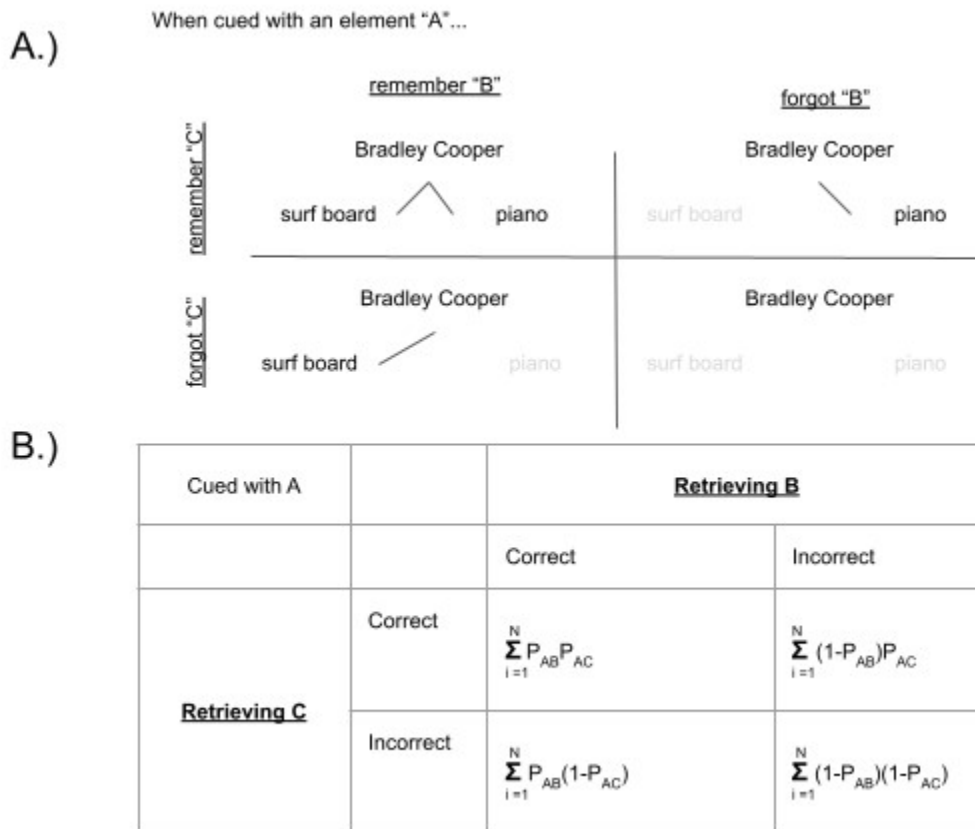


**Figure 9:** Calculation of Retrieval Dependency. A.) A visual aid for the calculation of retrieval dependency in the current design. Panel A illustrates an AbAc contingency table. B.) Table detailing the calculation of the expected proportion of retrievals in each cell of the AbAc contingency table under the assumption of independence.

If individuals differ in their ability to holistically remember social-emotional and visual-spatial focused mnemonic representations respectively, then I would expect retrieval dependency for famous person triads in session 1 to be more strongly correlated with their retrieval dependency for famous person triads in session 2 than to their retrieval dependency for famous place triads on sessions 1 or 2. The same logic would apply to performance on famous person triads. Importantly, all correlations would be run across participants. In other words, a separate retrieval dependency score would be calculated for each condition (famous person, famous place) for each session (session 1, session 2) for each participant. I will test my hypothesis of interest in the following manner. I will use a pair of partial correlation tests. Specifically, I will perform the following two statistical tests: a.) the partial correlation of famous person dependency in session 1 on famous person dependency in session 2 controlling for famous place dependency in sessions 1 and 2; b.) the partial correlation of famous place dependency in session 1 on famous place dependency in session 2 controlling for famous person dependency in session 1 and 2. These partial correlation tests should succeed if participants have an intrinsic ability for holistically recalling one type of information versus the other. Importantly, these partial correlation tests should control for participant's overall episodic memory ability and for a main effect of session. For the purposes of our independent segments stopping rule procedure (see **3.2.1 Participants** for more details), we will use the maximum p-value of these two tests as our critical p-value for determining whether to stop data collection.

## 3.3 RESULTS

### 3.3.1 Overall Accuracy

Overall accuracy refers to the proportion of cued recall response prompts that were given a correct answer. Participants performed moderately well but varied widely on the task ( $M = 0.57$ ,  $SD = 0.281$ ,  $min = 0.01$ ,  $max = 1$ ). To determine if participants' accuracy differed as a function of session (session 1, session2) and triad type (famous person, famous place), I fit a logistic mixed model to predict accurate cued recall using session and triad type. This model included triad type, session, and the trial type x session interaction as random effects (formula:  $\sim$ trial\_type \* session | subject\_id). The model's total explanatory power was substantial (conditional  $R^2 = 0.52$ ) and the part related to the fixed effects alone (marginal  $R^2$ ) was 0.01. The effect of session [session2] was statistically non-significant and negative ( $\beta = -0.12$ , 95% CI [-0.39, 0.14],  $p = 0.357$ , Std.  $\beta = -0.06$ ). The effect of condition [famous place] was statistically significant and negative ( $\beta = -0.49$ , 95% CI [-0.76, -0.23],  $p < .001$ , Std.  $\beta = -0.23$ ). The effect of session [session2]  $\times$  condition [famous place] was statistically non-significant and negative ( $\beta = -0.07$ , 95% CI [-0.36, 0.21],  $p = 0.601$ , Std.  $\beta = -0.04$ ). This model suggests that participants were more accurate when triads contained a famous person compared to when they contained a famous place (see **Figure 10**).

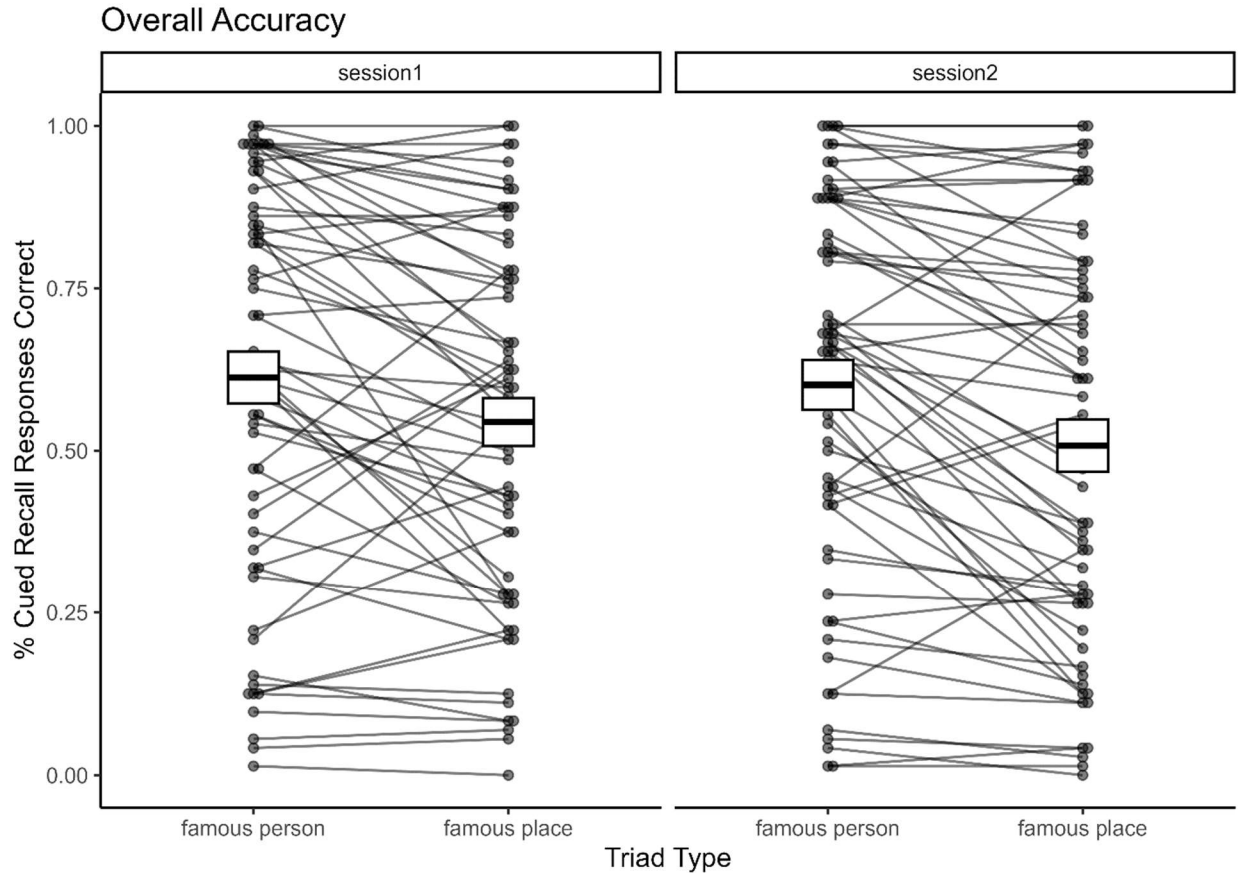


**Figure 10:** *Overall Accuracy as a Function of Session and Triad Type.* Participants performed moderately well and varied widely on the multielement episodic memory task. Our data suggest that participants were more accurate when triads contained a famous person than when they contained a famous place.

### 3.3.2 Evidence for Content Biases in Retrieval Dependency

Previous studies using the multielement episodic retrieval task consistently show that participants, on average, display evidence for retrieval dependency (Bisby et al., 2018; e.g., Horner & Burgess, 2014; Ngo et al., 2021). To determine if my data were consistent with these previous reports, I first determined if my sample of participants displayed evidence for retrieval dependency collapsed across my conditions. As expected, I found evidence that the proportion of joint retrieval observed in the data was greater than the estimated proportion of joint retrieval under the independent model (difference = 0.14, 95% CI [0.12, 0.16],  $t(59) = 13.85$ ,  $p < .001$ ,

Cohen's  $d = 1.79$ ), indicating that my sample showed significant dependence in their retrieval. Next, I calculated an index called “dependency” by subtracting the estimated proportion of joined retrievals observed in the data from the estimated proportion of join retrievals under the independent model separately for each subject, session, and triad type (see **3.2.3 Analysis**). To determine if participants’ retrieval dependency differed as a function of session (session 1, session2) and triad type (famous person, famous place), I fit a linear mixed model to predict dependency using session and triad type. The model included session and triad type as random effects (formula =  $\sim$  session + triad\_type | subject\_id). The model’s total explanatory power was substantial (conditional  $R^2 = 0.73$ ) and the part related to the fixed effects alone (marginal  $R^2$ ) was 0.02. The effect of session [session2] was statistically non-significant and positive ( $\beta = 6.56e-04$ , 95% CI [-0.03, 0.03],  $t(229) = 0.04$ ,  $p = 0.964$ , Std.  $\beta = 6.17e-03$ ). The effect of condition [famous place] was statistically significant and positive ( $\beta = 0.04$ , 95% CI [9.67e-03, 0.06],  $t(229) = 2.68$ ,  $p = 0.008$ , Std.  $\beta = 0.34$ ). The effect of session [session2]  $\times$  condition [famous place] was statistically significant and negative ( $\beta = -0.04$ , 95% CI [-0.06, -7.22e-03],  $t(229) = -2.47$ ,  $p = 0.014$ , Std.  $\beta = -0.34$ ). This model suggests that participants displayed greater retrieval dependency in the famous place triad condition. This effect was smaller in session 2 compared with session 1 (see **Figure 11**).

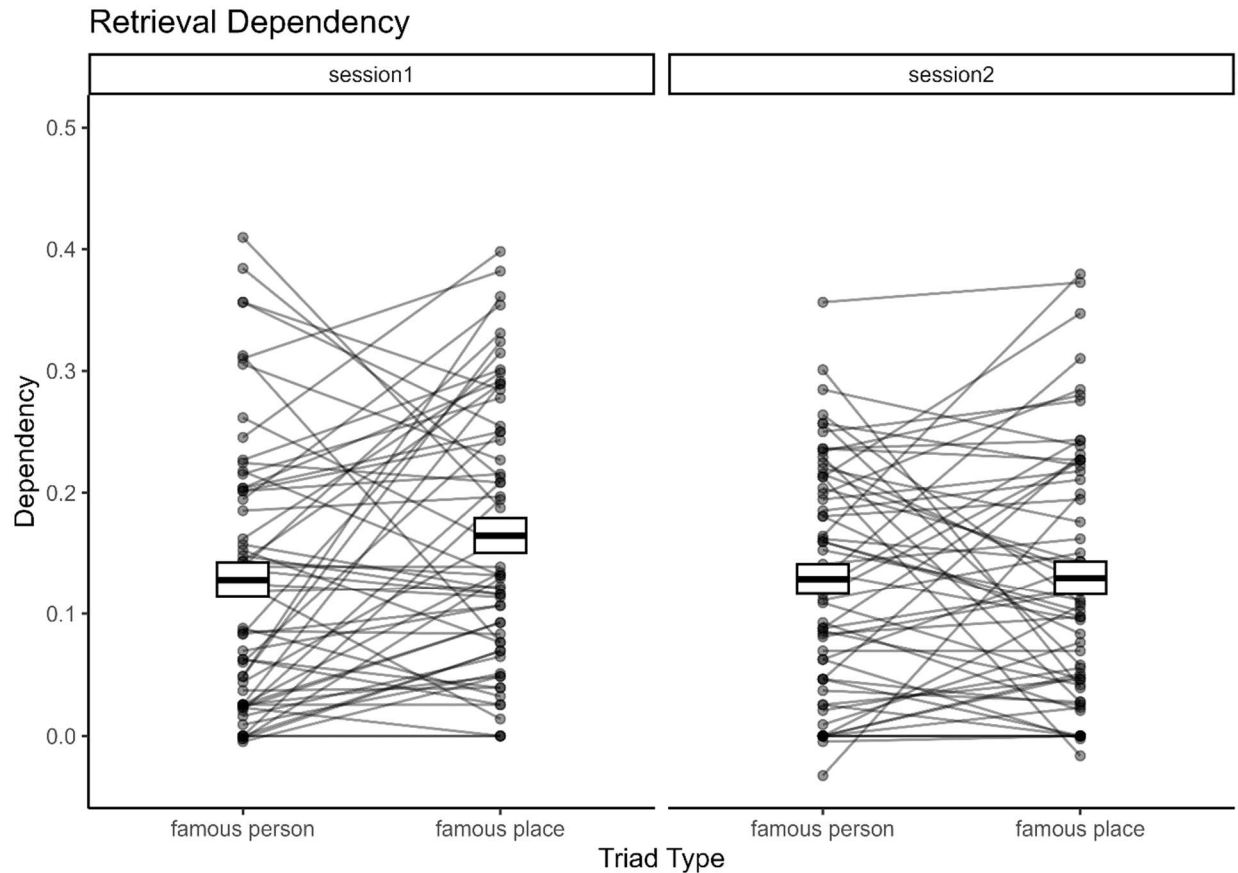


**Figure 11:** *Retrieval Dependency as a Function of Session and Triad Type.* Participants overall displayed strong evidence for retrieval dependency in their cued recalls. Participants additionally displayed more retrieval dependency for the famous place triads compared with the famous person triads. This effect was smaller in session 2 compared with session 1.

Lastly, to see if my data provided evidence for my key hypothesis, I ran a pair of partial correlation tests (see **3.2.3 Analysis**). Dependency in the famous person triad condition in session 1 was significantly correlated with dependency in the famous person triad condition in session 2 when controlling for dependency in the famous place triad condition in session 1 and session 2 ( $r = 0.500, t(56) = 4.318, p < 0.001$ ). Conversely, dependency in the famous place triad condition in session 1 was significantly correlated with dependency in the famous place triad condition in session 2 when controlling for dependency in the famous person triad condition in session 1 and session 2 ( $r = 0.359, t(56) = 2.874, p = 0.006$ ). As a result, data collection ceased after the first independent segment of  $N = 60$  (see **3.2.1 Participants**). To further understand

these results, I calculated a new measure, “person dependency bias” by subtracting retrieval dependency seen in the famous person triad condition from retrieval dependency seen in the famous place triad condition for each subject for each session. This measure essentially represents the slope of the lines seen in **Figure 11**. In **Figure 12a**, I plot person dependency bias measured in session 1 against person dependency bias measured in session 2. If person dependency bias is an intrinsic property of individuals, then I would expect person dependency bias measured in session 1 to be positively correlated with person dependency bias measured in session 2 -- indicating that participants remain consistent from session 1 to session 2. This was the case in my sample ( $r = 0.45$ , 95% CI [0.22, 0.63],  $t(58) = 3.80$ ,  $p < .001$ ). In **Figure 12b**, I plot participants’ dependency scores averaged over sessions in a scatterplot with the x-axis representing place dependency and the y-axis representing person dependency. Subjects that lie above and to the left of the diagonal in this plot (the red space) display a bias towards holistically remembering famous place triads and subjects that lie below and to the right of the diagonal (the blue space) display a bias towards holistically remembering famous person triads. Observing this space closely, it is evident that participants vary along the lower left to upper right diagonal, suggesting that there is an overall episodic memory capacity with some participants displaying overall more retrieval dependency than others. Importantly, it is also evident that participants vary off this diagonal, with some participants displaying a famous person or famous place bias in their holistic recollection. Taken together, these results suggest that participants differ in their intrinsic tendency to holistically recall information containing people and places, such that some individuals are better at holistically recalling triads containing famous places and some individuals are better at holistically recalling triads containing famous persons.

## Content Biases in Retrieval Dependency

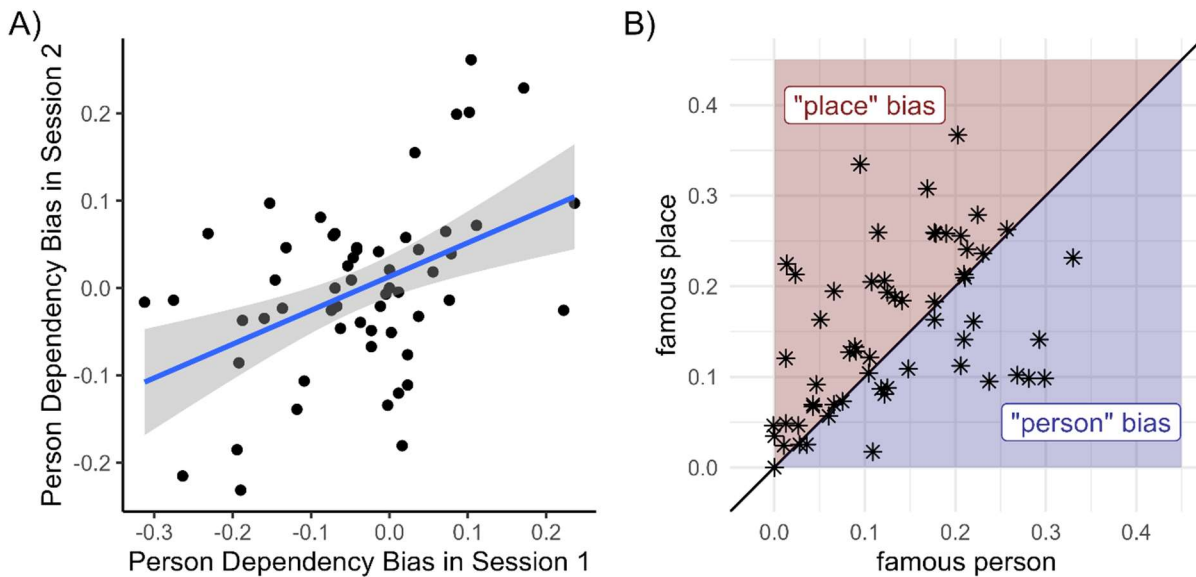


**Figure 12:** *Content Biases in Retrieval Dependency.* A.) Content biases in retrieval dependency are consistent over sessions, such that participants that have a content bias in session 1 tend to have a similar content bias in session 2. B.) Participants vary both in the overall amount of holistic retrieval (variability along the diagonal; black line) as well in their ability to holistically retrieve triads containing famous persons vs triads containing famous people (variability away from the diagonal). Bias = dependency in famous person triads – dependency in famous place triads.

### 3.3.3 Dependency and Overall Accuracy Are Strongly Related

As a follow up analysis, I wanted to determine if participants also displayed content biases in their overall cued recall accuracy. Before doing this, I wanted to better understand the relationship between retrieval dependency and overall cued recall accuracy. Retrieval dependency as reported in the literature is described as a measure that is independent from overall retrieval accuracy. This is because the calculation of retrieval dependency involves subtracting away the proportion of joint retrievals accounting for overall accuracy for different triad associations (i.e., the independent model; see **3.2.3 Analysis**; see also Horner & Burgess, 2014; Bisby et al. 2018; Ngo et al. 2021). However, this did not appear to be the case when considering variation across participants in my data. In **Figure 13**, I plot overall accuracy against

retrieval dependency across participants. As is evident from the figure, there is a strong quadratic relationship between overall accuracy and retrieval dependency such that participants who performed either at or near ceiling or at or near floor are the ones displaying little retrieval dependency. To statistically test for this, I fit a linear model of retrieval dependency (dependency) on overall accuracy (accuracy) containing a quadratic coefficient (model formula:  $\text{dependency} \sim \text{accuracy} + \text{accuracy}^2$ ). The model's explanatory power was substantial ( $R^2 = 0.75$ , adj.  $R^2 = 0.74$ ). The effect of accuracy is statistically significant and positive ( $\beta = 0.93$ , 95% CI [0.77, 1.08],  $t(57) = 12.18$ ,  $p < .001$ , Std.  $\beta = -0.32$ ). The effect of  $\text{accuracy}^2$  is statistically significant and negative ( $\beta = -0.89$ , 95% CI [-1.03, -0.75],  $t(57) = -12.87$ ,  $p < .001$ , Std.  $\beta = -0.92$ ).

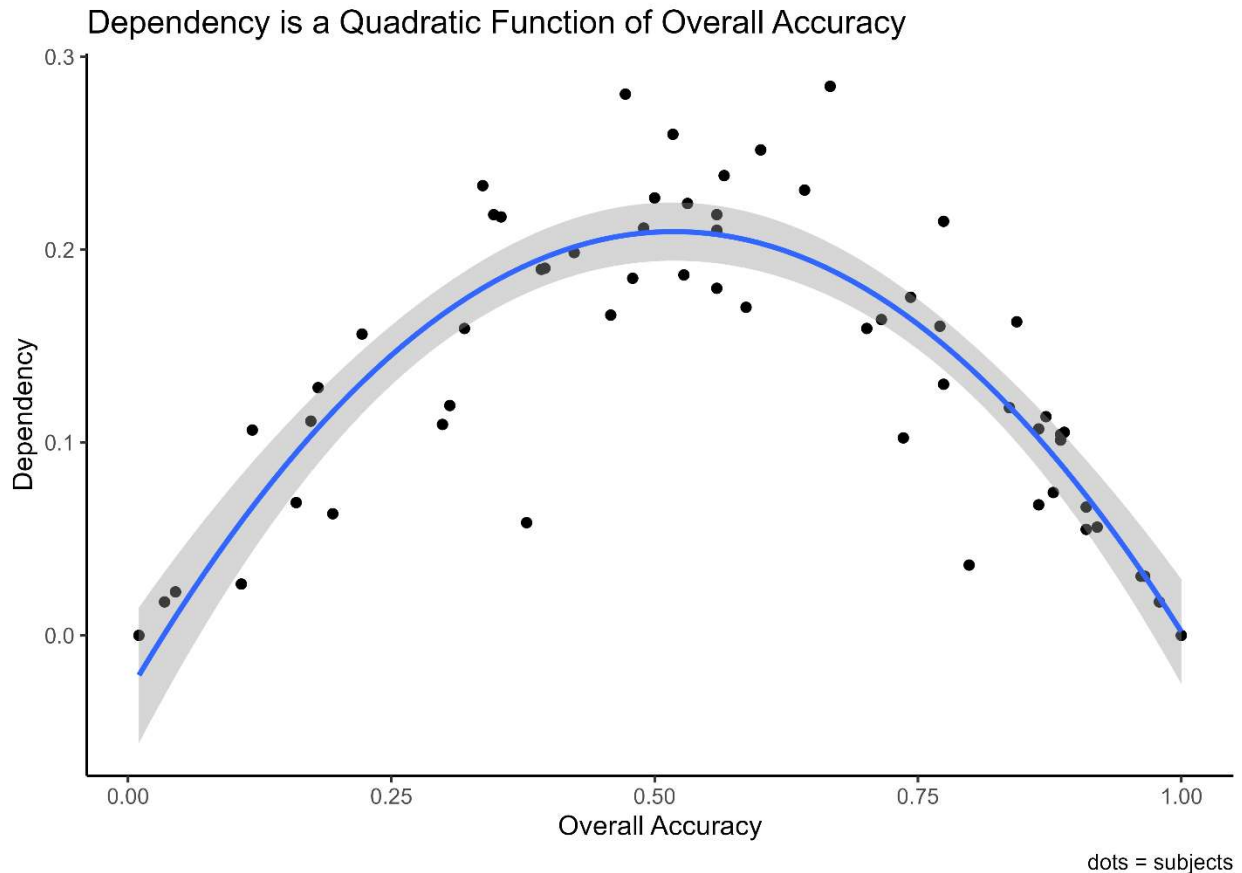


**Figure 13:** *Dependency is a Quadratic Function of Overall Accuracy.* Average retrieval dependency is a quadratic function of overall accuracy such that participants who are at or near ceiling or are at or near floor in terms of overall accuracy are also the participants who show the lowest retrieval dependency.

Upon further reflection, it became evident that this quadratic relationship is baked into the calculation of retrieval dependency. Specifically, participants who perform near ceiling or near floor must necessarily have similar amounts of observed joint retrievals and estimated joint retrievals under the independent model. In other words, performance near the floor and ceiling limits the range of possible retrieval dependency scores, resulting in the U-shaped function seen in **Figure 13**. I believe that the dependency measure can still be a valid measure of holistic retrieval if participants near the performance floor/ceiling are removed from the analysis. To perform a quick thought experiment as to why this makes sense, imagine a participant who performs perfectly on the experiment (100% accuracy). The proportion of observed joint recalls

for this participant will necessarily be 100% and the expected proportion of joint recalls under the independent model will also be 100%, resulting in a dependency measure of 0. However, this participant is NOT displaying 0 retrieval dependency. I cannot observe this participant's retrieval dependency because they performed so well on the experiment. We could, in theory, estimate their retrieval dependency on a more difficult retrieval test. A similar set of logic applies to participants near the performance floor.

To attempt to correct for this accuracy-dependency confound, I winsorized my data by removing participants who had extreme accuracy in any one of my experimental conditions. Specifically, I first removed participants who accurately recalled below 5% or above 95%, then removed those that accurately recalled below 10% and above 90%, and finally those that recalled below 25% and above 75% of recall prompts in any one of my experimental conditions. Winsorizing my data in this way resulted in revised sample sizes of 40, 33, and 17 respectively. The 5%/95% and 10%/90% samples still displayed a significant quadratic relationship between overall accuracy and dependency, but the 25%/75% sample showed no relationship between overall accuracy and retrieval dependency. I thus decided to rerun my analyses on the 25%/75% winsorized sample. The 25%/75% sample still displayed strong evidence for retrieval dependency (difference = 0.21, 95% CI [0.20, 0.23],  $t(16) = 24.94$ ,  $p < .001$ , Cohen's  $d = 6.05$ ). The results of the session x triad type model are unlike the original, with nonsignificant main effects of session and triad type and a non-significant interaction (see **S.8 Results in winsorized Subsample** for statistics). Dependency in the famous person triad condition in session 1 for this winsorized sample was not significantly correlated with dependency in the famous person triad condition in session 2 when controlling for dependency in the famous place TRIADs condition in session 1 and session 2 ( $r = 0.001$ ,  $t(13) = 0.007$ ,  $p = 0.99$ ). Dependency in the famous place

triad condition in session 1 was also not statistically significantly correlated with dependency in the famous place triad condition in session 2 when controlling for dependency in the person triad condition in session 1 and session 2 ( $r = -0.081$ ,  $t(13) = -0.454$ ,  $p = 0.65$ ). Thus, I am unable to reject the null hypothesis for either of my key statistical tests. Because I had to remove so many subjects, I may not have had sufficient statistical power remaining, and thus after this adjustment, my data are inconclusive with respect to my key hypothesis.

### 3.3.3 Content Biases in Overall Accuracy

Given the confound between overall accuracy and retrieval dependency, I decided to see if I could find evidence for intrinsic content biases in the overall accuracy data. Overall accuracy in the famous person triad condition in session 1 was significantly correlated with overall accuracy in the famous person triad condition in session 2 when controlling for overall accuracy in the famous place triad condition in session 1 and session 2 ( $r = 0.58$ ,  $t(56) = 5.283$ ,  $p < 0.001$ ). Conversely, overall accuracy in the famous place triad condition in session 1 was significantly correlated with overall accuracy in the famous place triad condition in session 2 when controlling for overall accuracy in the famous person triad condition in session 1 and session 2 ( $r = 0.540$ ,  $t(56) = 4.800$ ,  $p < 0.001$ ). Like with the analysis of retrieval dependency, I calculated a new measure “person accuracy bias” by subtracting overall accuracy in the famous person triad condition from overall accuracy seen in the famous place triad condition for each subject for each session. This measure essentially represents the slope of the lines seen in **Figure 10**. In **Figure 14a**, I plot person accuracy bias measured in session 1 against this person accuracy bias measured in session 2. If content bias in overall accuracy is an intrinsic property of individuals, then I would expect this person accuracy bias measured in session 1 to be positively correlated with person accuracy bias measured in session 2 -- indicating that participants remain consistent from session 1 to session 2. This was the case in my sample ( $r = 0.45$ , 95% CI [0.22, 0.63],  $t(58) = 3.80$ ,  $p < .001$ ). In **Figure 14b**, I plot participants’ cued recall accuracy averaged over sessions in a scatterplot with the x-axis representing accuracy in place triads and the y-axis accuracy in person triads. Subjects that lie above and to the left of the diagonal (the red space) display a bias towards recalling associations in famous place triads and subjects that lie below and to the right

of the diagonal (the blue space) display a bias towards accurately recalling associations from famous person triads. Observing this space closely, it is evident that there is an overall episodic memory capacity with participants displaying overall more accurate retrieval than others. In other words, participants are scattered along the lower left to upper right diagonal of this space. There is also evidence that participants vary off this diagonal, with some participants displaying a famous person or famous place bias in their overall accuracy. However, it appears that most of this variability lies below and to the right of this diagonal, reflecting the strong main effect of accuracy in the famous place condition compared with the famous person condition.

### Overall Accuracy

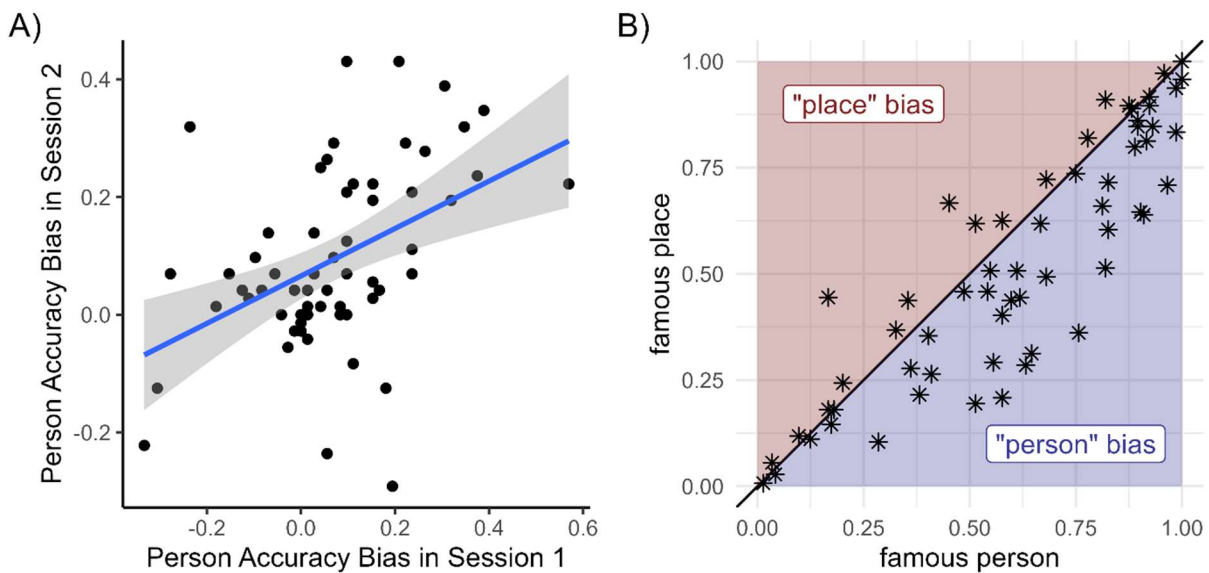


**Figure 14:** *Content Biases in Overall Accuracy.* A.) Content biases in overall accuracy replicate are consistent over sessions, such that participants that have a content bias in session 1 tend to have a similar content bias in session 2. B.) Participants are biased to accurately recall associations in famous person triads compared with famous place triads. Bias = cued recall accuracy in famous person triads – cued recall accuracy in famous place triads.

Because most participants showed a bias favoring memory for person triads, I additionally wanted to test whether there were other stimulus characteristics that could account for the retrieval accuracy results. Before completing the experiment, I asked participants to report their level of familiarity with each famous person and each famous place stimulus in the

experiment. As part of my experimental protocol, I selected the 14 (out of 28) most familiar famous person and famous place stimuli to serve as experimental stimuli for each participant (see **3.2.3 Procedure**). As a first step, I fit a linear mixed model to predict familiarity rating with session [session1, session2] and stimulus\_type [famous person, famous place]. The model included stimulus\_type as random effects (formula: ~stimType | subject\_id). The model's total explanatory power was substantial (conditional R<sup>2</sup> = 0.83) and the part related to the fixed effects alone (marginal R<sup>2</sup>) as 0.16. Within this model, the effect of session [session2] was statistically non-significant and negative ( $\beta = -4.49\text{e-}03$ , 95% CI [-0.13, 0.12],  $t(232) = -0.07$ ,  $p = 0.944$ , Std.  $\beta = -5.27\text{e-}03$ ), the effect of stimulus\_type [famous places] was statistically significant and negative ( $\beta = -0.58$ , 95% CI [-0.77, -0.39],  $t(232) = -6.08$ ,  $p < .001$ , Std.  $\beta = -0.68$ ), and the effect of session [session2]  $\times$  stimulus\_type [famous places] was statistically significant and negative ( $\beta = -0.20$ , 95% CI [-0.37, -0.02],  $t(232) = -2.17$ ,  $p = 0.031$ , Std.  $\beta = -0.23$ ). This model suggests that famous people were more familiar to participants than famous places. This effect was stronger in session two.

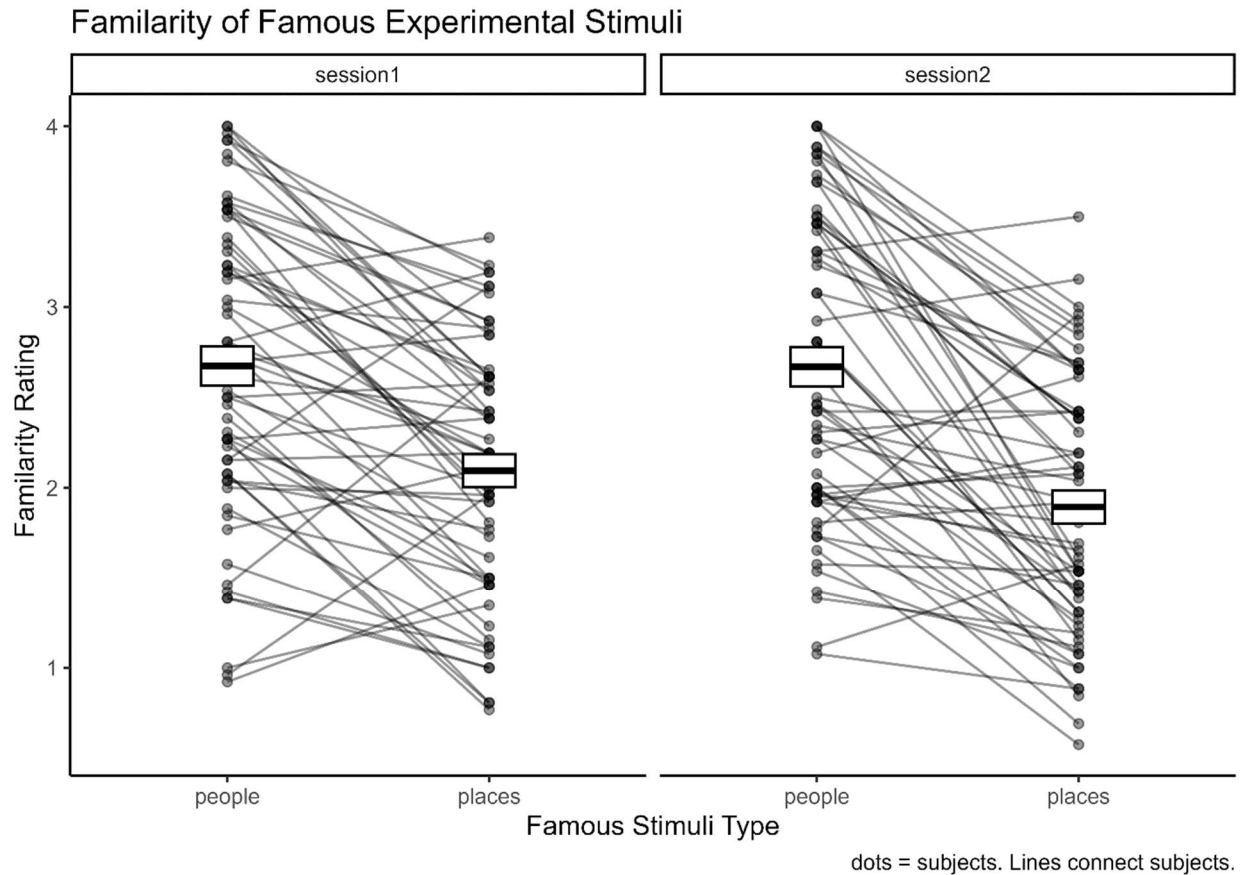


**Figure 15.** *Familiarity of Famous Experimental Stimuli.* My famous person stimuli were rated as much more familiar than my famous place stimuli.

Given that the famous people in my experiment were more familiar than famous places (see **Figure 15**) and given that overall cued recall accuracy was greater for the famous person triads compared with the famous place triads (see **Figure 10**), I was interested in determining if familiarity moderated the effect of overall recall accuracy on triad type. To determine if familiarity moderated the effect of triad type [person triad, place triad] on recall accuracy, I fit a logistic mixed model to predict overall accuracy with triad\_type, session and familiarity\_rating (formula:  $\text{accuracy} \sim \text{triad\_type} * \text{session} + \text{familiarity\_rating}$ ). The model included condition and rating as random effects (formula:  $\sim \text{condition} * \text{rating} \mid \text{subject\_id}$ ). The model's total explanatory power was substantial (conditional  $R^2 = 0.58$ ) and the part related to the fixed

effects alone (marginal R<sup>2</sup>) was 0.01. Within this model, the effect of triad\_type [famous place] was statistically significant and negative ( $\beta = -0.36$ , 95% CI [-0.59, -0.13],  $p = 0.002$ ; Std.  $\beta = -0.36$ , 95% CI [-0.59, -0.13]), the effect of session [session2] was statistically non-significant and negative ( $\beta = -0.03$ , 95% CI [-0.14, 0.09],  $p = 0.634$ ; Std.  $\beta = -0.03$ , 95% CI [-0.14, 0.09]), the effect of familiarity\_rating was statistically significant and positive ( $\beta = 0.20$ , 95% CI [0.11, 0.29],  $p < .001$ ; Std.  $\beta = 0.21$ , 95% CI [0.11, 0.31]), and the interaction effect of triad\_type [famous place]  $\times$  session [session2] was statistically non-significant and negative ( $\beta = -0.15$ , 95% CI [-0.31, 3.59e-03],  $p = 0.056$ ; Std.  $\beta = -0.15$ , 95% CI [-0.31, 3.55e-03]). This model suggests that familiarity with a stimulus does not completely moderate the effect of triad type on overall cued recall accuracy. In other words, accuracy in famous person triads is greater than accuracy in famous place triads even after accounting for the difference in familiarity.

### 3.4 SUMMARY

In summary, in Chapter 3 I report the results of an online behavioral experiment designed to test a neuroscience inspired hypothesis of the organization of individual differences in episodic remembering. Previous research on individual differences in memory has largely progressed independently of the parallel lines of research on the neurobiology underlying episodic memory (but see Ngo et al., 2021). Recent research on the neural architecture underlying episodic memory suggests that the default mode network (particularly its ventral components linked with the medial temporal lobes) supports the phenomenon. Furthermore, the default mode network itself is likely composed of highly related subnetworks that support different aspects of episodic remembering – a dorsal default mode subnetwork that is more involved with social-emotional aspects of cognition and a more ventral subnetwork that is

involved in visual-spatial aspects of cognition. The organization of the network underlying episodic remembering should inform how individuals differ in their episodic memory capacity. Specifically, I hypothesize that individuals should have at least three different episodic memory capacities – a social-emotional episodic memory capacity that relies on the efficient functioning of dorsal default mode subnetwork, a visual-spatial episodic memory capacity that relies on the efficient functioning of the ventral default mode subnetwork, and an overall episodic memory capacity that results from the efficient functioning and cooperation of the two related subsystems.

To test this hypothesis, I had a sample of 60 subjects complete a multielement episodic retrieval task. In this task, participants studied triads that contained either famous people or famous places across two sessions. The key measure from this memory task was retrieval dependency – a measure that has previously been used as an individual differences measure (Ngo et al., 2021) and a measure that I believed would closely index functioning of the ventral default mode network. The results of my experiment initially provided strong support for my hypothesis, but with a strong caveat. Upon further inspection of my data, I realized that the retrieval dependency measure – the key measure I used to test my hypothesis – had an unexpected inverted U-shaped relationship with overall cued recall accuracy. I showed that this was likely due to a mathematical necessity in the retrieval dependency calculation. After attempting to scrub my data of this confound, I found that evidence for my hypothesis was much weaker in the context of a much smaller sample size. Turning to overall accuracy, there was a strong bias for accurately retrieving association in famous person triads which persisted even when controlling for the fact that the famous person stimuli were rated as more familiar to participants than the famous place stimuli. Overall, the results were largely inconclusive, and it remains an open

question if individuals systematically differ in their ability to holistically recall different types of information from memory.

## DISCUSSION

I had three key aims for this dissertation. My first aim was to dissociate region-specific from network-wide contributions to episodic retrieval success in brain regions previously related to episodic cognition. I found that trialwise activation clustered into ventral and dorsal subnetworks and that, for the most part, these brain regions did *not* make region-specific contributions to episodic retrieval outcomes. Instead, these regions made subnetwork-wide contributions, with the ventral subnetwork predicting memory outcomes above and beyond the dorsal subnetwork, but not vice versa. My second aim was to investigate the neural basis of individual differences in episodic memory ability, with a specific focus on functional connectivity. In a series of hypothesis driven analyses, I found that functional connectivity of networks traditionally associated with episodic retrieval success was *not* related to individual differences in episodic memory ability. I did find, however, that a pattern of functional connectivity across the entire brain characterized by decoupling of somatomotor regions from default mode regions was predictive of episodic memory ability. Finally, my third aim was to test a neuroscience inspired hypothesis on how individuals differ in their memory ability. I hypothesized on the basis of cognitive neuroscience work that individuals would display content biases in their memory, such that some individuals would be better at retrieving events that are centered around famous persons while other individuals would be better at retrieving events that are centered around famous places. The results of my experiment were ultimately inconclusive, leaving open the possibility that individuals have different capacities for remembering events

involving different types of information. I will discuss the results of each of these studies in turn and conclude with a discussion of the broader implications of the research and future directions.

#### 4.1 INTEGRATING REGIONAL AND NETWORK APPROACHES

The results of Chapter 1 support the presence of dissociable subnetworks within the PM network (Andrews-Hanna et al., 2010; Barnett et al., 2021; Buckner & DiNicola, 2019; Cooper et al., 2021a). Previous studies have shown evidence for highly-related subnetworks during rest (Andrews-Hanna et al., 2010; Barnett et al., 2021) and during movie-watching (Cooper et al., 2021a). Our results extend these findings, showing evidence that a similar subnetwork organization explains the trialwise involvement of PM regions during retrieval of multi-feature events. Our models also showed that the coactivation of the vPMN makes contributions to memory quality that go above and beyond those made by coactivation of the dPMN (see **Figure 3**). The vPMN has previously been shown to modulate its connectivity in response to event transitions, and individual differences in episodic memory ability have been linked to dynamic changes in vPMN connectivity during movie watching (Cooper et al., 2021a). The vPMN regions have also been shown to represent similar information during a memory-guided decision-making task (Barnett et al., 2021). The vPMN is strongly related to episodic retrieval and autobiographical remembering, while portions of the dPMN have been linked to mentalizing about the mental states of others (Andrews-Hanna, Saxe, et al., 2014; Andrews-Hanna, Smallwood, et al., 2014). Additional evidence suggests that the vPMN may be particularly responsive to remembering and orienting towards visual-spatial information and the dPMN towards people (Peer et al., 2015; Silson et al., 2019) and the thematic elements of autobiographical remembrances (Gurguryan & Sheldon, 2019).

The fact that the vPMN in our dataset was uniquely related to overall memory quality could be reflective of our experimental design, which required the recollection of fine grained visual-spatial details. At least two other aspects of our results seem to support this conclusion. First, memory for the scene feature—which in our experimental design requires the recollection of the fine grained visual-spatial details—loaded most strongly onto our overall memory quality factor (see **Table 3**). Second, the vPMN significantly contributed only to scene feature memory in our memory feature models (see **Table 5**). The specific role of the vPMN in supporting scene memory is consistent with recent frameworks proposing that the anterior hippocampus and anterior regions of the neocortex support memory for coarse, gist-level, schematic details in memory whereas posterior regions of the hippocampus and the neocortex—including PHC, RSC, and posterior AG— support memory for fine grained perceptual details, especially spatial details (Robin & Moscovitch, 2017; Sekeres et al., 2018; Sheldon et al., 2019). In contrast, the dPMN was negatively correlated with scene memory and tended to be positively related to sound memory, which may have been mediated by relatively coarse representations of the sound valence that were sufficient to drive memory for this feature.

When taking into consideration the covariance among PM network regions, we did not find much evidence for independent, region-specific contributions, suggesting that the network-level effects could adequately account for their roles in predicting memory outcomes. Nevertheless, we had expected that there might be more region-specific effects, based on evidence that many of these regions play specialized roles in recollection. There are several reasons for why we did not see the region-specific effects that we had hypothesized. One possibility is that there is something unique about our experimental paradigm that did not allow us to observe region-specific contributions. For example, the hippocampus may have emerged as

making a region-specific contribution if we had operationalized our measure of memory success to target the hippocampus' proposed function more specifically. The hippocampus' contribution to predicting overall memory success may be subsumed by the network level contribution, but this may not be the case if the measure was more specific to successful pattern completion, for instance. Another possibility lies in how we modeled the neural response. In the current report, we modeled the neural response by assuming that it was transient, starting at the presentation of the memory cue during our 'remember' periods. Previous research suggests that the memory-related neural response in the angular gyrus is not transient with respect to the onset of recall, but is instead sustained throughout the duration of the recall period (Vilberg & Rugg, 2012, 2014). It is possible that modeling a sustained response throughout the recall period would allow for the identification of region-specific contributions of the angular gyrus. Our experimental design only allowed for 4 seconds for recall, so the responses captured here are likely to be similar to the transient responses seen in Vilberg & Rugg (2012, 2014). As an additional test of this possibility, all of our models were rerun using single trial estimates modeling the entire 4-second retrieval period. The key results of the current report remained unchanged. Another possible explanation is that the identification of region-specific contributions within our framework assumes that the operations and representations of individual regions can be decoupled. However, in a typically functioning brain, the activity of two brain regions may be highly correlated if the involvement of one brain region depends on the output of the other, even if they are performing otherwise separate functions. Thus, although the current results suggest strong evidence for network-level effects in the context of the typically functioning brain, the roles of individual brain regions may be better revealed in studies documenting the consequences of region-specific disruptions, such as studies of patients with focal brain damage (Corkin, 2002; Moscovitch & Winocur, 1992), or

in electrophysiological studies that can resolve fine temporal differences in information processing among regions in the same network (Fox et al., 2018; Treder et al., 2021).

The one region in which we found a region-specific effect was the MPFC. The MPFC has been commonly described as part of the PM network (Ritchey & Cooper, 2020; Rugg & Vilberg, 2013) and is thought to support the formation and retrieval of gist level, schema-based representations (Robin & Moscovitch, 2017; Schlichting & Preston, 2015; Sekeres et al., 2018; van Kesteren et al., 2012). Our results indicated that, after accounting for MPFC's participation in the dPMN subnetwork, the MPFC had a region-specific negative relationship with memory quality. The negative relationship between MPFC and memory success is not without precedent, with fMRI experiments of memory encoding often finding that less MPFC activation is associated with greater subsequent memory, particularly for objective compared to subjective memory judgments (Maillet & Rajah, 2014). This MPFC activation is thought to be associated with mind-wandering or off-task thoughts (Christoff et al., 2009) which interferes with the formation of a lasting memory trace. The current experiment, however, was primarily focused on retrieval where previous reports have indicated a positive relation between MPFC activity and measures of subjective memory success (H. Kim, 2016; McDermott et al., 2009; Spaniol et al., 2009). One possible explanation of this surprising result is that it reflects the role of the MPFC in schema-based memory. Our experimental design relies on participants arbitrarily associating event elements at a fine level of detail. If participants were relying on a schema to meet our task demands, this could potentially lead to decreased performance on the fine-grained memory measures in our experiment. However, in the absence of any independent measures of schema use in our experiment, another plausible interpretation is that the observed negative relationship may be the result of a statistical artifact. In the current study, the MPFC was only weakly

correlated with the quality with which events were remembered but was still positively correlated with other regions of the network (see **Table 1**). It was only after controlling for its subnetwork participation that we saw a strong negative contribution to memory. Thus, the result seen here could be the result of a conditioning-on-a-collider bias, also known as *Berkson's paradox* (Berkson, 1946; Lübke et al., 2020). In this paradox, two variables that do not have a statistical association are induced to have a negative association by statistically controlling for a variable that they both cause. In the current scenario, it could be the case that MPFC activation and memory quality are (at least in part) correlated with increases in PM network coactivation, but memory quality and MPFC activation are not related to one another.

The SEM methodology applied in Chapter 1 has several distinct advantages. Firstly, the current SEM approach has an advantage over previous reports of brain-behavior correlations in that it can simply and simultaneously capture the network-level and region-specific contributions of brain regions to behavioral phenomena. Second, the current report expanded upon previous deployments of this methodology (Bolt et al., 2018) by applying a multilevel SEM to simultaneously model within-subjects and between-subjects variation in the BOLD response, seeking to relate trial-by-trial, within-subjects variability in BOLD response to trial-by-trial variability in memory while controlling for individual differences. Thirdly, our dataset has a distinct advantage over previous studies of episodic remembering because it incorporates multiple measures of the quality of retrieval of an episode. This allowed us to model overall memory quality as a latent variable loading onto our measures of memory for 3 different features of each episode. By operationalizing memory success in this way, we were able to capture trial-to-trial variability in the joint remembering of event features. This is key, because holistic

recollection is thought to be a key characteristic separating episodic remembering from other forms of memory (Tulving, 1983).

Our SEM approach is related to, but distinct from, other methods for relating regions and networks to episodic remembering. For example, previous studies have used data-driven, hierarchical clustering methods to parcellate PMN subnetworks (Andrews-Hanna et al., 2010; Barnett et al., 2021; Cooper et al., 2021a), but did not relate trialwise coactivation within those subnetworks to episodic remembering. Another set of related methodological approaches is effective connectivity approaches. Specifically, some effective connectivity approaches also use SEM, but they use SEM to attempt to test hypothetical models of the underlying causal relations amongst regions of interest (e.g., McIntosh & Gonzalez-Lima, 1994; see McIntosh & Protzner, 2012 for review). The latent variable modeling approach applied here, in contrast, does not attempt to make such causal inferences. Instead, our approach uses a latent variable to capture the coactivation seen within a network and relates this coactivation to a behavioral variable of interest. Lastly, the current approach is conceptually similar to partial least squares (PLS) analyses (Krishnan et al., 2011; McIntosh et al., 1996; McIntosh & Lobaugh, 2004). PLS involves maximizing the covariation between signal extracted from voxels of the brain and behavior, extracting latent variables reflecting distributed coactivation across the brain that explains variance in some behavior of interest. The SEM approach used in the current report is similar to PLS in that it also estimates a latent variable using the covariation of regional activation profiles but has the advantage of being exclusively hypothesis driven and computationally and conceptually simpler. Many PLS applications (but not all Krishnan et al., 2011), in contrast, are data driven in nature. Additionally, PLS typically operates on all the

voxels collected during the course of an experiment, whereas the current approach operates on a set of hypothesized ROIs.

This chapter makes an important contribution to the literature on the role of the PM network in episodic remembering. It does, however, have its limitations. Our multilevel approach allowed us to model trialwise neural activation and behavioral profiles while controlling for individual differences. Multilevel SEM, however, also allows researchers to build models of individual differences in neural activation and behavior beyond simply controlling for this important source of variability. We did not attempt to model individual differences in the current report in large part because our dataset would be underpowered to do so. Future research could utilize larger sample sizes to model individual differences related to particular participant characteristics (see Bolt et al., 2018 for an SEM application to individual differences). Additionally, the current analysis was focused on a set of *a-priori* ROIs that were the same across individuals. Although this is a good starting point and is a strategy often adopted by researchers, recent research in high-precision functional mapping suggests that individually defined ROIs may provide more accurate insights into network organization and function (Buckner & DiNicola, 2019; Gilmore et al., 2021). Finally, although our memory measures captured multiple aspects of each episode (specifically, memory for multiple episodic features), they may not have adequately captured the functioning of core alliances within the PM network (Ritchey & Cooper, 2020).

## **4.2 FUNCTIONAL CONNECTIVITY AND MEMORY ABILITY**

Chapter 2 examined how individual differences in episodic memory ability related to intrinsic functional connectivity focusing specifically on the DMN-C subnetwork that has been

strongly implicated in episodic remembering (Ritchey & Cooper, 2020). Across a sample of 243 individuals, we found little evidence that DMN-C connections were related to episodic memory ability. We also found little evidence that average strength of hippocampal connections was related to episodic memory ability. We did find evidence, however, that network-wide patterns of functional connectivity could predict individual differences in memory. These predictive models were robust to analytic decisions and remained significant after controlling for age, self-reported biological sex, and average in-scanner movement. Probing these predictive models further revealed that superior memory ability was characterized by a decoupling of Somatomotor B regions and Default A regions and an increase in communication between Somatomotor B and visual processing regions. Together, these results suggest that there is limited evidence connecting individual differences in memory to measures of intrinsic functional connectivity among regions typically associated with memory function.

Contrary to my hypotheses, I found little evidence that the strength of intrinsic functional connections of DMN-C and hippocampal regions supports episodic memory ability. This finding fails to conceptually replicate previous reports that suggest that changes in functional connectivity of default mode (King et al., 2015; Lin et al., 2021; Sneve et al., 2017; van Buuren et al., 2019) and hippocampal regions (Touroutoglou et al., 2015; L. Wang, LaViolette, et al., 2010; L. Wang, Negreira, et al., 2010) scales with episodic memory ability. We believe that there are several possible reasons why this might be the case. One reason could be that the strength of “intrinsic” DMN-C and functional connections are not related to episodic memory ability, but the strength of “active” functional connections are. Measures of intrinsic functional connectivity, often obtained from resting-state scans that do not include an explicit cognitive task, have been widely used to study individual differences in cognition. Strong evidence has accumulated over

the years to suggest that these measures are related to behavioral phenotypes. Studies of the resting-state have found that there is a normative pattern of functional connections in the brain, such that brain regions form stable networks (between 7-17, Yeo et al., 2011). Recent work suggests that the majority of variability in the strength of these connections is attributable to stable individual differences away from this group-level pattern (as opposed to variation attributable to cognitive task or day-to-day variation; (Gratton et al., 2018). Furthermore, the strength of intrinsic connections has been shown to be predictive of a number of different behavioral phenotypes including neuroticism and extraversion (Hsu et al., 2018), trait-level anxiety (Z. Wang et al., 2021), fluid intelligence (Finn et al., 2015), creativity (Beaty et al., 2018), sustained attention (Rosenberg et al., 2016), and working memory ability (Avery et al., 2020). Patterns within the intrinsic functional connectome are so identifiable that they can be used to identify an individual from a group, acting a sort of “brain fingerprint” (Finn et al., 2015). Thus, it seemed reasonable to hypothesize that individual differences in intrinsic functional connectivity would be related to memory ability.

Other work critiques this line of research, however, suggesting that “intrinsic” functional connectivity calculated in the resting-state is less useful for predicting individual differences compared with “active” functional connectivity calculated while participants complete cognitive tasks (Greene et al., 2018, 2020; Lin et al., 2021). An analogy would be examining two cars and trying to determine which one is the better race car — you may not be able to tell the difference between an expensive race car and a Toyota civic by looking under the hood when they are sitting in a garage, but you may be able to tell the difference when you examine how their parts perform when engaged in a race. Supporting this idea, Greene and colleagues (2018) performed an analysis of a large openly available dataset where they attempted to predict individual

differences in fluid intelligence using functional connectivity calculated during a pair of resting state scans and functional connectivity calculated during each of 7 different cognitive task scans. Greene and colleagues (2018) showed that predictive performance improved dramatically when using the functional connectivity calculated during the cognitive tasks (from about 6% explained variance for resting-state connectivity to 20% explained variance for task connectivity), despite the fact that the cognitive tasks were not direct measures of fluid intelligence and had about half the amount of data compared with the resting-state task scans. Further work from Greene and colleagues (2020) suggests that this increase in predictive utility is due to the fact task scans increase inter-subject consistency in brain connectivity to an optimal point, whereby noise is minimized without obscuring important individual differences. The results of one of our supplemental analyses support these findings, with out-of-sample performance being significantly worse using the resting-state scan compared with the movie-watching or sensorimotor task data. Lin and colleagues (2021) came to a similar conclusion as Greene and colleagues (2018, 2020), suggesting that the functional connectomes calculated during encoding have greater predictive utility for predicting memory ability compared with resting-state scans. A closely related critique also questions the use of resting state networks for understanding how the brain supports cognition. This critique specifically puts forth the idea that the most important unit of analysis when relating brain measures to cognition is not networks identified via low-frequency coactivation during rest, but networks identified via high frequency coupling while participants complete highly controlled cognitive tasks (Cabeza & Moscovitch, 2013; S. W. Davis et al., 2017; Moscovitch et al., 2016). These high frequency couplings have been termed “process specific alliances” or PSAs. PSAs are small “teams” of brain regions that dynamically assemble to support a very specific cognitive operation. Key to the definition of

PSAs that differentiates them from resting-state networks is the rapidity with which they assemble and disassemble. Additionally, these PSA are often composed of nodes from resting-state networks, but can often straddle resting-state networks definitions. For example, a PSA involving the hippocampus and the left ventrolateral prefrontal cortex is thought to support successful episodic encoding (e.g., Wing et al., 2013), despite the fact that hippocampus is typically a member of the default mode network and left ventrolateral PFC is not (S. W. Davis et al., 2017). Thus, it could be the case that individual differences in behavior manifest themselves in individual differences in the strength of these high frequency and cognition specific PSAs and not in strength of low-frequency and cognition agnostic resting state networks. Thus, although we did not find a relationship between memory ability and intrinsic (i.e., task-independent) measures of functional connectivity in memory related brain regions, we hypothesize that this relationship may only be apparent when measuring brain activity while participants complete a memory-related task.

While we did not find evidence that hippocampal or DMN-C connections were related to memory ability, we did find that a multivariate brain-wide pattern of functional connectivity could predict memory ability reliably out-of-sample. Our predictive analyses suggest that the brains of superior rememberers are characterized by decoupling of somatomotor regions and DMN-A regions and increased communication between somatomotor regions and visual processing regions. This decoupling of default and sensory regions is in line with previous results from Sneve and colleagues (2017) who likewise showed evidence the superior rememberers were characterized by decoupling between default mode and sensory networks. However, contrary to this pattern, other studies have shown that increases in DMN connectivity are related to episodic memory ability. King and colleagues (2015), for example, showed that the

brains of superior rememberers were characterized by an increase in functional connectivity between hippocampal and DMN-C regions and the rest of the brain during episodic retrieval tasks. Van Burren and colleagues (2019) showed that lower MTL-DMN connectivity and higher DMN-frontal-parietal control regions predicted episodic memory ability. Lin and colleagues (2021) performed a similar computational lesion approach to the one performed in Chapter 2 and showed that the removal of any one network resulted in negligible decrements in predictive power, suggesting that the information contained within the functional connectome is widely distributed. What is clear from the results of Chapter 2 and the literature to date is that information about memory ability is likely contained within the functional connectome beyond brain networks classically linked to episodic remembering. The exact pattern of whole brain connectivity that predicts memory ability, however, remains inconsistent from study to study.

An important factor that may have influenced our results is our choice of memory measure. Here, we used a standard neuropsychological measure of memory that assessed an individual's ability to recall the details of a written short story – the logical memory subtest of the Wechsler Memory Scale (Wechsler, 1999). The logical memory subtest of the Wechsler Memory Scale was chosen because it was available for the largest number of subjects in the CamCan dataset, compared to other included memory measures, and this measure has been previously shown to correlate with individual differences in brain activity in response to event boundaries during the CamCan movie watching scan (Reagh et al., 2020). Reliance on a single memory measure to capture an individual's memory ability, however, may be problematic given previous research suggesting that individuals have aptitudes for different types of memory tasks (Unsworth, 2019). We speculate that differences in how memory ability is operationalized could explain the mixed state of the literature – all of the previous research relating individual

differences in memory ability and functional connectivity have taken a unique approach to operationalizing memory ability (King et al., 2015; Lin et al., 2021; Sneve et al., 2017; van Buuren et al., 2019). King and colleagues (2015) and Sneve and Colleagues (2017) relied on performance in source memory recognition tasks; Lin and colleagues (2021) relied on performance on a remember/know/new recognition memory paradigm; van Burren and colleagues (2019) relied on performance on an object-location memory task; Setton and colleagues (2022) used the number of internal details generated during an autobiographical memory interview. It is currently unclear how performance on these different memory tasks relates to one another. Future research on individual differences in memory ability should, ideally, use multiple memory measures to get an unbiased measure of individuals' overall memory ability.

While these previous studies have considered individual differences in objective evaluations of participants' memory, other studies have looked at measures of individuals' subjective evaluations of their own memory when relating individual differences to brain function (Petrican et al., 2020; Sheldon et al., 2016). Sheldon and colleagues (2016), for example, examined the relationship between the strength of functional connectivity of the parahippocampal cortex and subjects reports of episodic memory tendencies measured by the Survey of Autobiographical Memory (SAM) survey (Palombo et al., 2013). The SAM measures participants' self-reported mnemonic traits, measuring their tendency, for example, to remember specific event and contextual details when recalling events (episodic subscale) versus their tendency to remember facts about oneself, events, or the world that lack contextual detail (semantic subscale). There is some evidence that individual differences in self-reported mnemonic traits measured by the episodic subscale of the SAM relies on a similar resting-state

functional connectivity profile as individual differences measured using a visual, laboratory based episodic memory task (Petrican et al., 2020). Future work should consider the relationship between subjective and objective measures of memory function (e.g., Cooper & Ritchey, 2022), as well as how these measures relate to individual differences in brain function.

Another important consideration for individual differences research is how to approach controlling for covariates of no interest. Here, we controlled for the influence of age, sex, and subject motion. Subject motion has long been known to be a major source of variability in functional connectivity (Power et al., 2012). Far fewer reports, however, attempt to control for age and sex when doing individual differences research. Age, for example, is known to have a strong relationship with intrinsic functional connectivity (Dosenbach et al., 2010) and with various measures of personality and cognition. Recent research also supports the idea that males and females engage different neural networks when remembering information (Spets et al., 2019; Spets & Slotnick, 2021). If researchers are interested in the direct relationship between functional connectivity and memory, we feel it is crucial to control for age even in age restricted samples of younger adults. In addition to statistical controls for both age and sex, we additionally attempted to maximize our statistical power by 1.) using a large openly available dataset and, crucially 2.) collapsing data across functional runs when calculating the functional connectome. This last point we feel is what really sets our analysis apart from previous literature. We were persuaded by recent findings suggesting that intrinsic individual differences dominate task differences in terms of variance explained in functional connectivity and findings that showed that 6-8 minutes of data is often underpowered for detecting a functional connectome that is intrinsic to individuals – an assumption that previous studies have made when utilizing a single resting-state scan.

An intriguing future direction is to look at other *facets* of brain connectivity and how they may be related to episodic memory ability. There are at least three facets of brain connectivity that could theoretically support individual differences in cognition: variability in connectional strength, variability in the spatial localization of brain regions, and variability in large-scale network topology (i.e., large scale networks have different sets of constituent nodes across subjects (Gordon & Nelson, 2021)). The current study, like many of studies that have come before, focused on how variability of the *strength* of functional connections related to individual differences in memory ability. Recent work, however, suggests that there are substantial individual differences in the *size* and *organization* of functional brain areas (Gordon, Laumann, Adeyemo, et al., 2017; Gordon & Nelson, 2021; Kong et al., 2019; Laumann et al., 2015). Gordon and Nelson (2021) display a striking example of this type of idiosyncrasy, where the posterior medial precuneus node of the default mode network for one subject is translated along the cortical surface such that the node wraps around to the lateral side of the brain. These differences in the spatial topography of functional nodes on the cortical surface also appear to have behavioral relevance. Kong and colleagues (2019) estimated individual specific network topologies and showed that they could successfully predict behavioral outcomes by using both similarities in overall network topology and similarity in the size of different networks as predictors. Recent work has also identified individual differences in large-scale network topology, such that nodes that are the same across individuals are a part of different large scale networks (Gordon & Nelson, 2021; Laumann et al., 2015; Seitzman et al., 2019). Laumann and colleagues (2015) for example analyzed data from a case study where a single individual was scanned over 100 times. They showed that this individual has a small cortical region in the lateral frontal cortex that is a part of the frontal-parietal control network in most individuals, but

for this individual is a part of the cingulo-opercular network. This phenomenon has recently been termed a “network variant” (Seitzman et al., 2019). Network variants appear to occur in specific regions of the brain, particularly in default mode regions, and are observed in some datasets in approximately 33% of individuals. Like with individual differences in node size and location, the behavioral relevance of these network variants is unclear (but see Kong et al., 2019). Another intriguing possibility is that individual differences in memory ability could be related to the presence or absence of network variants in default mode regions.

In conclusion, we found little evidence in support for a relationship between memory ability and intrinsic functional connectivity among cortical and hippocampal networks commonly associated with episodic memory. We did find a multivariate brain wide pattern of functional connectivity that was predictive of memory ability, characterized by decoupling of somatomotor regions from default mode regions. Our findings agree with previous research that suggests that information about memory ability is contained in functional connections in regions outside of regions classically linked to episodic memory. The exact nature of this brain connectivity pattern that predicts memory ability remains unclear. We believe this is due to variability in how memory ability is operationalized and the low power of previous studies both in terms of number of subjects collected and in the amount of data collected per subject. Future research on the relationship between individual differences in memory and functional brain networks should incorporate multiple measures to operationalize memory ability unbiased toward a particular task (Unsworth, 2019), collect a large amount of data (Gordon, Laumann, Adeyemo, et al., 2017; Marek et al., 2022), ideally task-related data (Greene et al., 2018), and examine facets of brain organization other than functional connectivity strength (Gordon & Nelson, 2021).

### 4.3 NEURAL INSPIRED ORGANIZATION OF MEMORY ABILITY

In Chapter 3 I reported the results of an online behavioral experiment designed to test a neuroscience inspired hypothesis of the organization of individual differences in episodic remembering. In general, the results were inconclusive, and it remains an open question if individuals systematically differ in their ability to holistically recall events centered around different types of information from memory. The study reported in Chapter 3 was focused on individual differences in memory based on the content of the memoranda, i.e., person and place information. Previous psychometric studies have looked at individual differences in performance for different types of memory content, but memory content was operationalized along different dimensions than the one used in Chapter 3. Some studies, for example, had participants complete tests for pictorial and verbal content (item recognition words vs item recognition pictures; Unsworth & Brewer, 2009) and others have had participants complete tests for nonsensical content and meaningful content (Carroll, 1993 “meaningful memory” vs “visual memory”; e.g., Hakstian & Cattell, 1974-- “associative memory” vs “meaningful memory”; Kelley, 1954 “route memory” vs “meaningful memory”). Evidence compiled across studies looking at the factor structure of memory abilities, however, is largely consistent with the idea of a hierarchical factor structure with an overall memory ability and separate abilities for different types of criterial tasks (Unsworth, 2019). It remains to be seen, however, whether there are individual capacities for remembering visuo-spatial versus socio-emotional information. In addition, prior studies have not investigated how memories are bound around different kinds of content, as we did here with the retrieval dependency measure (but see Ngo et al., 2021).

I chose the dependency measure for this experiment because this measure best captures the integrative, (re)constructive, multielement binding processes that are attributed to the default

mode network and the posterior medial network (Ritchey & Cooper, 2020). What is appealing about this measure is that it is described as being a “pure” measure of episodic binding that is independent of overall memory performance. Overall memory performance, relative to dependency, may be more likely to be driven by individual differences in motivation and attention paid during the task. Because the dependency measure accounts for overall memory performance in its calculation (Bisby et al., 2018; Horner & Burgess, 2013, 2014; James et al., 2020), I believed that it was also likely to be dissociable from nuisance variables like motivation, attention, and simple task engagement. It has also been successfully used in an individual differences context previously (Ngo et al., 2021). Chapter 3 of my dissertation discovered, however, that this measure is closely related to memory accuracy, displaying a quadratic relationship with dependency. A recent publication that performed a simulation study examining the statistical characteristics of 6 different retrieval dependency calculations supports my conclusion drawn here, noting that the retrieval dependency measure used here, although a valid way to measure dependency on average across conditions or subjects, is highly related to memory accuracy when used as an individual differences measure (Schreiner & Meiser, 2022). Future studies interested in testing this hypothesis should try and identify a behavioral measure that can capture the integrative, constructive, multielement binding processes of the default mode network independent of overall performance on the task.

In light of these observations, I decided to look for evidence for my hypothesis by looking at a secondary measure: overall cued recall accuracy. I did not find, however, strong evidence for my neuroscience inspired hypothesis when analyzing the overall performance measure. Although participants displayed a content-specific bias in their overall accuracy that replicated over sessions and was independent of overall performance, this content-specific bias

did not span the entire famous person, famous place space like my original hypothesis predicted. Instead, my overall performance findings suggest that participants displayed a consistent bias for remembering associations from famous person triads over famous place triads.

Why did the results of this overall accuracy analysis not turn out as predicted? One possibility is that the assumptions of my hypothesis were not met with this analysis – perhaps, for example, cued recall accuracy for associations from famous people and famous places is not a great indicator of dorsal and ventral DMN function respectively. Future studies would need to be run with behavioral measures that are more strongly related to ventral and dorsal PMN function respectively. Another possibility is that the overall accuracy measure was strongly related to participants' familiarity with the famous person and famous place stimuli used in this analysis. Follow up analyses suggested that this might be a possibility because the famous person stimuli used in my experiment were consistently rated as more familiar to participants and this fact partially explained why associations from famous person triads were remembered better than those from famous place triads. Future research should attempt to equate preexperiment familiarity with person and place triads to rule of a familiarity based explanation of the results.

Previous psychometric research suggests that individuals have particular capacities for different types of memory tests (see Unsworth, 2019 for review). In Chapter 3 of my dissertation, I tested an alternative hypothesis on individual differences in memory ability that was rooted in the cognitive neuroscience literature, although my findings were ultimately inconclusive. Specifically, the cognitive neuroscience literature suggests that episodic memory retrieval is supported by the default mode network, specifically two subnetworks of the default mode network that are closely related to the hippocampus and the medial temporal lobes. These two subnetworks of the default mode network are often linked to different cognitive operations that

differ on the specific operation and, importantly, on the content that is being processed. The more dorsal of the default mode subnetworks, for example, is often linked to tasks involved in theory of mind – a cognitive operation that relies on memory for and processing of a person and their mental states. The more ventral subnetwork, on the other hand, is often linked to tasks involved in spatial navigation – a cognitive operation that relies on memory for and the processing of complex, associative spatial layouts. Given this difference in cognitive operation of these mnemonic networks, I hypothesized that individuals would, as a result, systematically differ on a task that taxed the episodic memory system when episodic representations differed on the content that they contained – in this case a famous person and a famous place. This is because biological substrates should shape how individuals differ because biological substrates are what are ultimately responsible for our behavior.

To better understand the logic of this prediction, consider the following analogy in a different context – athletics. Human beings are capable of performing a range of athletic feats and these athletic feats are supported by the biology of our muscular system. The muscular system is composed of two interrelated but dissociable types of muscle fibers – fast twitch muscle fibers and slow twitch muscle fibers. These muscle fibers support two different types of physical activity – short bursts of physical effort and long, sustained amounts of physical effort respectively. This biological reality explains the ways in which athletes differ – some athletes, like weightlifters, are great at short bursts of athletic performance. Other athletes, like marathon runners, are great at long bouts of sustained athletic output. In other words, a good model of athletic ability is one in which we place athletes in an athletic space spanned by two dimensions related to the muscular system – a dimension composed of performance on short bursts of athletic performance and a dimension composed of sustained performance over longer periods of

time. I hypothesize that individual differences in memory ability should work in the same way as individual differences in athletic ability.

If given the opportunity, I would redesign the experiment by greatly expanding the amount of data collected per subject. Specifically, I would replicate the experiment over three sessions and I would include a number of additional memory tests that contained social-emotional and visual-spatial content. By having replications over more sessions, I can be more confident that I have precisely captured a true trait-like measure of participants' performance on particular tasks. More importantly, additional replications and more types of memory tests would allow me to use a structural equation model to more directly examine the fit of the hierarchical model implied by my hypothesis. Specifically, I would have participants complete memory tests that are common in the cognitive neuroscience literature, like old/new recognition, free recall, and the multi elemental continuous reconstruction task used in Chapter 1, on events that contain social-emotional and visual-spatial content. By having such a wide variety of memory tests completed across events that systematically varied in their type of content, I could compare the fit of at least three different theoretical models – a model that contains only a single overall memory capacity that loads onto all tasks, a model that contains two latent variables that load onto memory tests that contain social-emotional information and visual-spatial information respectively that themselves load onto a higher-order overall memory capacity latent variable, and a model that contains latent variables for the criterial tasks that is analogous to the one from Unsworth (2019).

#### 4.4 FUTURE DIRECTIONS & CONCLUDING THOUGHTS

Across three studies, I investigated the cognitive and neural bases of episodic memory. In Chapter 1, I found that brain regions related to episodic cognition formed ventral and dorsal subnetworks across the trials of an episodic retrieval task and that the contributions of these regions to episodic recollection were largely made at the subnetwork level. In Chapter 2, I found that individual differences in memory ability were not related to functional connectivity of brain regions related to memory, but instead related to a whole brain pattern of functional connectivity. In Chapter 3, I found inconclusive evidence when testing a neuroscience inspired hypothesis on how individuals differ in their memory ability. Given all of these findings, what are the running themes and takeaways from my dissertation? Where should research go from here? I believe that there are three themes that run throughout my dissertation that I discuss in turn: 1) The brain should be studied as a series of networks. 2) More cross talk needs to occur between cognitive neuroscience and psychometric research. Finally, 3) Future research needs to do a better job of addressing methodological issues to ensure replicability.

*The brain should be studied as a series of networks.* We have learned a lot about studying individual brain regions. Studies of neuropsychological patients with focal brain damage, including the famous patient H.M., have been highly influential on our current understanding of how the brain works. Future work, however, needs to continue to embrace the multidimensionality of the brain. Across Chapter 1 and Chapter 2 I took network-based approaches to studying the neural correlates of memory. Chapter 1 specifically challenges the idea that memory-related brain regions make unique contributions to memory retrieval outside of their participation in dissociable subnetworks. Chapter 2 follows up on and expands this idea in an individual differences context. When restricting analyses to only memory-related brain

regions, I was unable to build a model to predict memory ability. However, when incorporating information from the brain as a whole, I was able to predict memory ability. Both of these findings emphasize that although individual regions have strong links to cognitive processes (e.g., the hippocampus and memory), these regions do not support cognitive processes in isolation, and we must consider how they are embedded within a broader neural context (McIntosh, 2000).

*More cross talk is needed between cognitive neuroscience and psychometrics.* Across Chapter 2 and Chapter 3 I studied individual differences in episodic memory ability. In Chapter 2, I took a close look at the cognitive neuroscience literature, attempting to predict memory ability using neural data. In Chapter 3, I took a close look at the psychometric literature on memory ability. What surprised me is how little cross talk there was between these two lines of literature – cognitive neuroscientists often do not factor in the psychometric properties of the behavioral tasks that they use while psychologists often do not factor in the underlying brain networks that support their cognitive abilities of interest. If we take the philosophical stance that the brain gives rise to cognition, then we must consider how the brain is structured when thinking about how individuals differ. Future research should attempt to map out the psychometric properties of influential cognitive neuroscience of memory tasks, including the multi element retrieval task, mnemonic similarity task, classic recognition tasks, source memory/associative memory tasks, and autobiographical memory tasks. Interesting recent work towards this end suggests that cognitive neuroscientists should begin to predict phenotypes that express themselves as a pattern across behavioral variables, instead of just as a single variable (e.g., He et al., 2022). Future research in the psychology of memory should likewise incorporate what we know about neural networks into their models and theories of how individuals differ.

*Methodological issues present in psychology and cognitive neuroscience research.* Much cognitive neuroscience research has progressed without a thorough understanding of the basic psychometric properties of the behavioral tests and neural measures that they use. For example, we have limited understanding of how cognitive neuroscience memory tasks relate to one another, how reliable our memory tasks are, how many trials we typically need to achieve good reliability in our behavioral measures, and how much data we need to achieve reliability in our neural measures. This is beginning to change, however. Recent studies have shown that we need to collect more trials per subject for many tasks used in cognitive neuroscience studies in order to achieve adequate reliability (Kadlec et al., 2023). A recently completed study scanning the same individual 100s times has mapped out the reliability curve for functional connectivity measures (Laumann et al., 2015). Future cognitive neuroscience studies on individual differences in cognition should take note of these recent methodological demonstrations to collect a) more subjects, b) more/longer scans per subject, c) a sufficient number of trials per subject, and d) a variety of different tasks that are all thought to tap into a cognitive ability of interest.

In summary, the brain is simultaneously composed of large-scale brain networks and individual regions composing those networks. Future research on the cognitive neuroscience of memory should factor in the network organization of memory processes, as interactions among brain regions may be better predictors of memory quality than individual brain regions alone. These interactions may be best understood in a task context, as the intrinsic functional connectivity of memory networks does not appear to predict individual differences in overall episodic memory ability. Future work should seek to expand our knowledge of individual differences in both brain and behavior by conducting high quality replicable research that precisely measures individuals' brain function and their cognitive abilities.

## SUPPLEMENTAL MATERIAL

### S.1 Chapter 1 Model Summaries

Model	Description	Estimator	Chi-square (df)	RMSEA	CFI	SRMR_W	SRMR_B
Preliminary							
1	Neural Preliminary	MLR	2951.578 (36), $p < .001$	.144	.000	.047	.352
2	Behavioral Preliminary	WLSMV	20.882 (6), $p = .002$	.025	.958	.000	.634
Measurement models							
3	One Factor Neural	MLR	290.442 (20), $p < .001$	.059	.905	.063	.005
4	Two Factor Neural	MLR	90.096 (19), $p < .001$	.031	.975	.035	.003
5	Latent Variable Behavioral	WLSMV	0.163 (2), $p = .922$	.000	1.000	.001	.022
6	Stitched Model	WLSMV	534.782 (59), $p < .001$	.046	.974	.034	.043
8	Stitched Model Without Behavioral Latent Variable	WLSMV	683.198 (37), $p < .001$	.067	.965	.030	.000
Structural models							
7	Behavioral Latent Variable	WLSMV	See <b>Table 4</b> and <b>Figure 3</b>				
9	Without Behavioral Latent Variable	WLSMV	See <b>Table 5</b> and <b>Figure 4</b>				

**Supplemental Table 1.** *Summaries of all Models Included in Chapter 1.* The preliminary models were used to establish the appropriateness of the multi-level modeling approach for the neural (Model 1) and behavioral (2) data. The measurement models characterized the loading of individual measures onto their corresponding latent variables, separately for the neural (3, 4) and behavioral (5) data. Measurement models were stitched together into combined models with (6) and without (8) the latent variable for overall memory quality. Finally, structural models were used to test the paths connecting the neural and behavioral latent variables with each other and with the individual measures, for both the overall memory quality (7) and memory feature (9) analyses.

## S.2 Memory Feature Model Parameters

paramHeader	param	est	se	pval
VPMN.BY	RSC	0.627	0.006	< 0.001
	PHC	0.567	0.008	< 0.001
	PAG	0.608	0.007	< 0.001
DPMN.BY	MPFC	0.516	0.006	< 0.001
	PHIPP	0.438	0.008	< 0.001
	PREC	0.647	0.007	< 0.001
	PCC	0.685	0.004	< 0.001
	AAG	0.711	0.005	< 0.001
SCENE.ON	VPMN	0.277	0.043	< 0.001
	DPMN	-0.147	0.040	< 0.001
COLOR.ON	VPMN	-0.004	0.047	0.933
	DPMN	0.041	0.050	0.417
SOUND.ON	VPMN	0.006	0.043	0.882
	DPMN	0.114	0.059	0.052
DPMN.WITH	VPMN	0.634	0.008	< 0.001
SCENE.WITH	COLOR	0.340	0.025	< 0.001
	SOUND	0.313	0.026	< 0.001
	COLOR.WITH SOUND	0.232	0.026	< 0.001
Variances	VPMN	1	0	999
	DPMN	1	0	999
	PHIPP	0.809	0.007	< 0.001
	PREC	0.581	0.009	< 0.001
	PCC	0.531	0.006	< 0.001
	MPFC	0.734	0.006	< 0.001
	PHC	0.679	0.009	< 0.001

RSC	0.607	0.008	< 0.001
AAG	0.495	0.007	< 0.001
PAG	0.630	0.008	< 0.001

**Supplemental Table 2:** *Parameter Estimates for the within-subjects Part of our Feature Specific Memory Model* (Model 9; see **Figure 4**). This table was created using the R package *MplusAutomation* (Hallquist & Wiley, 2018). Parameter headers (paramHeader) follow standard Mplus syntax, where the ON keyword indicates a path parameter from the variable listed in the “param” column to variable listed in the “paramHeader” column, the BY keyword indicates a loading parameter (lambda  $\lambda$ ), and the WITH keyword indicates a covariance parameter (theta  $\theta$ ). param = parameter, est = standardized estimate, se = standard error, pval = p value. See **Figure 2** caption for abbreviations.

### S.3 FM RIPREP Boilerplate

The following is an edited version of the recommended boilerplate output by *fMRIPrep* after processing the data. The original boilerplate contained redundant descriptions of the operations performed by the software. What appears below is a detailed description of the processing steps with the redundant descriptions removed.

Results included in this manuscript come from preprocessing performed using *fMRIPrep 20.2.0* (Esteban et al., 2019), which is based on *Nipype 1.5.1* (Esteban et al., 2017; Gorgolewski et al., 2011).

#### S.3.1 Anatomical data preprocessing

A total of 1 T1-weighted (T1w) images were found within the input BIDS dataset. The T1-weighted (T1w) image was corrected for intensity non-uniformity (INU) with **N4BiasFieldCorrection** (Tustison et al., 2010), distributed with ANTs 2.3.3 (Avants et al., 2008), and used as T1w-reference throughout the workflow. The T1w-reference was then skull-stripped with a *Nipype* implementation of the **antsBrainExtraction.sh** workflow (from ANTs), using OASIS30ANTs as target template. Brain tissue segmentation of cerebrospinal fluid (CSF), white-matter (WM) and gray-matter (GM) was performed on the brain-extracted T1w using **fast**

(FSL 5.0.9; Zhang et al., 2001). Volume-based spatial normalization to one standard space (MNI152NLin2009cAsym) was performed through nonlinear registration with `antsRegistration` (ANTs 2.3.3), using brain-extracted versions of both T1w reference and the T1w template. The following template was selected for spatial normalization: *ICBM 152 Nonlinear Asymmetrical template version 2009c* (Fonov et al., 2009 TemplateFlow ID: MNI152NLin2009cAsym).

### S.3.2 Functional data preprocessing

For each of the 3 BOLD runs found per subject (across all tasks and sessions), the following preprocessing was performed. First, a reference volume and its skull-stripped version were generated from the shortest echo of the BOLD run using a custom methodology of *fMRIPrep*. A B0-nonuniformity map (or *fieldmap*) was estimated based on a phase-difference map calculated with a dual-echo GRE (gradient-recall echo) sequence, processed with a custom workflow of *SDCFlows* inspired by the `epidewarp.fsl` script and further improvements in HCP Pipelines (Glasser et al., 2013). The *fieldmap* was then co-registered to the target EPI (echo-planar imaging) reference run and converted to a displacements field map (amenable to registration tools such as ANTs) with FSL's `fugue` and other *SDCFlows* tools. Based on the estimated susceptibility distortion, a corrected EPI (echo-planar imaging) reference was calculated for a more accurate co-registration with the anatomical reference. The BOLD reference was then co-registered to the T1w reference using `flirt` (FSL 5.0.9, Jenkinson & Smith, 2001) with the boundary-based registration (Greve & Fischl, 2009) cost-function. Co-registration was configured with nine degrees of freedom to account for distortions remaining in the BOLD reference. Head-motion parameters with respect to the BOLD reference (transformation matrices, and six corresponding rotation and translation parameters) are estimated before any spatiotemporal filtering using `mcflirt` (FSL 5.0.9, Jenkinson et al., 2002). BOLD runs were slice-

time corrected using **3dTshift** from AFNI 20160207 (Cox & Hyde, 1997). The BOLD time-series (including slice-timing correction when applied) were resampled onto their original, native space by applying a single, composite transform to correct for head-motion and susceptibility distortions. These resampled BOLD time-series will be referred to as *preprocessed BOLD in original space*, or just *preprocessed BOLD*. A T2\* map was estimated from the preprocessed BOLD by fitting to a monoexponential signal decay model with nonlinear regression, using T2\*/S0 estimates from a log-linear regression fit as initial values. For each voxel, the maximal number of echoes with reliable signal in that voxel were used to fit the model. The calculated T2\* map was then used to optimally combine preprocessed BOLD across echoes following the method described in (Posse et al., 1999). The optimally combined time series was carried forward as the *preprocessed BOLD*. The BOLD time-series were resampled into standard space, generating a *preprocessed BOLD run in MNI152NLin2009cAsym space*. Several confounding time-series were calculated based on the *preprocessed BOLD*: framewise displacement (FD), DVARS and three region-wise global signals. FD was computed using two formulations following Power (absolute sum of relative motions, Power et al., 2014) and Jenkinson (relative root mean square displacement between affines, Jenkinson et al., 2002). FD and DVARS are calculated for each functional run, both using their implementations in *Nipype* (following the definitions by Power et al., 2014). The three global signals are extracted within the CSF, the WM, and the whole-brain masks. Additionally, a set of physiological regressors were extracted to allow for component-based noise correction (CompCor, Behzadi et al., 2007). Principal components are estimated after high-pass filtering the preprocessed BOLD time-series (using a discrete cosine filter with 128s cut-off) for the two *CompCor* variants: temporal (tCompCor) and anatomical (aCompCor). tCompCor components are then calculated from the top 2% variable

voxels within the brain mask. For aCompCor, three probabilistic masks (CSF, WM and combined CSF+WM) are generated in anatomical space. The implementation differs from that of Behzadi et al. in that instead of eroding the masks by 2 pixels on BOLD space, the aCompCor masks are subtracted a mask of pixels that likely contain a volume fraction of GM. This mask is obtained by thresholding the corresponding partial volume map at 0.05, and it ensures components are not extracted from voxels containing a minimal fraction of GM. Finally, these masks are resampled into BOLD space and binarized by thresholding at 0.99 (as in the original implementation). Components are also calculated separately within the WM and CSF masks. For each CompCor decomposition, the  $k$  components with the largest singular values are retained, such that the retained components' time series are sufficient to explain 50 percent of variance across the nuisance mask (CSF, WM, combined, or temporal). The remaining components are dropped from consideration. The head-motion estimates calculated in the correction step were also placed within the corresponding confounds file. The confound time series derived from head motion estimates and global signals were expanded with the inclusion of temporal derivatives and quadratic terms for each (Satterthwaite et al., 2013). Frames that exceeded a threshold of 0.5 mm FD or 1.5 standardized DVARS were annotated as motion outliers. All resamplings can be performed with *a single interpolation step* by composing all the pertinent transformations (i.e. head-motion transform matrices, susceptibility distortion correction when available, and co-registrations to anatomical and output spaces). Gridded (volumetric) resamplings were performed using `antsApplyTransforms` (ANTs), configured with Lanczos interpolation to minimize the smoothing effects of other kernels (Lanczos, 1964). Non-gridded (surface) resamplings were performed using `mri_vol2surf` (FreeSurfer).

Many internal operations of *fMRIPrep* use *Nilearn* 0.6.2 (Abraham et al., 2014), mostly within the functional processing workflow. For more details of the pipeline, see [the section corresponding to workflows in fMRIPrep's documentation](#).

## S.4 Global Signal Regression

Global signal regression (GSR) involves statistically removing the global mean signal from the timecourse of each voxel in the brain prior to calculating functional connectivity between brain regions (see Murphy & Fox, 2017 for a review). GSR was originally thought to be an effective way to remove artifactual signals (e.g., motion) from voxel time series and was implemented in task-based fMRI experiments. This preprocessing step, however, mathematically mandates negative connectivity estimates between brain regions (Murphy et al., 2009), muddying the interpretation of resulting anti-correlations. Recent research, however, suggests that GSR helps analyses whose aim is to predict behavior using functional connectivity estimates (Finn & Bandettini, 2021; Li et al., 2019). In our pre-registration, we did not include GSR in our preprocessing pipeline, though we have since been convinced that this step may be important for individual difference analyses. For completeness, we reran our analyses *excluding* GSR from our preprocessing pipeline and report the results below. Removing GSR had no impact on our pre-registered, hypothesis-driven analyses targeting the DMN-C (see **Supplemental Table 3-5**). However, there were two differences in the other results: First, removing GSR results in a statistically significant relationship between average hippocampal connectivity on memory ability, whereby average hippocampal connectivity was inversely related to memory ability (see **Supplemental Table 6**). Second, removing GSR resulted in a substantially weaker ability to predict memory ability in the CBPM analysis ( $r_{\{\text{observed}, \text{predicted}\}} = 0.081, p = 0.099$ ).

Characteristic	Model 1		Model 2		Model 3	
	Beta <sup>1</sup>	SE <sup>2</sup>	Beta <sup>1</sup>	SE <sup>2</sup>	Beta <sup>1</sup>	SE <sup>2</sup>
within	-0.29	0.225	-0.27	0.225	-0.18	0.204
age			-0.05	0.027	-0.05	0.026
sex <sup>3</sup>			-0.91*	0.446	-1.0*	0.414
fd			-6.4	5.70	2.0	5.21
acer					1.1***	0.243
cattell					0.83***	0.237
No. Obs.	243		243		235	
R <sup>2</sup>	0.007		0.048		0.238	

<sup>1</sup>p<0.05; <sup>2</sup>p<0.01; <sup>3</sup>p<0.001

<sup>2</sup>SE = Standard Error

<sup>3</sup>Female = 0, Male = 1.

**Supplemental Table 3.** *Regression Results of Average Within DMN-C Connectivity on Memory Ability Removing GSR from Our Analysis Pipeline.* within = average strength of connection among DMN-C regions; acer = cognitive capacity score, cattell = fluid intelligence score.

Characteristic	Model 4		Model 5		Model 6	
	Beta <sup>1</sup>	SE <sup>2</sup>	Beta <sup>1</sup>	SE <sup>2</sup>	Beta <sup>1</sup>	SE <sup>2</sup>
between	-0.35	0.224	-0.22	0.231	-0.07	0.208
age			-0.04	0.027	-0.05	0.026
sex <sup>3</sup>			-0.95*	0.444	-1.0*	0.414
fd			-5.6	5.86	1.9	5.33
acer					1.1***	0.244
cattell					0.82***	0.237
No. Obs.	243		243		235	
R <sup>2</sup>	0.010		0.046		0.235	

<sup>1</sup>p<0.05; <sup>2</sup>p<0.01; <sup>3</sup>p<0.001

<sup>2</sup>SE = Standard Error

<sup>3</sup>Female = 0, Male = 1.

**Supplemental Table 4:** *Regression Results of Average DMNC--DMNA Connectivity on Memory Ability Removing GSR from Our Analysis Pipeline.* between = average strength of connection between DMNC and DMNA regions; acer = cognitive capacity score, cattell = fluid intelligence score.

Characteristic	Model 7		Model 8		Model 9	
	Beta <sup>1</sup>	SE <sup>2</sup>	Beta <sup>1</sup>	SE <sup>2</sup>	Beta <sup>1</sup>	SE <sup>2</sup>
extra	-0.60**	0.222	-0.40	0.252	-0.31	0.230
age			-0.04	0.028	-0.04	0.026
sex <sup>3</sup>			-0.85	0.449	-0.94*	0.417
fd			-3.2	6.15	4.3	5.57
acer					1.1***	0.243
cattell					0.84***	0.237
No. Obs.	243		243		235	
R <sup>2</sup>	0.030		0.052		0.241	

<sup>1</sup>p<0.05; <sup>2</sup>p<0.01; <sup>3</sup>p<0.001

<sup>2</sup>SE = Standard Error

<sup>3</sup>Female = 0, Male = 1.

**Supplemental Table 5:** Regression Results of Average DMNC Connectivity with the Rest of the Brain on Memory Ability Removing GSR from Our Analysis Pipeline. extra = average strength of connection between DMNC regions and regions not in the DMNC or DMNA; acer = cognitive capacity score, cattell = fluid intelligence score.

Characteristic	Model 10		Model 11		Model 12	
	Beta <sup>1</sup>	SE <sup>2</sup>	Beta <sup>1</sup>	SE <sup>2</sup>	Beta <sup>1</sup>	SE <sup>2</sup>
hipp	-0.74***	0.220	-0.57*	0.241	-0.44*	0.218
age			-0.04	0.027	-0.04	0.026
sex <sup>3</sup>			-0.73	0.451	-0.84*	0.421
fd			-2.4	5.95	4.8	5.39
acer					1.1***	0.242
cattell					0.81***	0.235
No. Obs.	243		243		235	
R <sup>2</sup>	0.044		0.065		0.249	

<sup>1</sup>p<0.05; <sup>2</sup>p<0.01; <sup>3</sup>p<0.001

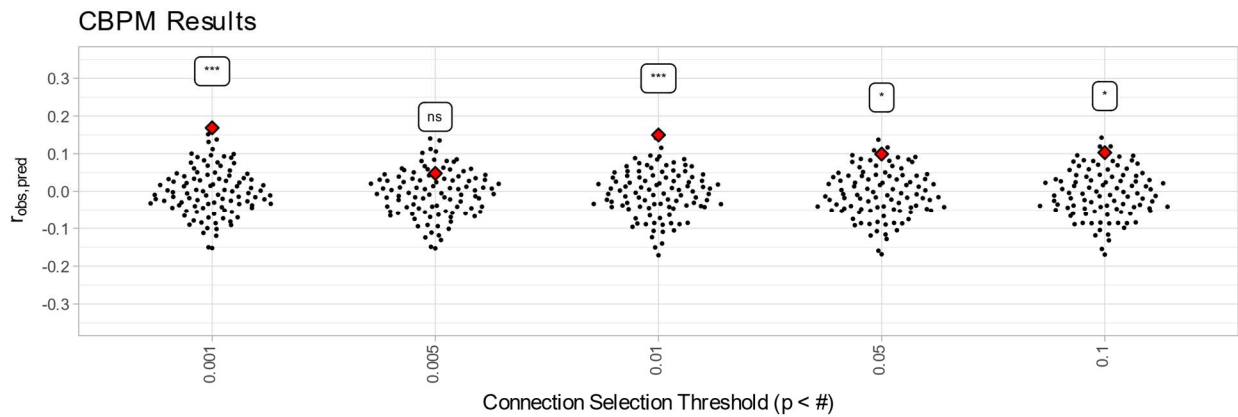
<sup>2</sup>SE = Standard Error

<sup>3</sup>Female = 0, Male = 1.

**Supplemental Table 6:** Regression Results of Average Hippocampal Connectivity on Memory Ability Removing GSR from Our Analysis Pipeline. hipp = average strength of connection of hippocampal regions; acer = cognitive capacity score, cattell = fluid intelligence score.

## S.5 CBPM Connection Defining Threshold

Our study used Connectome Based Predictive Modeling (CBPM; Shen et al., 2017) to determine if information contained within the functional connectome is useful for predicting memory ability. This approach involves setting an arbitrary threshold for defining which connections are used to make behavioral predictions. Analyses reported in this manuscript used a connection selection threshold of  $p \leq .01$ . It is unclear, however, whether this arbitrary choice of threshold has any impact on our results. We reran our key CBPM analysis (i.e., predicting memory ability while controlling for age, sex, and average framewise displacement) using a range of connection selection thresholds:  $p = [0.001 \ 0.005 \ 0.01 \ 0.05 \ 0.1]$ . Results are reported in **Supplemental Figure 1**. Analyses using all selection thresholds were statistically significant with one exception – when the selection threshold was set to  $p < 0.005$ . It is currently unclear why this specific analysis failed — selecting an even stricter threshold (i.e.,  $p < 0.001$ ) resulted in restored predictive performance. We take this pattern of results as evidence that the CBPM approach is robust to connection selection threshold, in line with previous reports (Finn et al., 2015; Jangraw et al., 2018; CBPM; Shen et al., 2017).



**Supplemental Figure 1:** *CBPM Results are Robust to Selection of Connection Selection Threshold.* Red diamonds indicate observed results, black dots indicate results of 100 null simulations. \*\*\*  $p \leq 0.001$ , \*\*  $p \leq 0.01$ , \*  $p \leq 0.05$ , ns =  $p > 0.05$ .

## S.6 Combining Data Across Tasks

Our analyses combined data across tasks to increase the reliability of our functional connectivity estimates (Elliott et al., 2019). This approach assumes that intrinsic functional connectivity would not vary substantially across tasks. Indeed, a recent study suggests that variability in the functional connectome is dominated by a normative pattern, patterns unique to individuals, and patterns unique to how individuals complete certain tasks (Gratton et al., 2018). To test the validity of this approach, we calculated the functional connectome separately for each task for each subject (i.e., movie watching, rest, sensorimotor) and correlated the resulting task-specific functional connectomes. **Supplemental Table 7** displays the mean, standard deviation, minimum, and maximum similarity for each pair of tasks across our sample of 243 subjects. All correlations between tasks were performed on the subset of subjects that had a pair of valid scans. The movie-watching connectome was notably less similar to the rest and sensorimotor task connectomes. We suspect that this could be due to stimulus-driven changes in brain activation.

Task Pair	N	min	max	mean	sd
movie-smt	240	0.20	0.69	0.51	0.06
rest-movie	227	0.18	0.66	0.49	0.06
rest-smt	226	0.47	0.79	0.63	0.07

**Supplemental Table 7:** *How Similar are Connectomes Calculated Using Data from Different Tasks? Similarity between connectomes was calculated using a Pearson's correlation.*

To see how this impacted our results, we reran our CBPM analyses using functional connectomes calculated using only the movie-watching data (“movie”), only the resting-state data (“rest”), and only the sensorimotor (“smt”) tasks data. The results of these CBPM analyses are reported in **Supplemental Figure 2**. Functional connectomes calculated using the resting-state ( $r_{\{\text{observed, predicted}\}} = -0.007, p = 0.39$ ) and sensorimotor task ( $r_{\{\text{observed, predicted}\}} = 0.083, p = 0.12$ ) data were insufficient for predicting memory ability. Functional connectomes calculated using the movie watching data, however, were sufficient for predicting memory ability ( $r_{\{\text{observed, predicted}\}} = 0.113, p = 0.03$ ). Interestingly, all the task specific predictive models performed worse compared with our predictive model that used a combined “intrinsic” connectome for each subject by averaging across tasks ( $r_{\{\text{observed, predicted}\}} = 0.1498, p < 0.01$ ).



**Supplemental Figure 2:** *How do Predictive Models built using Connectomes from Individual Tasks Compare? Movie = movie watching, rest = resting-state, smt = sensorimotor task.*

## S.7 Experimental Stimuli

<b>object</b>		<b>famous people</b>			<b>famous places</b>	
		<i>first</i>	<i>last</i>			
1	bowling ball	1	Adam	Sandler	1	The Acropolis of Athens
2	bowling pin	2	Adele		2	The Amazon River, Brazil
3	brick	3	Albert	Einstein	3	Alcatraz, San Francisco
4	button	4	Amy	Poehler	4	Arc de Triomphe, Paris
5	calculator	5	Amy	Schumer	5	The Bank of England, London
6	candle	6	Angelina	Jolie	6	Big Ben, London
7	chalk	7	Anne	Hathaway	7	The Bird's Nest, Beijing
8	dart board	8	Ariana	Grande	8	The Blue Domes of Santorini
9	earrings	9	Audrey	Hepburn	9	The Brandenburg Gate, Berlin
10	envelope	10	Barack	Obama	10	The British Museum, London
11	hammer	11	Beyonce		11	The Brooklyn Bridge, New York
12	handcuffs	12	Bill	Clinton	12	Buckingham Palace, London
13	harmonica	13	Bill	Gates	13	Burj Al Arab, Dubai
14	horseshoe	14	Brad	Pitt	14	Burj Khalifa, Dubai
15	mail box	15	Bradley	Cooper	15	Capitol Hill, Washington D.C.
16	ring	16	Bruce	Willis	16	Carnegie Hall, New York
17	ruler	17	Bruno	Mars	17	Central Park, New York
18	scissors	18	Charli	Damelio	18	Chichen Itza, Mexico
19	screw	19	Chris	Hemsworth	19	Cristo Redentor, Rio de Janeiro
20	skateboard	20	Chris	Pratt	20	The CN Tower, Toronto
21	snowman	21	Condoleezza	Rice	21	The Colosseum, Rome
22	wrench	22	The Dalai	Lama	22	Easter Island, Chile
23	surf board	23	Daniel	Radcliffe	23	Edinburgh Castle, Scotland
24	toothbrush	24	Denzel	Washington	24	The Eiffel Tower, Paris
25	umbrella	25	Dwayne	Johnson	25	Epcot Center, Orlando
26	windmill	26	Ellen	Degeneres	26	The Empire State Building, New York

27	zipper	27	Emily	Blunt	27	Fenway Park, Boston
28	dog house	28	Emma	Watson	28	The Forbidden City, Beijing
29	football	29	George	Clooney	29	The Gateway Arch, St. Louis
30	golf ball	30	Halle	Berry	30	The Gherkin, London
31	guitar case	31	Hillary	Clinton	31	The Golden Gate Bridge, San Francisco
32	kite	32	Hugh	Jackman	32	The Grand Canal, Venice
33	lawn mower	33	Idris	Elba	33	The Grand Canyon, Arizona
34	light switch	34	Jamie	Foxx	34	La Grande Arche, Paris
35	locker	35	Jennifer	Aniston	35	The Great Buddha, Japan
36	mattress	36	Jennifer	Lawrence	36	The Great Sphinx of Giza
37	pool table	37	Jennifer	Lopez	37	The Great Wall of China
38	school bus	38	Jimmy	Fallon	38	Hagia Sophia, Istanbul
39	soccer ball	39	John	Krasinski	39	The Hollywood Sign, Los Angeles
40	swing	40	John	Travolta	40	The Kremlin, Moscow
41	wheelchair	41	John F.	Kennedy	41	La Sagrada Familia, Barcelona
42	accordion	42	Julia	Roberts	42	The Lincoln Memorial, Washington D.C.
43	binoculars	43	Julianne	Moore	43	The London Eye
44	dice	44	Julie	Andrews	44	The Louvre, Paris
45	fire hydrant	45	Justin	Bieber	45	Machu Picchu, Peru
46	fork	46	Keira	Knightley	46	Mecca, Saudi Arabia
47	funnel	47	Kevin	Hart	47	Mount Everest, Nepal
48	key	48	Kim	Kardashian	48	Mount Fuji, Japan
49	lipstick	49	Kristen	Wiig	49	Mount Rushmore, South Dakota
50	microscope	50	Lady	Diana	50	Neuschwanstein Castle, Germany
51	pencil	51	Lady	Gaga	51	Niagara Falls
52	staples	52	Leonardo	Dicaprio	52	One World Trade Center, New York
53	thermometer	53	Liam	Hemsworth	53	The Palm Islands, Dubai
54	toaster	54	Liam	Neeson	54	The Pentagon, Washington D.C.
55	violin	55	Lindsay	Lohan	55	Pompeii, Italy
56	nunchucks	56	Madonna		56	The Pont du Gard, France

57	apron	57	Mahatma	Gandhi	57	The Pyramids of Giza
58	banjo	58	Margot	Robbie	58	The Sistine Chapel, Vatican City
59	basketball	59	Marilyn	Monroe	59	The Space Needle, Seattle
60	battery	60	Mark	Zuckerberg	60	The Spanish Steps, Rome
61	belt	61	Martin	Luther King	61	The Statue of Liberty, New York
62	bow	62	Matt	Damon	62	Stonehenge, United Kingdom
63	chain	63	Matthew	McConaughey	63	Table Mountain, South Africa
64	cigarette	64	Meghan	Markle	64	The Taj Mahal, India
65	drum sticks	65	Melissa	McCarthy	65	Times Square, New York
66	exit sign	66	Meryl	Streep	66	Tower Bridge, London
67	frisbee	67	Michael	Jackson	67	The Tower of Pisa, Italy
68	ladder	68	Michael	Jordan	68	Uluru, Australia
69	lighter	69	Michael	Phelps	69	United Nations Headquarters, New York
70	compass	70	Michelle	Obama	70	Vatican City, Italy
71	measuring cup	71	Miley	Cyrus	71	The Palace of Versailles, France
72	parachute	72	Mindy	Kaling	72	The Western Wall, Jerusalem
73	rubik cube	73	Morgan	Freeman	73	Westminster Abbey, London
74	sand castle	74	Mother	Teresa	74	The White House, Washington D.C.
75	scarf	75	Nelson	Mandela	75	Windsor Castle, United Kingdom
76	screwdriver	76	Nicholas	Cage	76	Old Faithful, Yellowstone National Park
77	sewing machine	77	Nicole	Kidman	77	The Hoover Dam, Nevada
78	shirt	78	Octavia	Spencer	78	The Las Vegas Strip
79	snowboard	79	Oprah		79	Napa Valley, California
80	stapler	80	Orlando	Bloom	80	Notre-Dame, Paris
81	telescope	81	Paul	McCartney	81	The University of Oxford, England
82	tennis ball	82	Penelope	Cruz	82	The Sahara Desert, Africa
83	broom	83	Prince	William	83	The Serengeti, Africa
84	mouse trap	84	Queen	Elizabeth	84	The Washington Monument, Washington D.C.

85	anchor	85	Rachel	McAdams		
86	arrow	86	Reese	Witherspoon		
87	bird house	87	Rihanna			
88	blender	88	Robert	Deniro		
89	bullet	89	Robert	Downey Jr.		
90	cannon	90	Robert	Pattinson		
91	cash register	91	Robin	Williams		
92	disco ball	92	Rosa	Parks		
93	dream catcher	93	Ryan	Reynolds		
94	hockey stick	94	Samuel	L. Jackson		
95	hula hoop	95	Sandra	Bullock		
96	nutcracker	96	Sandra	Oh		
97	toolbox	97	Scarlett	Johansson		
98	trampoline	98	Sean	Connery		
99	tricycle	99	Selena	Gomez		
100	trophy	100	Serena	Williams		
101	ashtray	101	Shakira			
102	cd	102	Stephen	Curry		
103	clock	103	Stephen	Hawking		
104	eraser	104	Steve	Carell		
105	eye patch	105	Steve	Jobs		
106	iron	106	Taylor	Swift		
107	lamp	107	Timothee	Chalamet		
108	match	108	Tom	Cruise		
109	paint brush	109	Tom	Hanks		
110	plate	110	Whoopi	Goldberg		
111	sandal	111	Will	Smith		
112	spoon	112	Zendaya			
113	toilet paper					
114	tile					

115	wheelbarrow				
116	book				
117	bridge				
118	bumper car				
119	cigar				
120	escalator				
121	fly swatter				
122	helicopter				
123	rake				
124	lighthouse				

**Supplemental Table 8:** *Famous Person, Famous Place, and Common Object Stimuli Used in Chapter 3.*

## S.8 Results in winsorized Subsample

To determine if participants' dependency differed as a function of session (session 1, session2) and triad type (famous person, famous place) in the 25%/75% winsorized sample, I fit a linear mixed model to predict dependency using session and triad type. The model included session and triad type as random effects (formula =  $\sim$  session + triad\_type | subject\_id). The model's total explanatory power is substantial (conditional R<sup>2</sup> = 0.58) and the part related to the fixed effects alone (marginal R<sup>2</sup>) is 0.03. The effect of session [session2] is statistically non-significant and positive ( $\beta = -1.74e-03$ , 95% CI [-0.04, 0.03],  $t(149) = -0.09$ ,  $p = 0.925$ , Std.  $\beta = -0.02$ ). The effect of triad type [famous place] is statistically non-significant and positive ( $\beta = 0.03$ , 95% CI [-5.74e-03, 0.07],  $t(149) = 1.67$ ,  $p = 0.098$ , Std.  $\beta = 0.31$ ). The effect of session [session2]  $\times$  triad type [famous place] is statistically significant and negative ( $\beta = -0.04$ , 95% CI [-0.08, -2.18e-03],  $t(149) = -2.08$ ,  $p = 0.039$ , Std.  $\beta = -0.43$ ).

## REFERENCES

- Abraham, A., Pedregosa, F., Eickenberg, M., Gervais, P., Mueller, A., Kossaifi, J., Gramfort, A., Thirion, B., & Varoquaux, G. (2014). Machine learning for neuroimaging with scikit-learn. *Frontiers in Neuroinformatics*, *8*, 14. <https://doi.org/10.3389/fninf.2014.00014>
- Addis, D. R., Leclerc, C. M., Muscatell, K. A., & Kensinger, E. A. (2010). There are age-related changes in neural connectivity during the encoding of positive, but not negative, information. *Cortex*, *46*(4), 425–433. <https://doi.org/10.1016/j.cortex.2009.04.011>
- Anderson, J. S., Ferguson, M. A., Lopez-Larson, M., & Yurgelun-Todd, D. (2011). Reproducibility of single-subject functional connectivity measurements. *AJNR. American Journal of Neuroradiology*, *32*(3), 548–555. <https://doi.org/10.3174/ajnr.A2330>
- Andrews-Hanna, J. R., Reidler, J. S., Sepulcre, J., Poulin, R., & Buckner, R. L. (2010). Functional-anatomic fractionation of the brain's default network. *Neuron*, *65*(4), 550–562. <https://doi.org/10.1016/j.neuron.2010.02.005>
- Andrews-Hanna, J. R., Saxe, R., & Yarkoni, T. (2014). Contributions of episodic retrieval and mentalizing to autobiographical thought: evidence from functional neuroimaging, resting-state connectivity, and fMRI meta-analyses. *NeuroImage*, *91*, 324–335. <https://doi.org/10.1016/j.neuroimage.2014.01.032>
- Andrews-Hanna, J. R., Smallwood, J., & Spreng, R. N. (2014). The default network and self-generated thought: component processes, dynamic control, and clinical relevance. *Annals of the New York Academy of Sciences*, *1316*, 29–52. <https://doi.org/10.1111/nyas.12360>
- Avants, B. B., Epstein, C. L., Grossman, M., & Gee, J. C. (2008). Symmetric diffeomorphic image registration with cross-correlation: evaluating automated labeling of elderly and neurodegenerative brain. *Medical Image Analysis*, *12*(1), 26–41. <https://doi.org/10.1016/j.media.2007.06.004>
- Avery, E. W., Yoo, K., Rosenberg, M. D., Greene, A. S., Gao, S., Na, D. L., Scheinost, D., Constable, T. R., & Chun, M. M. (2020). Distributed Patterns of Functional Connectivity Predict Working Memory Performance in Novel Healthy and Memory-impaired Individuals. *Journal of Cognitive Neuroscience*, *32*(2), 241–255. [https://doi.org/10.1162/jocn\\_a\\_01487](https://doi.org/10.1162/jocn_a_01487)
- Barnett, A. J., Reilly, W., Dimsdale-Zucker, H. R., Mizrak, E., Reagh, Z., & Ranganath, C. (2021). Intrinsic connectivity reveals functionally distinct cortico-hippocampal networks in the human brain. *PLoS Biology*, *19*(6), e3001275. <https://doi.org/10.1371/journal.pbio.3001275>
- Bates, D., Mächler, M., Bolker, B., & Walker, S. (2015). Fitting Linear Mixed-Effects Models Using lme4. In *Journal of Statistical Software* (Vol. 67, Issue 1, pp. 1–48). <https://doi.org/10.18637/jss.v067.i01>
- Beaty, R. E., Kenett, Y. N., Christensen, A. P., Rosenberg, M. D., Benedek, M., Chen, Q., Fink, A., Qiu, J., Kwapil, T. R., Kane, M. J., & Silvia, P. J. (2018). Robust prediction of individual creative ability from brain functional connectivity. *Proceedings of the National Academy of Sciences of the United States of America*, *115*(5), 1087–1092.

<https://doi.org/10.1073/pnas.1713532115>

- Behzadi, Y., Restom, K., Liao, J., & Liu, T. T. (2007). A component based noise correction method (CompCor) for BOLD and perfusion based fMRI. *NeuroImage*, *37*(1), 90–101. <https://doi.org/10.1016/j.neuroimage.2007.04.042>
- Ben-Shachar, M. S., Lüdtke, D., & Makowski, D. (2020). effectsize: Estimation of Effect Size Indices and Standardized Parameters. In *Journal of Open Source Software* (Vol. 5, Issue 56, p. 2815). The Open Journal. <https://doi.org/10.21105/joss.02815>
- Berkson, J. (1946). Limitations of the application of fourfold table analysis to hospital data. *Biometrics*, *2*(3), 47–53. <https://doi.org/10.2307/3002000>
- Berryhill, M. E., Phuong, L., Picasso, L., Cabeza, R., & Olson, I. R. (2007). Parietal lobe and episodic memory: bilateral damage causes impaired free recall of autobiographical memory. *The Journal of Neuroscience: The Official Journal of the Society for Neuroscience*, *27*(52), 14415–14423. <https://doi.org/10.1523/JNEUROSCI.4163-07.2007>
- Bisby, J. A., Horner, A. J., Bush, D., & Burgess, N. (2018). Negative emotional content disrupts the coherence of episodic memories. *Journal of Experimental Psychology. General*, *147*(2), 243–256. <https://doi.org/10.1037/xge0000356>
- Bolt, T., Prince, E. B., Nomi, J. S., Messinger, D., Llabre, M. M., & Uddin, L. Q. (2018). Combining region- and network-level brain-behavior relationships in a structural equation model. *NeuroImage*, *165*, 158–169. <https://doi.org/10.1016/j.neuroimage.2017.10.007>
- Bradley, M. M., & Lang, P. J. (2007). The International Affective Digitized Sounds (IADS-2): Affective ratings of sounds and instruction manual. *University of Florida, Gainesville, FL, Tech. Rep. B-3*.
- Brady, T. F., Konkle, T., Gill, J., Oliva, A., & Alvarez, G. A. (2013). Visual long-term memory has the same limit on fidelity as visual working memory. *Psychological Science*, *24*(6), 981–990. <https://doi.org/10.1177/0956797612465439>
- Brodeur, M. B., Dionne-Dostie, E., Montreuil, T., & Lepage, M. (2010). The Bank of Standardized Stimuli (BOSS), a new set of 480 normative photos of objects to be used as visual stimuli in cognitive research. *PloS One*, *5*(5), e10773. <https://doi.org/10.1371/journal.pone.0010773>
- Brodeur, M. B., Guérard, K., & Bouras, M. (2014). Bank of Standardized Stimuli (BOSS) phase II: 930 new normative photos. *PloS One*, *9*(9), e106953. <https://doi.org/10.1371/journal.pone.0106953>
- Buckner, R. L., & DiNicola, L. M. (2019). The brain’s default network: updated anatomy, physiology and evolving insights. *Nature Reviews Neuroscience*. <https://doi.org/10.1038/s41583-019-0212-7>
- Cabeza, R., & Moscovitch, M. (2013). Memory Systems, Processing Modes, and Components: Functional Neuroimaging Evidence. *Perspectives on Psychological Science: A Journal of the Association for Psychological Science*, *8*(1), 49–55. <https://doi.org/10.1177/1745691612469033>
- Carroll, J. B. (1993). *Human Cognitive Abilities: A Survey of Factor-Analytic Studies*. Cambridge University Press. [https://play.google.com/store/books/details?id=jp9dt4\\_0\\_cIC](https://play.google.com/store/books/details?id=jp9dt4_0_cIC)

- Chen, J., Leong, Y. C., Honey, C. J., Yong, C. H., Norman, K. A., & Hasson, U. (2017). Shared memories reveal shared structure in neural activity across individuals. *Nature Neuroscience*, *20*(1), 115–125. <https://doi.org/10.1038/nn.4450>
- Christoff, K., Gordon, A. M., Smallwood, J., Smith, R., & Schooler, J. W. (2009). Experience sampling during fMRI reveals default network and executive system contributions to mind wandering. *Proceedings of the National Academy of Sciences*, *106*(21), 8719–8724. <https://doi.org/10.1073/pnas.0900234106>
- Clark, I. A., Monk, A. M., Hotchin, V., Pizzamiglio, G., Liefgreen, A., Callaghan, M. F., & Maguire, E. A. (2020). Does hippocampal volume explain performance differences on hippocampal-dependant tasks? *NeuroImage*, *221*, 117211. <https://doi.org/10.1016/j.neuroimage.2020.117211>
- Cooper, R. A., Kurkela, K. A., Davis, S. W., & Ritchey, M. (2021a). Mapping the organization and dynamics of the posterior medial network during movie watching. *NeuroImage*, *236*, 118075. <https://doi.org/10.1016/j.neuroimage.2021.118075>
- Cooper, R. A., Kurkela, K. A., Davis, S. W., & Ritchey, M. (2021b). Mapping the organization and dynamics of the posterior medial network during movie watching. *NeuroImage*, *236*, 118075. <https://doi.org/10.1016/j.neuroimage.2021.118075>
- Cooper, R. A., Plaisted-Grant, K. C., Baron-Cohen, S., & Simons, J. S. (2017). Eye movements reveal a dissociation between memory encoding and retrieval in adults with autism. *Cognition*, *159*, 127–138. <https://doi.org/10.1016/j.cognition.2016.11.013>
- Cooper, R. A., & Ritchey, M. (2019). Cortico-hippocampal network connections support the multidimensional quality of episodic memory. *eLife*, *8*. <https://doi.org/10.7554/eLife.45591>
- Cooper, R. A., & Ritchey, M. (2022). Patterns of episodic content and specificity predicting subjective memory vividness. *Memory & Cognition*. <https://doi.org/10.3758/s13421-022-01291-5>
- Corkin, S. (2002). What's new with the amnesic patient H.M.? *Nature Reviews Neuroscience*, *3*(2), 153–160. <https://doi.org/10.1038/nrn726>
- Cox, R. W., & Hyde, J. S. (1997). Software tools for analysis and visualization of fMRI data. *NMR in Biomedicine*, *10*(4-5), 171–178. [https://doi.org/10.1002/\(sici\)1099-1492\(199706/08\)10:4/5<171::aid-nbm453>3.0.co;2-1](https://doi.org/10.1002/(sici)1099-1492(199706/08)10:4/5<171::aid-nbm453>3.0.co;2-1)
- Damasio, A. R., Eslinger, P. J., Damasio, H., Van Hoesen, G. W., & Cornell, S. (1985). Multimodal amnesic syndrome following bilateral temporal and basal forebrain damage. *Archives of Neurology*, *42*(3), 252–259. <https://doi.org/10.1001/archneur.1985.04060030070012>
- Davachi, L. (2006). Item, context and relational episodic encoding in humans. *Current Opinion in Neurobiology*, *16*(6), 693–700. <https://doi.org/10.1016/j.conb.2006.10.012>
- Davachi, L., Mitchell, J. P., & Wagner, A. D. (2003). Multiple routes to memory: distinct medial temporal lobe processes build item and source memories. *Proceedings of the National Academy of Sciences of the United States of America*, *100*(4), 2157–2162. <https://doi.org/10.1073/pnas.0337195100>
- Davis, M. H. (1983). Measuring individual differences in empathy: Evidence for a

- multidimensional approach. *Journal of Personality and Social Psychology*, 44(1), 113–126. <https://doi.org/10.1037//0022-3514.44.1.113>
- Davis, S. W., Stanley, M. L., Moscovitch, M., & Cabeza, R. (2017). Resting-state networks do not determine cognitive function networks: a commentary on Campbell and Schacter (2016). *Language, Cognition and Neuroscience*, 32(6), 669–673. <https://doi.org/10.1080/23273798.2016.1252847>
- Diana, R. A., Yonelinas, A. P., & Ranganath, C. (2007). Imaging recollection and familiarity in the medial temporal lobe: a three-component model. *Trends in Cognitive Sciences*, 11(9), 379–386. <https://doi.org/10.1016/j.tics.2007.08.001>
- Diana, R. A., Yonelinas, A. P., & Ranganath, C. (2010). Medial temporal lobe activity during source retrieval reflects information type, not memory strength. *Journal of Cognitive Neuroscience*, 22(8), 1808–1818. <https://doi.org/10.1162/jocn.2009.21335>
- DiNicola, L. M., Braga, R. M., & Buckner, R. L. (2020). Parallel distributed networks dissociate episodic and social functions within the individual. *Journal of Neurophysiology*, 123(3), 1144–1179. <https://doi.org/10.1152/jn.00529.2019>
- Donovan, C. L., & Miller, M. B. (2008). *An investigation of individual variability in brain activity during episodic encoding and retrieval*. CALIFORNIA UNIV SANTA BARBARA DEPT OF PSYCHOLOGY. <https://apps.dtic.mil/docs/citations/ADA505787>
- Dosenbach, N. U. F., Nardos, B., Cohen, A. L., Fair, D. A., Power, J. D., Church, J. A., Nelson, S. M., Wig, G. S., Vogel, A. C., Lessov-Schlaggar, C. N., Barnes, K. A., Dubis, J. W., Feczko, E., Coalson, R. S., Pruett, J. R., Jr, Barch, D. M., Petersen, S. E., & Schlaggar, B. L. (2010). Prediction of individual brain maturity using fMRI. *Science*, 329(5997), 1358–1361. <https://doi.org/10.1126/science.1194144>
- Duarte, A., Ranganath, C., & Knight, R. T. (2005). Effects of unilateral prefrontal lesions on familiarity, recollection, and source memory. *The Journal of Neuroscience: The Official Journal of the Society for Neuroscience*, 25(36), 8333–8337. <https://doi.org/10.1523/JNEUROSCI.1392-05.2005>
- Ebbinghaus, H. (1964). *Memory: A contribution to experimental psychology* (H. A. Ruger & C. E. Bussenius, trans.). Dover Publications, Inc. (Original work published 1885)
- Eichenbaum, H., Yonelinas, A. P., & Ranganath, C. (2007). The medial temporal lobe and recognition memory. *Annual Review of Neuroscience*, 30, 123–152. <https://doi.org/10.1146/annurev.neuro.30.051606.094328>
- Elliott, M. L., Knodt, A. R., Cooke, M., Kim, M. J., Melzer, T. R., Keenan, R., Ireland, D., Ramrakha, S., Poulton, R., Caspi, A., Moffitt, T. E., & Hariri, A. R. (2019). General functional connectivity: Shared features of resting-state and task fMRI drive reliable and heritable individual differences in functional brain networks. *NeuroImage*, 189, 516–532. <https://doi.org/10.1016/j.neuroimage.2019.01.068>
- Esteban, O., Birman, D., Schaer, M., Koyejo, O. O., Poldrack, R. A., & Gorgolewski, K. J. (2017). MRIQC: Advancing the automatic prediction of image quality in MRI from unseen sites. *PloS One*, 12(9), e0184661. <https://doi.org/10.1371/journal.pone.0184661>
- Esteban, O., Blair, R., Markiewicz, C. J., Berleant, S. L., Moodie, C., Ma, F., Isik, A. I.,

- Erramuzpe, A., Kent, M., Goncalves, M., & Others. (2018). fmriprep. *Software: Practice & Experience*.
- Esteban, O., Markiewicz, C. J., Blair, R. W., Moodie, C. A., Isik, A. I., Erramuzpe, A., Kent, J. D., Goncalves, M., DuPre, E., Snyder, M., Oya, H., Ghosh, S. S., Wright, J., Durnez, J., Poldrack, R. A., & Gorgolewski, K. J. (2019). fMRIPrep: a robust preprocessing pipeline for functional MRI. *Nature Methods*, *16*(1), 111–116. <https://doi.org/10.1038/s41592-018-0235-4>
- Finn, E. S., & Bandettini, P. A. (2021). Movie-watching outperforms rest for functional connectivity-based prediction of behavior. *NeuroImage*, *235*, 117963. <https://doi.org/10.1016/j.neuroimage.2021.117963>
- Finn, E. S., Shen, X., Scheinost, D., Rosenberg, M. D., Huang, J., Chun, M. M., Papademetris, X., & Constable, R. T. (2015). Functional connectome fingerprinting: identifying individuals using patterns of brain connectivity. *Nature Neuroscience*, *18*(11), 1664–1671. <https://doi.org/10.1038/nn.4135>
- Fonov, V. S., Evans, A. C., McKinstry, R. C., Alml, C. R., & Collins, D. L. (2009). Unbiased nonlinear average age-appropriate brain templates from birth to adulthood. *NeuroImage*, *47*, S102. [https://doi.org/10.1016/S1053-8119\(09\)70884-5](https://doi.org/10.1016/S1053-8119(09)70884-5)
- Fornito, A., Harrison, B. J., Zalesky, A., & Simons, J. S. (2012). Competitive and cooperative dynamics of large-scale brain functional networks supporting recollection. *Proceedings of the National Academy of Sciences of the United States of America*, *109*(31), 12788–12793. <https://doi.org/10.1073/pnas.1204185109>
- Fox, K. C. R., Foster, B. L., Kucyi, A., Daitch, A. L., & Parvizi, J. (2018). Intracranial Electrophysiology of the Human Default Network. *Trends in Cognitive Sciences*, *22*(4), 307–324. <https://doi.org/10.1016/j.tics.2018.02.002>
- Gadian, D. G., Aicardi, J., Watkins, K. E., & Porter, D. A. (2000). Developmental amnesia associated with early hypoxic–ischaemic injury. *Brain: A Journal of Neurology*. <https://academic.oup.com/brain/article-abstract/123/3/499/348744>
- Geib, B. R., Stanley, M. L., Wing, E. A., Laurienti, P. J., & Cabeza, R. (2017). Hippocampal Contributions to the Large-Scale Episodic Memory Network Predict Vivid Visual Memories. *Cerebral Cortex*, *27*(1), 680–693. <https://doi.org/10.1093/cercor/bhv272>
- Gilmore, A. W., Nelson, S. M., & McDermott, K. B. (2021). Precision functional mapping of human memory systems. *Current Opinion in Behavioral Sciences*, *40*, 52–57. <https://doi.org/10.1016/j.cobeha.2020.12.013>
- Glasser, M. F., Sotiropoulos, S. N., Wilson, J. A., Coalson, T. S., Fischl, B., Andersson, J. L., Xu, J., Jbabdi, S., Webster, M., Polimeni, J. R., Van Essen, D. C., Jenkinson, M., & WU-Minn HCP Consortium. (2013). The minimal preprocessing pipelines for the Human Connectome Project. *NeuroImage*, *80*, 105–124. <https://doi.org/10.1016/j.neuroimage.2013.04.127>
- Gohel, D., & Skintzos, P. (2023). *flextable: Functions for Tabular Reporting*. <https://CRAN.R-project.org/package=flextable>
- Gordon, E. M., Laumann, T. O., Adeyemo, B., & Petersen, S. E. (2017). Individual Variability of

- the System-Level Organization of the Human Brain. *Cerebral Cortex*, 27(1), 386–399. <https://doi.org/10.1093/cercor/bhv239>
- Gordon, E. M., Laumann, T. O., Gilmore, A. W., Newbold, D. J., Greene, D. J., Berg, J. J., Ortega, M., Hoyt-Drazen, C., Grattton, C., Sun, H., Hampton, J. M., Coalson, R. S., Nguyen, A. L., McDermott, K. B., Shimony, J. S., Snyder, A. Z., Schlaggar, B. L., Petersen, S. E., Nelson, S. M., & Dosenbach, N. U. F. (2017). Precision Functional Mapping of Individual Human Brains. *Neuron*, 95(4), 791–807.e7. <https://doi.org/10.1016/j.neuron.2017.07.011>
- Gordon, E. M., & Nelson, S. M. (2021). Three types of individual variation in brain networks revealed by single-subject functional connectivity analyses. *Current Opinion in Behavioral Sciences*, 40, 79–86. <https://doi.org/10.1016/j.cobeha.2021.02.014>
- Gorgolewski, K., Burns, C. D., Madison, C., Clark, D., Halchenko, Y. O., Waskom, M. L., & Ghosh, S. S. (2011). Nipype: a flexible, lightweight and extensible neuroimaging data processing framework in python. *Frontiers in Neuroinformatics*, 5, 13. <https://doi.org/10.3389/fninf.2011.00013>
- Grattton, C., Laumann, T. O., Nielsen, A. N., Greene, D. J., Gordon, E. M., Gilmore, A. W., Nelson, S. M., Coalson, R. S., Snyder, A. Z., Schlaggar, B. L., Dosenbach, N. U. F., & Petersen, S. E. (2018). Functional Brain Networks Are Dominated by Stable Group and Individual Factors, Not Cognitive or Daily Variation. *Neuron*, 98(2), 439–452.e5. <https://doi.org/10.1016/j.neuron.2018.03.035>
- Greene, A. S., Gao, S., Noble, S., Scheinost, D., & Constable, R. T. (2020). How Tasks Change Whole-Brain Functional Organization to Reveal Brain-Phenotype Relationships. *Cell Reports*, 32(8), 108066. <https://doi.org/10.1016/j.celrep.2020.108066>
- Greene, A. S., Gao, S., Scheinost, D., & Constable, R. T. (2018). Task-induced brain state manipulation improves prediction of individual traits. *Nature Communications*, 9(1), 1–13. <https://doi.org/10.1038/s41467-018-04920-3>
- Greicius, M. D., Krasnow, B., Reiss, A. L., & Menon, V. (2003). Functional connectivity in the resting brain: a network analysis of the default mode hypothesis. *Proceedings of the National Academy of Sciences of the United States of America*, 100(1), 253–258. <https://doi.org/10.1073/pnas.0135058100>
- Greicius, M. D., Srivastava, G., Reiss, A. L., & Menon, V. (2004). Default-mode network activity distinguishes Alzheimer’s disease from healthy aging: evidence from functional MRI. *Proceedings of the National Academy of Sciences of the United States of America*, 101(13), 4637–4642. <https://doi.org/10.1073/pnas.0308627101>
- Greve, D. N., & Fischl, B. (2009). Accurate and robust brain image alignment using boundary-based registration. *NeuroImage*, 48(1), 63–72. <https://doi.org/10.1016/j.neuroimage.2009.06.060>
- Gurguryan, L., & Sheldon, S. (2019). Retrieval orientation alters neural activity during autobiographical memory recollection. *NeuroImage*, 199, 534–544. <https://doi.org/10.1016/j.neuroimage.2019.05.077>
- Hakstian, A. R., & Cattell, R. B. (1974). THE CHECKING OF PRIMARY ABILITY STRUCTURE ON A BROADER BASIS OF PERFORMANCES. *The British Journal of Educational Psychology*, 44(2), 140–154. <https://doi.org/10.1111/j.2044->

8279.1974.tb02281.x

- Hallquist, M. N., & Wiley, J. F. (2018). MplusAutomation: An R Package for Facilitating Large-Scale Latent Variable Analyses in Mplus. *Structural Equation Modeling*, 25(4), 621–638. <https://doi.org/10.1080/10705511.2017.1402334>
- He, T., An, L., Chen, P., Chen, J., Feng, J., Bzdok, D., Holmes, A. J., Eickhoff, S. B., & Yeo, B. T. T. (2022). Meta-matching as a simple framework to translate phenotypic predictive models from big to small data. *Nature Neuroscience*, 25(6), 795–804. <https://doi.org/10.1038/s41593-022-01059-9>
- Horner, A. J., Bisby, J. A., Bush, D., Lin, W.-J., & Burgess, N. (2015). Evidence for holistic episodic recollection via hippocampal pattern completion. *Nature Communications*, 6. <https://doi.org/10.1038/ncomms8462>
- Horner, A. J., & Burgess, N. (2013). The associative structure of memory for multi-element events. *Journal of Experimental Psychology. General*, 142(4), 1370–1383. <https://doi.org/10.1037/a0033626>
- Horner, A. J., & Burgess, N. (2014). Pattern completion in multielement event engrams. *Current Biology: CB*, 24(9), 988–992. <https://doi.org/10.1016/j.cub.2014.03.012>
- Hsu, W.-T., Rosenberg, M. D., Scheinost, D., Constable, R. T., & Chun, M. M. (2018). Resting-state functional connectivity predicts neuroticism and extraversion in novel individuals. *Social Cognitive and Affective Neuroscience*, 13(2), 224–232. <https://doi.org/10.1093/scan/nsy002>
- Hu, L., & Bentler, P. M. (1999). Cutoff criteria for fit indexes in covariance structure analysis: Conventional criteria versus new alternatives. *Structural Equation Modeling*, 6(1), 1–55. <https://doi.org/10.1080/10705519909540118>
- Humphreys, G. F., Lambon Ralph, M. A., & Simons, J. S. (2021). A Unifying Account of Angular Gyrus Contributions to Episodic and Semantic Cognition. *Trends in Neurosciences*, 44(6), 452–463. <https://doi.org/10.1016/j.tins.2021.01.006>
- Iidaka, T., Matsumoto, A., Nogawa, J., Yamamoto, Y., & Sadato, N. (2006). Frontoparietal network involved in successful retrieval from episodic memory. Spatial and temporal analyses using fMRI and ERP. *Cerebral Cortex*, 16(9), 1349–1360. <https://doi.org/10.1093/cercor/bhl040>
- Im, K., Lee, J.-M., Yoon, U., Shin, Y.-W., Hong, S. B., Kim, I. Y., Kwon, J. S., & Kim, S. I. (2006). Fractal dimension in human cortical surface: multiple regression analysis with cortical thickness, sulcal depth, and folding area. *Human Brain Mapping*, 27(12), 994–1003. <https://doi.org/10.1002/hbm.20238>
- Inc., T. M. (2022). *MATLAB version: 9.13.0 (R2022b)*. The MathWorks Inc. <https://www.mathworks.com>
- Jak, S. (2019). Cross-Level Invariance in Multilevel Factor Models. *Structural Equation Modeling*, 26(4), 607–622. <https://doi.org/10.1080/10705511.2018.1534205>
- Jak, S., Oort, F. J., & Dolan, C. V. (2013). A Test for Cluster Bias: Detecting Violations of Measurement Invariance Across Clusters in Multilevel Data. *Structural Equation Modeling*, 20(2), 265–282. <https://doi.org/10.1080/10705511.2013.769392>

- James, E., Ong, G., Henderson, L. M., & Horner, A. J. (2020). Make or break it: boundary conditions for integrating multiple elements in episodic memory. *Royal Society Open Science*, 7(9), 200431. <https://doi.org/10.1098/rsos.200431>
- Jangraw, D. C., Gonzalez-Castillo, J., Handwerker, D. A., Ghane, M., Rosenberg, M. D., Panwar, P., & Bandettini, P. A. (2018). A functional connectivity-based neuromarker of sustained attention generalizes to predict recall in a reading task. *NeuroImage*, 166, 99–109. <https://doi.org/10.1016/j.neuroimage.2017.10.019>
- Jeffreys, H. (1961). *Theory of Probability* (3rd ed.). Oxford University Press.
- Jenkinson, M., Bannister, P., Brady, M., & Smith, S. (2002). Improved optimization for the robust and accurate linear registration and motion correction of brain images. *NeuroImage*, 17(2), 825–841. <https://doi.org/10.1006/nimg.2002.1132>
- Jenkinson, M., & Smith, S. (2001). A global optimisation method for robust affine registration of brain images. *Medical Image Analysis*, 5(2), 143–156. [https://doi.org/10.1016/s1361-8415\(01\)00036-6](https://doi.org/10.1016/s1361-8415(01)00036-6)
- Josselyn, S. A., & Tonegawa, S. (2020). Memory engrams: Recalling the past and imagining the future. *Science*, 367(6473). <https://doi.org/10.1126/science.aaw4325>
- Kadlec, J., Walsh, C., Sadé, U., Amir, A., Rissman, J., & Ramot, M. (2023). Putting cognitive tasks on trial: A measure of reliability convergence. In *bioRxiv* (p. 2023.07.03.547563). <https://doi.org/10.1101/2023.07.03.547563>
- Kelley, H. P. (1954). A factor analysis of memory ability. *ETS Research Bulletin Series*, 1954(1), i – 183. <https://doi.org/10.1002/j.2333-8504.1954.tb00928.x>
- Kim, E. S., Dedrick, R. F., Cao, C., & Ferron, J. M. (2016). Multilevel Factor Analysis: Reporting Guidelines and a Review of Reporting Practices. *Multivariate Behavioral Research*, 51(6), 881–898. <https://doi.org/10.1080/00273171.2016.1228042>
- Kim, H. (2011). Neural activity that predicts subsequent memory and forgetting: a meta-analysis of 74 fMRI studies. *NeuroImage*, 54(3), 2446–2461. <https://doi.org/10.1016/j.neuroimage.2010.09.045>
- Kim, H. (2013). Differential neural activity in the recognition of old versus new events: an activation likelihood estimation meta-analysis. *Human Brain Mapping*, 34(4), 814–836. <https://doi.org/10.1002/hbm.21474>
- Kim, H. (2016). Default network activation during episodic and semantic memory retrieval: A selective meta-analytic comparison. *Neuropsychologia*, 80, 35–46. <https://doi.org/10.1016/j.neuropsychologia.2015.11.006>
- Kim, S. (2015). *ppcor: Partial and Semi-Partial (Part) Correlation*. <https://CRAN.R-project.org/package=ppcor>
- King, D. R., de Chastelaine, M., Elward, R. L., Wang, T. H., & Rugg, M. D. (2015). Recollection-related increases in functional connectivity predict individual differences in memory accuracy. *Journal of Neuroscience*, 35(4), 1763–1772. <https://doi.org/10.1523/JNEUROSCI.3219-14.2015>
- Kong, R., Li, J., Orban, C., Sabuncu, M. R., Liu, H., Schaefer, A., Sun, N., Zuo, X.-N., Holmes,

- A. J., Eickhoff, S. B., & Yeo, B. T. T. (2019). Spatial Topography of Individual-Specific Cortical Networks Predicts Human Cognition, Personality, and Emotion. *Cerebral Cortex*, 29(6), 2533–2551. <https://doi.org/10.1093/cercor/bhy123>
- Krishnan, A., Williams, L. J., McIntosh, A. R., & Abdi, H. (2011). Partial Least Squares (PLS) methods for neuroimaging: a tutorial and review. *NeuroImage*, 56(2), 455–475. <https://doi.org/10.1016/j.neuroimage.2010.07.034>
- Kurkela, K. A., Cooper, R. A., Ryu, E., & Ritchey, M. (2022a). Integrating region- and network-level contributions to episodic recollection using multilevel structural equation modeling. In *bioRxiv* (p. 2022.02.08.478511). <https://doi.org/10.1101/2022.02.08.478511>
- Kurkela, K. A., Cooper, R. A., Ryu, E., & Ritchey, M. (2022b). Integrating Region- and Network-level Contributions to Episodic Recollection Using Multilevel Structural Equation Modeling. *Journal of Cognitive Neuroscience*, 34(12), 2341–2359. [https://doi.org/10.1162/jocn\\_a\\_01904](https://doi.org/10.1162/jocn_a_01904)
- Lanczos, C. (1964). Evaluation of Noisy Data. *Journal of the Society for Industrial and Applied Mathematics Series B Numerical Analysis*, 1(1), 76–85. <https://doi.org/10.1137/0701007>
- Laumann, T. O., Gordon, E. M., Adeyemo, B., Snyder, A. Z., Joo, S. J., Chen, M.-Y., Gilmore, A. W., McDermott, K. B., Nelson, S. M., Dosenbach, N. U. F., Schlaggar, B. L., Mumford, J. A., Poldrack, R. A., & Petersen, S. E. (2015). Functional System and Areal Organization of a Highly Sampled Individual Human Brain. *Neuron*, 87(3), 657–670. <https://doi.org/10.1016/j.neuron.2015.06.037>
- LePort, A. K. R., Mattfeld, A. T., Dickinson-Anson, H., Fallon, J. H., Stark, C. E. L., Kruggel, F., Cahill, L., & McGaugh, J. L. (2012). Behavioral and neuroanatomical investigation of Highly Superior Autobiographical Memory (HSAM). *Neurobiology of Learning and Memory*, 98(1), 78–92. <https://doi.org/10.1016/j.nlm.2012.05.002>
- Libby, L. A., Ekstrom, A. D., Ragland, J. D., & Ranganath, C. (2012). Differential connectivity of perirhinal and parahippocampal cortices within human hippocampal subregions revealed by high-resolution functional imaging. *The Journal of Neuroscience: The Official Journal of the Society for Neuroscience*, 32(19), 6550–6560. <https://doi.org/10.1523/JNEUROSCI.3711-11.2012>
- Li, J., Kong, R., Liégeois, R., Orban, C., Tan, Y., Sun, N., Holmes, A. J., Sabuncu, M. R., Ge, T., & Yeo, B. T. T. (2019). Global signal regression strengthens association between resting-state functional connectivity and behavior. *NeuroImage*, 196, 126–141. <https://doi.org/10.1016/j.neuroimage.2019.04.016>
- Lin, Q., Yoo, K., Shen, X., Constable, T. R., & Chun, M. M. (2021). Functional Connectivity during Encoding Predicts Individual Differences in Long-Term Memory. *Journal of Cognitive Neuroscience*, 1–18. [https://doi.org/10.1162/jocn\\_a\\_01759](https://doi.org/10.1162/jocn_a_01759)
- Lübke, K., Gehrke, M., Horst, J., & Szepannek, G. (2020). Why We Should Teach Causal Inference: Examples in Linear Regression With Simulated Data. *Journal of Statistics Education*, 28(2), 133–139. <https://doi.org/10.1080/10691898.2020.1752859>
- Maguire, E. A., Gadian, D. G., Johnsrude, I. S., Good, C. D., Ashburner, J., Frackowiak, R. S., & Frith, C. D. (2000). Navigation-related structural change in the hippocampi of taxi drivers. *Proceedings of the National Academy of Sciences of the United States of America*, 97(8),

- 4398–4403. <https://doi.org/10.1073/pnas.070039597>
- Maillet, D., & Rajah, M. N. (2014). Dissociable roles of default-mode regions during episodic encoding. *NeuroImage*, *89*, 244–255. <https://doi.org/10.1016/j.neuroimage.2013.11.050>
- Makowski, D., Lüdecke, D., Patil, I., Thériault, R., Ben-Shachar, M. S., & Wiernik, B. M. (2023). Automated Results Reporting as a Practical Tool to Improve Reproducibility and Methodological Best Practices Adoption. In *CRAN*. <https://easystats.github.io/report/>
- Malmi, R. A., Underwood, B. J., & Carroll, J. B. (1979). The interrelationships among some associative learning tasks. *Bulletin of the Psychonomic Society*, *13*(3), 121–123. <https://doi.org/10.3758/BF03335032>
- Marek, S., Tervo-Clemmens, B., Calabro, F. J., Montez, D. F., Kay, B. P., Hatoum, A. S., Donohue, M. R., Foran, W., Miller, R. L., Hendrickson, T. J., Malone, S. M., Kandala, S., Feczko, E., Miranda-Dominguez, O., Graham, A. M., Earl, E. A., Perrone, A. J., Cordova, M., Doyle, O., ... Dosenbach, N. U. F. (2022). Reproducible brain-wide association studies require thousands of individuals. *Nature*, *603*(7902), 654–660. <https://doi.org/10.1038/s41586-022-04492-9>
- Marks, D. F. (1973). Vividness of Visual Imagery Questionnaire. *British Journal of Psychology* *Journal of Mental Imagery*. <https://doi.org/10.1037/t05959-000>
- Marr, D. (1971). Simple memory: a theory for archicortex. *Philosophical Transactions of the Royal Society of London*, *262*(841), 23–81. <https://doi.org/10.1098/rstb.1971.0078>
- Mazoyer, B., Zago, L., Mellet, E., Bricogne, S., Etard, O., Houdé, O., Crivello, F., Joliot, M., Petit, L., & Tzourio-Mazoyer, N. (2001). Cortical networks for working memory and executive functions sustain the conscious resting state in man. *Brain Research Bulletin*, *54*(3), 287–298. [https://doi.org/10.1016/s0361-9230\(00\)00437-8](https://doi.org/10.1016/s0361-9230(00)00437-8)
- Mazzoni, G., Clark, A., De Bartolo, A., Guerrini, C., Nahouli, Z., Duzzi, D., De Marco, M., McGeown, W., & Venneri, A. (2019). Brain activation in highly superior autobiographical memory: The role of the precuneus in the autobiographical memory retrieval network. *Cortex; a Journal Devoted to the Study of the Nervous System and Behavior*, *120*, 588–602. <https://doi.org/10.1016/j.cortex.2019.02.020>
- McCormick, C., Moscovitch, M., Protzner, A. B., Huber, C. G., & McAndrews, M. P. (2010). Hippocampal-neocortical networks differ during encoding and retrieval of relational memory: functional and effective connectivity analyses. *Neuropsychologia*, *48*(11), 3272–3281. <https://doi.org/10.1016/j.neuropsychologia.2010.07.010>
- McCormick, C., St-Laurent, M., Ty, A., Valiante, T. A., & McAndrews, M. P. (2015). Functional and effective hippocampal-neocortical connectivity during construction and elaboration of autobiographical memory retrieval. *Cerebral Cortex*, *25*(5), 1297–1305. <https://doi.org/10.1093/cercor/bht324>
- McDermott, K. B., Szpunar, K. K., & Christ, S. E. (2009). Laboratory-based and autobiographical retrieval tasks differ substantially in their neural substrates. *Neuropsychologia*, *47*(11), 2290–2298. <https://doi.org/10.1016/j.neuropsychologia.2008.12.025>
- McIntosh, A. R. (2000). Towards a network theory of cognition. *Neural Networks: The Official*

- Journal of the International Neural Network Society*, 13(8-9), 861–870.  
[https://doi.org/10.1016/s0893-6080\(00\)00059-9](https://doi.org/10.1016/s0893-6080(00)00059-9)
- McIntosh, A. R., Bookstein, F. L., Haxby, J. V., & Grady, C. L. (1996). Spatial pattern analysis of functional brain images using partial least squares. *NeuroImage*, 3(3), 143–157.  
<https://doi.org/10.1006/nimg.1996.0016>
- McIntosh, A. R., & Gonzalez-Lima, F. (1994). Structural equation modeling and its application to network analysis in functional brain imaging. *Human Brain Mapping*, 2(1-2), 2–22.  
<https://doi.org/10.1002/hbm.460020104>
- McIntosh, A. R., & Lobaugh, N. J. (2004). Partial least squares analysis of neuroimaging data: applications and advances. *NeuroImage*. <https://doi.org/10.1016/j.neuroimage.2004.07.020>
- McIntosh, A. R., & Protzner, A. B. (2012). Structural equation models of imaging data. In R. H. Hoyle (Ed.), *Handbook of structural equation modeling* (Vol. 740, pp. 636–649). The Guilford Press.
- Miller, J., & Ulrich, R. (2021). A simple, general, and efficient method for sequential hypothesis testing: The independent segments procedure. *Psychological Methods*, 26(4), 486–497.  
<https://doi.org/10.1037/met0000350>
- Miller, M. B., Donovan, C.-L., Bennett, C. M., Aminoff, E. M., & Mayer, R. E. (2012). Individual differences in cognitive style and strategy predict similarities in the patterns of brain activity between individuals. *NeuroImage*, 59(1), 83–93.  
<https://doi.org/10.1016/j.neuroimage.2011.05.060>
- Miller, M. B., Donovan, C.-L., Van Horn, J. D., German, E., Sokol-Hessner, P., & Wolford, G. L. (2009). Unique and persistent individual patterns of brain activity across different memory retrieval tasks. *NeuroImage*, 48(3), 625–635.  
<https://doi.org/10.1016/j.neuroimage.2009.06.033>
- Miller, M. B., Van Horn, J. D., Wolford, G. L., Handy, T. C., Valsangkar-Smyth, M., Inati, S., Grafton, S., & Gazzaniga, M. S. (2002). Extensive individual differences in brain activations associated with episodic retrieval are reliable over time. *Journal of Cognitive Neuroscience*, 14(8), 1200–1214. <https://doi.org/10.1162/089892902760807203>
- Misaki, M., Kim, Y., Bandettini, P. A., & Kriegeskorte, N. (2010). Comparison of multivariate classifiers and response normalizations for pattern-information fMRI. *NeuroImage*, 53(1), 103–118. <https://doi.org/10.1016/j.neuroimage.2010.05.051>
- Morey, R. D., & Rouder, J. N. (2021). *BayesFactor: Computation of Bayes Factors for Common Designs*. <https://CRAN.R-project.org/package=BayesFactor>
- Moscovitch, M., Cabeza, R., Winocur, G., & Nadel, L. (2016). Episodic Memory and Beyond: The Hippocampus and Neocortex in Transformation. *Annual Review of Psychology*, 67, 105–134. <https://doi.org/10.1146/annurev-psych-113011-143733>
- Moscovitch, M., & Winocur, G. (1992). The neuropsychology of memory and aging. In F. I. M. Craik (Ed.), *The handbook of aging and cognition* (Vol. 586, pp. 315–372). Lawrence Erlbaum Associates.
- Mumford, J. A., Turner, B. O., Ashby, F. G., & Poldrack, R. A. (2012). Deconvolving BOLD activation in event-related designs for multivoxel pattern classification analyses.

- NeuroImage*, 59(3), 2636–2643. <https://doi.org/10.1016/j.neuroimage.2011.08.076>
- Murphy, K., Birn, R. M., Handwerker, D. A., Jones, T. B., & Bandettini, P. A. (2009). The impact of global signal regression on resting state correlations: are anti-correlated networks introduced? *NeuroImage*, 44(3), 893–905. <https://doi.org/10.1016/j.neuroimage.2008.09.036>
- Murphy, K., & Fox, M. D. (2017). Towards a consensus regarding global signal regression for resting state functional connectivity MRI. *NeuroImage*, 154, 169–173. <https://doi.org/10.1016/j.neuroimage.2016.11.052>
- Muthén, L. K., & Muthén, B. O. (1997-2017). *Mplus User's Guide* (Eight Edition). Los Angeles, CA: Muthén & Muthén.
- Newsome, R. N., Trelle, A. N., Fidalgo, C., Hong, B., Smith, V. M., Jacob, A., Ryan, J. D., Rosenbaum, R. S., Cowell, R. A., & Barense, M. D. (2018). Dissociable contributions of thalamic nuclei to recognition memory: novel evidence from a case of medial dorsal thalamic damage. *Learning & Memory*, 25(1), 31–44. <https://doi.org/10.1101/lm.045484.117>
- Ngo, C. T., Michelmann, S., Olson, I. R., & Newcombe, N. S. (2021). Pattern separation and pattern completion: Behaviorally separable processes? *Memory & Cognition*, 49(1), 193–205. <https://doi.org/10.3758/s13421-020-01072-y>
- Norman, K. A., & O'Reilly, R. C. (2003). Modeling hippocampal and neocortical contributions to recognition memory: a complementary-learning-systems approach. *Psychological Review*, 110(4), 611–646. <https://doi.org/10.1037/0033-295X.110.4.611>
- Nyberg, L. (1994). A structural equation modeling approach to the multiple memory systems question. *Journal of Experimental Psychology: Learning, Memory, and Cognition*, 20(2), 485–491. <https://doi.org/10.1037/0278-7393.20.2.485>
- O'Keefe, J., Nadel, L., Keightley, S., & Kill, D. (1975). Fornix lesions selectively abolish place learning in the rat. *Experimental Neurology*, 48(1), 152–166. [https://doi.org/10.1016/0014-4886\(75\)90230-7](https://doi.org/10.1016/0014-4886(75)90230-7)
- Palombo, D. J., Sheldon, S., & Levine, B. (2018). Individual Differences in Autobiographical Memory. *Trends in Cognitive Sciences*, 22(7), 583–597. <https://doi.org/10.1016/j.tics.2018.04.007>
- Palombo, D. J., Williams, L. J., Abdi, H., & Levine, B. (2013). The survey of autobiographical memory (SAM): a novel measure of trait mnemonics in everyday life. *Cortex; a Journal Devoted to the Study of the Nervous System and Behavior*, 49(6), 1526–1540. <https://doi.org/10.1016/j.cortex.2012.08.023>
- Parker, E. S., Cahill, L., & McGaugh, J. L. (2006). A case of unusual autobiographical remembering. *Neurocase*, 12(1), 35–49. <https://doi.org/10.1080/13554790500473680>
- Peer, M., Salomon, R., Goldberg, I., Blanke, O., & Arzy, S. (2015). Brain system for mental orientation in space, time, and person. *Proceedings of the National Academy of Sciences*, 112(35), 11072–11077. <https://doi.org/10.1073/pnas.1504242112>
- Petrican, R., Palombo, D. J., Sheldon, S., & Levine, B. (2020). The Neural Dynamics of Individual Differences in Episodic Autobiographical Memory. *eNeuro*, 7(2). <https://doi.org/10.1523/ENEURO.0531-19.2020>

- Poppenk, J., & Moscovitch, M. (2011). A hippocampal marker of recollection memory ability among healthy young adults: contributions of posterior and anterior segments. *Neuron*, 72(6), 931–937. <https://doi.org/10.1016/j.neuron.2011.10.014>
- Posse, S., Wiese, S., Gembris, D., Mathiak, K., Kessler, C., Grosse-Ruyken, M. L., Elghahwagi, B., Richards, T., Dager, S. R., & Kiselev, V. G. (1999). Enhancement of BOLD-contrast sensitivity by single-shot multi-echo functional MR imaging. *Magnetic Resonance in Medicine: Official Journal of the Society of Magnetic Resonance in Medicine / Society of Magnetic Resonance in Medicine*, 42(1), 87–97. [https://doi.org/10.1002/\(sici\)1522-2594\(199907\)42:1<87::aid-mrm13>3.0.co;2-o](https://doi.org/10.1002/(sici)1522-2594(199907)42:1<87::aid-mrm13>3.0.co;2-o)
- Power, J. D., Barnes, K. A., Snyder, A. Z., Schlaggar, B. L., & Petersen, S. E. (2012). Spurious but systematic correlations in functional connectivity MRI networks arise from subject motion. *NeuroImage*, 59(3), 2142–2154. <https://doi.org/10.1016/j.neuroimage.2011.10.018>
- Power, J. D., Mitra, A., Laumann, T. O., Snyder, A. Z., Schlaggar, B. L., & Petersen, S. E. (2014). Methods to detect, characterize, and remove motion artifact in resting state fMRI. *NeuroImage*, 84, 320–341. <https://doi.org/10.1016/j.neuroimage.2013.08.048>
- Przeździk, I., Faber, M., Fernández, G., Beckmann, C. F., & Haak, K. V. (2019). The functional organisation of the hippocampus along its long axis is gradual and predicts recollection. *Cortex; a Journal Devoted to the Study of the Nervous System and Behavior*, 119, 324–335. <https://doi.org/10.1016/j.cortex.2019.04.015>
- Raichle, M. E., MacLeod, A. M., Snyder, A. Z., Powers, W. J., Gusnard, D. A., & Shulman, G. L. (2001). A default mode of brain function. *Proceedings of the National Academy of Sciences of the United States of America*, 98(2), 676–682. <https://doi.org/10.1073/pnas.98.2.676>
- Rajah, M. N., & McIntosh, A. R. (2005). Overlap in the functional neural systems involved in semantic and episodic memory retrieval. *Journal of Cognitive Neuroscience*, 17(3), 470–482. <https://doi.org/10.1162/0898929053279478>
- Ramanan, S., Piguet, O., & Irish, M. (2018). Rethinking the Role of the Angular Gyrus in Remembering the Past and Imagining the Future: The Contextual Integration Model. *The Neuroscientist*, 24(4), 342–352. <https://doi.org/10.1177/1073858417735514>
- Ramirez, S., Liu, X., Lin, P.-A., Suh, J., Pignatelli, M., Redondo, R. L., Ryan, T. J., & Tonegawa, S. (2013). Creating a false memory in the hippocampus. *Science*, 341(6144), 387–391. <https://doi.org/10.1126/science.1239073>
- Ranganath, C. (2010). Binding Items and Contexts: The Cognitive Neuroscience of Episodic Memory. *Current Directions in Psychological Science*, 19(3), 131–137. <https://doi.org/10.1177/0963721410368805>
- Ranganath, C., & Ritchey, M. (2012). Two cortical systems for memory-guided behaviour. *Nature Reviews. Neuroscience*, 13(10), 713–726. <https://doi.org/10.1038/nrn3338>
- Ranganath, C., Yonelinas, A. P., Cohen, M. X., Dy, C. J., Tom, S. M., & D’Esposito, M. (2004). Dissociable correlates of recollection and familiarity within the medial temporal lobes. *Neuropsychologia*, 42(1), 2–13. <https://doi.org/10.1016/j.neuropsychologia.2003.07.006>
- R Core Team. (2022). *R: A Language and Environment for Statistical Computing*. R Foundation

for Statistical Computing. <https://www.R-project.org/>

- Reagh, Z. M., Delarazan, A. I., Garber, A., & Ranganath, C. (2020). Aging alters neural activity at event boundaries in the hippocampus and Posterior Medial network. *Nature Communications*, *11*(1), 3980. <https://doi.org/10.1038/s41467-020-17713-4>
- Richter, F. R., Cooper, R. A., Bays, P. M., & Simons, J. S. (2016). Distinct neural mechanisms underlie the success, precision, and vividness of episodic memory. *eLife*, *5*. <https://doi.org/10.7554/eLife.18260>
- Riedel, G., Micheau, J., Lam, A. G., Roloff, E. L., Martin, S. J., Bridge, H., de Hoz, L., Poeschel, B., McCulloch, J., & Morris, R. G. (1999). Reversible neural inactivation reveals hippocampal participation in several memory processes. *Nature Neuroscience*, *2*(10), 898–905. <https://doi.org/10.1038/13202>
- Ritchey, M., & Cooper, R. A. (2020). Deconstructing the Posterior Medial Episodic Network. *Trends in Cognitive Sciences*. <https://doi.org/10.1016/j.tics.2020.03.006>
- Ritchey, M., Montchal, M. E., Yonelinas, A. P., & Ranganath, C. (2015). Delay-dependent contributions of medial temporal lobe regions to episodic memory retrieval. *eLife*, *4*. <https://doi.org/10.7554/eLife.05025>
- Ritchey, M., Yonelinas, A. P., & Ranganath, C. (2014). Functional connectivity relationships predict similarities in task activation and pattern information during associative memory encoding. *Journal of Cognitive Neuroscience*, *26*(5), 1085–1099. [https://doi.org/10.1162/jocn\\_a\\_00533](https://doi.org/10.1162/jocn_a_00533)
- Robin, J., & Moscovitch, M. (2017). Details, gist and schema: hippocampal–neocortical interactions underlying recent and remote episodic and spatial memory. *Current Opinion in Behavioral Sciences*, *17*, 114–123. <https://doi.org/10.1016/j.cobeha.2017.07.016>
- Rosenbaum, R. S., Furey, M. L., Horwitz, B., & Grady, C. L. (2010). Altered connectivity among emotion-related brain regions during short-term memory in Alzheimer’s disease. *Neurobiology of Aging*, *31*(5), 780–786. <https://doi.org/10.1016/j.neurobiolaging.2008.06.002>
- Rosenberg, M. D., Finn, E. S., Scheinost, D., Papademetris, X., Shen, X., Constable, R. T., & Chun, M. M. (2016). A neuromarker of sustained attention from whole-brain functional connectivity. *Nature Neuroscience*, *19*(1), 165–171. <https://doi.org/10.1038/nn.4179>
- Rugg, M. D., & King, D. R. (2018). Ventral lateral parietal cortex and episodic memory retrieval. *Cortex*, *107*, 238–250. <https://doi.org/10.1016/j.cortex.2017.07.012>
- Rugg, M. D., & Vilberg, K. L. (2013). Brain networks underlying episodic memory retrieval. *Current Opinion in Neurobiology*, *23*(2), 255–260. <https://doi.org/10.1016/j.conb.2012.11.005>
- Satterthwaite, T. D., Elliott, M. A., Gerraty, R. T., Ruparel, K., Loughhead, J., Calkins, M. E., Eickhoff, S. B., Hakonarson, H., Gur, R. C., Gur, R. E., & Wolf, D. H. (2013). An improved framework for confound regression and filtering for control of motion artifact in the preprocessing of resting-state functional connectivity data. *NeuroImage*, *64*, 240–256. <https://doi.org/10.1016/j.neuroimage.2012.08.052>
- Schaefer, A., Kong, R., Gordon, E. M., Laumann, T. O., Zuo, X.-N., Holmes, A. J., Eickhoff, S.

- B., & Yeo, B. T. T. (2018). Local-Global Parcellation of the Human Cerebral Cortex from Intrinsic Functional Connectivity MRI. *Cerebral Cortex*, *28*(9), 3095–3114. <https://doi.org/10.1093/cercor/bhx179>
- Schedlbauer, A. M., Copara, M. S., Watrous, A. J., & Ekstrom, A. D. (2014). Multiple interacting brain areas underlie successful spatiotemporal memory retrieval in humans. *Scientific Reports*, *4*, 6431. <https://doi.org/10.1038/srep06431>
- Schlichting, M. L., & Preston, A. R. (2015). Memory integration: neural mechanisms and implications for behavior. *Current Opinion in Behavioral Sciences*, *1*, 1–8. <https://doi.org/10.1016/j.cobeha.2014.07.005>
- Schreiner, M. R., & Meiser, T. (2022). Measuring binding effects in event-based episodic representations. *Behavior Research Methods*. <https://doi.org/10.3758/s13428-021-01769-1>
- Scoville, W. B., & Milner, B. (1957). Loss of recent memory after bilateral hippocampal lesions. *Journal of Neurology, Neurosurgery, and Psychiatry*, *20*(1), 11–21. <https://doi.org/10.1136/jnnp.20.1.11>
- Seitzman, B. A., Gratton, C., Laumann, T. O., Gordon, E. M., Adeyemo, B., Dworetzky, A., Kraus, B. T., Gilmore, A. W., Berg, J. J., Ortega, M., Nguyen, A., Greene, D. J., McDermott, K. B., Nelson, S. M., Lessov-Schlaggar, C. N., Schlaggar, B. L., Dosenbach, N. U. F., & Petersen, S. E. (2019). Trait-like variants in human functional brain networks. *Proceedings of the National Academy of Sciences of the United States of America*. <https://doi.org/10.1073/pnas.1902932116>
- Sekeres, M. J., Winocur, G., & Moscovitch, M. (2018). The hippocampus and related neocortical structures in memory transformation. *Neuroscience Letters*, *680*, 39–53. <https://doi.org/10.1016/j.neulet.2018.05.006>
- Setton, R., Mwilambwe-Tshilobo, L., Sheldon, S., Turner, G. R., & Spreng, R. N. (2022). Hippocampus and temporal pole functional connectivity is associated with age and individual differences in autobiographical memory. *Proceedings of the National Academy of Sciences of the United States of America*, *119*(41), e2203039119. <https://doi.org/10.1073/pnas.2203039119>
- Shafto, M. A., Tyler, L. K., Dixon, M., Taylor, J. R., Rowe, J. B., Cusack, R., Calder, A. J., Marslen-Wilson, W. D., Duncan, J., Dalgleish, T., Henson, R. N., Brayne, C., Matthews, F. E., & Cam-CAN. (2014). The Cambridge Centre for Ageing and Neuroscience (Cam-CAN) study protocol: a cross-sectional, lifespan, multidisciplinary examination of healthy cognitive ageing. *BMC Neurology*, *14*, 204. <https://doi.org/10.1186/s12883-014-0204-1>
- Sheldon, S., Farb, N., Palombo, D. J., & Levine, B. (2016). Intrinsic medial temporal lobe connectivity relates to individual differences in episodic autobiographical remembering. *Cortex; a Journal Devoted to the Study of the Nervous System and Behavior*, *74*, 206–216. <https://doi.org/10.1016/j.cortex.2015.11.005>
- Sheldon, S., Fenerci, C., & Gurguryan, L. (2019). A Neurocognitive Perspective on the Forms and Functions of Autobiographical Memory Retrieval. *Frontiers in Systems Neuroscience*, *13*, 4. <https://doi.org/10.3389/fnsys.2019.00004>
- Shen, X., Finn, E. S., Scheinost, D., Rosenberg, M. D., Chun, M. M., Papademetris, X., & Constable, R. T. (2017). Using connectome-based predictive modeling to predict individual

- behavior from brain connectivity. *Nature Protocols*, 12(3), 506–518.  
<https://doi.org/10.1038/nprot.2016.178>
- Silson, E. H., Steel, A., Kidder, A., Gilmore, A. W., & Baker, C. I. (2019). Distinct subdivisions of human medial parietal cortex support recollection of people and places. *eLife*, 8.  
<https://doi.org/10.7554/eLife.47391>
- Simons, J. S., Peers, P. V., Mazuz, Y. S., Berryhill, M. E., & Olson, I. R. (2010). Dissociation between memory accuracy and memory confidence following bilateral parietal lesions. *Cerebral Cortex*, 20(2), 479–485. <https://doi.org/10.1093/cercor/bhp116>
- Sjoberg, D., Whiting, K., Curry, M., Lavery, J., & Larmarange, J. (2021). Reproducible Summary Tables with the gtsummary Package. *The R Journal*, 13(1), 570.  
<https://doi.org/10.32614/rj-2021-053>
- Sneve, M. H., Grydeland, H., Amlien, I. K., Langnes, E., Walhovd, K. B., & Fjell, A. M. (2017). Decoupling of large-scale brain networks supports the consolidation of durable episodic memories. *NeuroImage*, 153, 336–345. <https://doi.org/10.1016/j.neuroimage.2016.05.048>
- Spaniol, J., Davidson, P. S. R., Kim, A. S. N., Han, H., Moscovitch, M., & Grady, C. L. (2009). Event-related fMRI studies of episodic encoding and retrieval: meta-analyses using activation likelihood estimation. *Neuropsychologia*, 47(8-9), 1765–1779.  
<https://doi.org/10.1016/j.neuropsychologia.2009.02.028>
- Spets, D. S., Jeye, B. M., & Slotnick, S. D. (2019). Different patterns of cortical activity in females and males during spatial long-term memory. *NeuroImage*, 199, 626–634.  
<https://doi.org/10.1016/j.neuroimage.2019.06.027>
- Spets, D. S., & Slotnick, S. D. (2021). Are there sex differences in brain activity during long-term memory? A systematic review and fMRI activation likelihood estimation meta-analysis. *Cognitive Neuroscience*, 12(3-4), 163–173.  
<https://doi.org/10.1080/17588928.2020.1806810>
- Spiers, H. J., Maguire, E. A., & Burgess, N. (2001). Hippocampal amnesia. *Neurocase*, 7(5), 357–382. <https://doi.org/10.1076/neur.7.5.357.16245>
- Spreng, R. N., & Grady, C. L. (2010). Patterns of brain activity supporting autobiographical memory, prospection, and theory of mind, and their relationship to the default mode network. *Journal of Cognitive Neuroscience*, 22(6), 1112–1123.  
<https://doi.org/10.1162/jocn.2009.21282>
- Spunt, R. P., Satpute, A. B., & Lieberman, M. D. (2011). Identifying the what, why, and how of an observed action: an fMRI study of mentalizing and mechanizing during action observation. *Journal of Cognitive Neuroscience*, 23(1), 63–74.  
<https://doi.org/10.1162/jocn.2010.21446>
- Squire, L. R. (1992). Memory and the hippocampus: a synthesis from findings with rats, monkeys, and humans. *Psychological Review*, 99(2), 195–231.  
<https://doi.org/10.1037/0033-295x.99.2.195>
- Squire, L. R., & Zola-Morgan, S. (1991). The medial temporal lobe memory system. *Science*, 253(5026), 1380–1386. <https://www.ncbi.nlm.nih.gov/pubmed/1896849>
- Sutherland, R. J., & McDonald, R. J. (1990). Hippocampus, amygdala, and memory deficits in

- rats. *Behavioural Brain Research*, 37(1), 57–79. [https://doi.org/10.1016/0166-4328\(90\)90072-m](https://doi.org/10.1016/0166-4328(90)90072-m)
- Tambini, A., Ketz, N., & Davachi, L. (2010). Enhanced brain correlations during rest are related to memory for recent experiences. *Neuron*, 65(2), 280–290. <https://doi.org/10.1016/j.neuron.2010.01.001>
- Taylor, J. R., Williams, N., Cusack, R., Auer, T., Shafto, M. A., Dixon, M., Tyler, L. K., Cam-Can, & Henson, R. N. (2017). The Cambridge Centre for Ageing and Neuroscience (Cam-CAN) data repository: Structural and functional MRI, MEG, and cognitive data from a cross-sectional adult lifespan sample. *NeuroImage*, 144(Pt B), 262–269. <https://doi.org/10.1016/j.neuroimage.2015.09.018>
- Thakral, P. P., Madore, K. P., & Schacter, D. L. (2020). The core episodic simulation network dissociates as a function of subjective experience and objective content. *Neuropsychologia*, 136, 107263. <https://doi.org/10.1016/j.neuropsychologia.2019.107263>
- Touroutoglou, A., Andreano, J. M., Barrett, L. F., & Dickerson, B. C. (2015). Brain network connectivity-behavioral relationships exhibit trait-like properties: Evidence from hippocampal connectivity and memory. *Hippocampus*, 25(12), 1591–1598. <https://doi.org/10.1002/hipo.22480>
- Treder, M. S., Charest, I., Michelmann, S., Martín-Buro, M. C., Roux, F., Carceller-Benito, F., Ugalde-Canitrot, A., Rollings, D. T., Sawlani, V., Chelvarajah, R., Wimber, M., Hanslmayr, S., & Staresina, B. P. (2021). The hippocampus as the switchboard between perception and memory. *Proceedings of the National Academy of Sciences*, 118(50). <https://doi.org/10.1073/pnas.2114171118>
- Tulving, E. (1983). *Elements of episodic memory*. Oxford University Press.
- Tulving, E. (2002). Episodic memory: from mind to brain. *Annual Review of Psychology*, 53, 1–25. <https://doi.org/10.1146/annurev.psych.53.100901.135114>
- Tustison, N. J., Avants, B. B., Cook, P. A., Zheng, Y., Egan, A., Yushkevich, P. A., & Gee, J. C. (2010). N4ITK: improved N3 bias correction. *IEEE Transactions on Medical Imaging*, 29(6), 1310–1320. <https://doi.org/10.1109/TMI.2010.2046908>
- Underwood, B. J., Boruch, R. F., & Malmi, R. A. (1978). Composition of episodic memory. *Journal of Experimental Psychology. General*, 107(4), 393–419. <https://doi.org/10.1037/0096-3445.107.4.393>
- Unsworth, N. (2010). On the division of working memory and long-term memory and their relation to intelligence: A latent variable approach. *Acta Psychologica*, 134(1), 16–28. <https://doi.org/10.1016/j.actpsy.2009.11.010>
- Unsworth, N. (2019). Individual differences in long-term memory. *Psychological Bulletin*, 145(1), 79–139. <https://doi.org/10.1037/bul0000176>
- Unsworth, N., & Brewer, G. A. (2009). Examining the relationships among item recognition, source recognition, and recall from an individual differences perspective. *Journal of Experimental Psychology. Learning, Memory, and Cognition*, 35(6), 1578–1585. <https://doi.org/10.1037/a0017255>
- Unsworth, N., & Brewer, G. A. (2010). Individual differences in false recall: A latent variable

- analysis. *Journal of Memory and Language*, 62(1), 19–34.  
<https://doi.org/10.1016/j.jml.2009.08.002>
- Valenstein, E., Bowers, D., Verfaellie, M., Heilman, K. M., Day, A., & Watson, R. T. (1987). Retrosplenial amnesia. *Brain: A Journal of Neurology*, 110 ( Pt 6), 1631–1646.  
<https://doi.org/10.1093/brain/110.6.1631>
- van Buuren, M., Wagner, I. C., & Fernández, G. (2019). Functional network interactions at rest underlie individual differences in memory ability. *Learning & Memory*, 26(1), 9–19.  
<https://doi.org/10.1101/lm.048199.118>
- van Kesteren, M. T. R., Ruiters, D. J., Fernández, G., & Henson, R. N. (2012). How schema and novelty augment memory formation. *Trends in Neurosciences*, 35(4), 211–219.  
<https://doi.org/10.1016/j.tins.2012.02.001>
- Van Petten, C. (2004). Relationship between hippocampal volume and memory ability in healthy individuals across the lifespan: review and meta-analysis. *Neuropsychologia*, 42(10), 1394–1413. <https://doi.org/10.1016/j.neuropsychologia.2004.04.006>
- Vilberg, K. L., & Rugg, M. D. (2012). The neural correlates of recollection: transient versus sustained fMRI effects. *Journal of Neuroscience*, 32(45), 15679–15687.  
<https://doi.org/10.1523/JNEUROSCI.3065-12.2012>
- Vilberg, K. L., & Rugg, M. D. (2014). Temporal dissociations within the core recollection network. *Cognitive Neuroscience*, 5(2), 77–84.  
<https://doi.org/10.1080/17588928.2013.860088>
- Vincent, J. L., Snyder, A. Z., Fox, M. D., Shannon, B. J., Andrews, J. R., Raichle, M. E., & Buckner, R. L. (2006). Coherent spontaneous activity identifies a hippocampal-parietal memory network. *Journal of Neurophysiology*, 96(6), 3517–3531.  
<https://doi.org/10.1152/jn.00048.2006>
- Wang, L., LaViolette, P., O’Keefe, K., Putcha, D., & Bakkour, A. (2010). Intrinsic connectivity between the hippocampus and posteromedial cortex predicts memory performance in cognitively intact older individuals. *NeuroImage*.  
<https://www.sciencedirect.com/science/article/pii/S1053811910002144>
- Wang, L., Negreira, A., LaViolette, P., Bakkour, A., Sperling, R. A., & Dickerson, B. C. (2010). Intrinsic interhemispheric hippocampal functional connectivity predicts individual differences in memory performance ability. *Hippocampus*, 20(3), 345–351.  
<https://doi.org/10.1002/hipo.20771>
- Wang, Z., Goerlich, K. S., Ai, H., Aleman, A., Luo, Y.-J., & Xu, P. (2021). Connectome-Based Predictive Modeling of Individual Anxiety. *Cerebral Cortex*, 31(6), 3006–3020.  
<https://doi.org/10.1093/cercor/bhaa407>
- Watrous, A. J., Tandon, N., Conner, C. R., Pieters, T., & Ekstrom, A. D. (2013). Frequency-specific network connectivity increases underlie accurate spatiotemporal memory retrieval. *Nature Neuroscience*, 16(3), 349–356. <https://doi.org/10.1038/nn.3315>
- Weschler, C. J. (1999). *Weschler Memory Scale* (Third UK edition).
- Whitfield-Gabrieli, S., & Nieto-Castanon, A. (2012). Conn: a functional connectivity toolbox for correlated and anticorrelated brain networks. *Brain Connectivity*, 2(3), 125–141.

<https://doi.org/10.1089/brain.2012.0073>

- Wickham, H. (2016). *ggplot2: Elegant Graphics for Data Analysis*. Springer-Verlag New York. <https://ggplot2.tidyverse.org>
- Wing, E. A., Marsh, E. J., & Cabeza, R. (2013). Neural correlates of retrieval-based memory enhancement: an fMRI study of the testing effect. *Neuropsychologia*, *51*(12), 2360–2370. <https://doi.org/10.1016/j.neuropsychologia.2013.04.004>
- Wolf, E. J., Harrington, K. M., Clark, S. L., & Miller, M. W. (2013). Sample Size Requirements for Structural Equation Models: An Evaluation of Power, Bias, and Solution Propriety. *Educational and Psychological Measurement*, *76*(6), 913–934. <https://doi.org/10.1177/0013164413495237>
- Xiao, J., Ehinger, K. A., Oliva, A., & Torralba, A. (2012). Recognizing scene viewpoint using panoramic place representation. *2012 IEEE Conference on Computer Vision and Pattern Recognition*, 2695–2702. <https://doi.org/10.1109/CVPR.2012.6247991>
- Xia, Y., & Yang, Y. (2019). RMSEA, CFI, and TLI in structural equation modeling with ordered categorical data: The story they tell depends on the estimation methods. *Behavior Research Methods*, *51*(1), 409–428. <https://doi.org/10.3758/s13428-018-1055-2>
- Yarkoni, T., Poldrack, R. A., Nichols, T. E., Van Essen, D. C., & Wager, T. D. (2011). Large-scale automated synthesis of human functional neuroimaging data. *Nature Methods*, *8*(8), 665–670. <https://doi.org/10.1038/nmeth.1635>
- Yeo, B. T. T., Krienen, F. M., Sepulcre, J., Sabuncu, M. R., Lashkari, D., Hollinshead, M., Roffman, J. L., Smoller, J. W., Zöllei, L., Polimeni, J. R., Fischl, B., Liu, H., & Buckner, R. L. (2011). The organization of the human cerebral cortex estimated by intrinsic functional connectivity. *Journal of Neurophysiology*, *106*(3), 1125–1165. <https://doi.org/10.1152/jn.00338.2011>
- Zhang, Y., Brady, M., & Smith, S. (2001). Segmentation of brain MR images through a hidden Markov random field model and the expectation-maximization algorithm. *IEEE Transactions on Medical Imaging*, *20*(1), 45–57. <https://doi.org/10.1109/42.906424>
- Zola-Morgan, S., & Squire, L. R. (1985). Medial temporal lesions in monkeys impair memory on a variety of tasks sensitive to human amnesia. *Behavioral Neuroscience*, *99*(1), 22–34. <https://doi.org/10.1037//0735-7044.99.1.22>
- Zola-Morgan, S., & Squire, L. R. (1986). Memory impairment in monkeys following lesions limited to the hippocampus. *Behavioral Neuroscience*, *100*(2), 155–160. <https://doi.org/10.1037//0735-7044.100.2.155>
- Zola-Morgan, S., Squire, L. R., & Amaral, D. G. (1986). Human amnesia and the medial temporal region: enduring memory impairment following a bilateral lesion limited to field CA1 of the hippocampus. *The Journal of Neuroscience: The Official Journal of the Society for Neuroscience*, *6*(10), 2950–2967. <https://doi.org/10.1523/JNEUROSCI.06-10-02950.1986>
- Zola-Morgan, S., Squire, L. R., Amaral, D. G., & Suzuki, W. A. (1989). Lesions of perirhinal and parahippocampal cortex that spare the amygdala and hippocampal formation produce severe memory impairment. *The Journal of Neuroscience: The Official Journal of the*

*Society for Neuroscience*, 9(12), 4355–4370. <https://doi.org/10.1523/JNEUROSCI.09-12-04355.1989>